EVOLUTION OF NOVEL MATERIAL PROPERTIES AND THE EMERGENCE OF GROUP-LEVEL HERITABILITY IN THE TRANSITION TO MULTICELLULARITY

A Dissertation
Presented to
The Academic Faculty

By

Seyed Alireza Zamani Dahaj

In Partial Fulfillment
of the Requirements for the Degree
Doctor of Philosophy in the
Quantitative Biosciences
School of Physics

Georgia Institute of Technology

May 2021

© Seyed Alireza Zamani Dahaj 2021

EVOLUTION OF NOVEL MATERIAL PROPERTIES AND THE EMERGENCE OF GROUP-LEVEL HERITABILITY IN THE TRANSITION TO MULTICELLULARITY

Thesis committee:

Prof. Peter J. Yunker, Advisor
School of Physics
Georgia Institute of Technology

Prof. Daniel B. Weissman
Department of Physics
Emory University

Prof. William C. Ratcliff, Co-advisor
School of Biological Sciences
Georgia Institute of Technology

Prof. Raphael F. Rosenzweig
School of Biological Sciences
Georgia Institute of Technology

Prof. Joshua S. Weitz
School of Biological Sciences
Georgia Institute of Technology

Date approved: April 30, 2021

Life can only be understood backwards; but it must be lived forwards.

Søren Kierkegaard.

To my parents

ACKNOWLEDGMENTS

Through out my life I have had the help, support and friendship of many wonderful people that it's impossible to do justice to them with mere words. But I would like to express my gratitude and appreciation of a few individuals.

First and foremost I'm eternally grateful to my family. My father who flamed the love of science in me since I can remember and my mother who her love was always inspiring me to be the best version of my self.

People are considering themselves lucky if they have a good PhD advisor. But very few have the chance of working with two amazing advisor like I did. My deepest gratitude goes to Prof. Peter Yunker and Prof. Will Ratcliff. Their passion for science, welcoming attitude, encouraging personality, and patience with me was the key to my success. I I will forever remember your lessons and mentorship.

I am beholden to Prof. Joshua Weitz for his support and guidance. He encouraged me to apply to Qunatitative biosciences program at Georgia tech and since then whenever I needed help or guidance he was always there to make sure I am on the right track. I learn many valuable lessons from him and will never forget his generosity and wisdom. In addition, I thank the remaining members of my thesis committee, Prof. Raphael F. Rosenzweig, and Prof. Daniel Weissman for taking the time to guide, comment, and review my thesis research.

I also want to especially thank Matthew D. Herron and Gonensin Ozan Bozdag who generated some of the main ideas that lead to this thesis and without their incredible collaboration and invaluable input it was impossible to finish these projects. I also want to thank Prof. Matteo Smerlak for helping me developing some of the analytical models. During my PhD I also had the chance to collaboration with many bright and intelligent people including: Thomas C. Day, Anthony J. Burnetti and Penelope C. Kahn. Additionally, I thank my fellow members of the Yunker lab and Ratcliff past and present for their

friendship and inteltual input. These include the numerous undergraduate and high school researchers who have passed though the lab over the years, and fellow graduate students , Thomas C. Day, Arben Kalziqi, Jonathan Michel, David Yanni, Pablo A Bravo, Aawaz R Pokhrel, Jennifer Pentz, Pedro Márquez-Zacarías, Kai Tong, Katie Wendorf MacGillivray and Rozenn Pineau as well as post-doctoral researchers Anthony J. Burnetti, Gonensin Ozan Bozdag, Gabi Steinbach, Peter Conlin and Skanda Vivek.

I also like to thank all the friends that I had the chance to met during my time in Atlanta. I owe a word of thanks to Elma and Jessica who without their support and friendship I couldn't last long and they always were there whenever I needed help.

TABLE OF CONTENTS

LIST OF TABLES

LIST OF FIGURES

SUMMARY

Evolutionary Transitions in Individuality (ETIs) describe the history of increasing complexity of life and emergence of hierarchical organization in an elegant framework. Each transition is characterized by a group of independent individuals coming together and forming a group that eventually can undergo Darwinian evolution and turns into a new individual level. One of the prominent examples of ETIs is the emergence of multicellularity. In this thesis I address two key questions about the transition to multicellularity: The emergence of heritability of higher level traits and its relationship to cell-level traits.

First, I discuss how the heritability of newly-formed group traits emerges as groups emerge. We introduce a simple theoretical model for calculating group-level trait heritability, where the trait is the linear function of a cell-level trait. For cases in which the relationship is more complex than a linear function, we developed a statistical simulation to model and explore different kinds of analytical functions based on biological examples of relationship between cell-level traits and collective-level traits. Finally, using the snowflake yeast model system we did an experiment that shows an ecologically relevant, emergent trait in a nascent multicellular organism can have a higher heritability across a range of conditions than the unicellular-level trait on which it is based.

The evolution of complex multicellularity presents an apparent paradox: nascent multicellular organisms are thought to require (relatively) large size to evolve complex traits, but at the same time maintaining large size requires complex organization at the cell and group levels. This poses a chicken and egg problem between large size and cellular development. Here, we show that over the course of a year snowflake yeast can increase its size multiple orders of magnitude with minimal change at the cell level by taking advantage of the physical properties of granular entangled materials.

CHAPTER 1
INTRODUCTION AND BACKGROUND

1.1 Overview

Life on earth has evolved from organic molecules capable of simple and erroneous replication [1] to on one hand clonal *Posidonia oceanica* spanning over thousands of acres and surviving for tens of thousands of years [2] and on the other hand *Homo sapiens* capable of changing the Earth's climate over the span of few centuries thus triggering a mass extinction event [3]. This colossal increase in structural complexity has happened due to the forces of natural selection and evolution acting continuously over billions of years through a semi-random process of trial and error.

One of the main features of life on earth is its hierarchical structure across many levels spanning from molecular to macroscopic scales [4, 5, 6]. For example, a bee colony is made out of bees that are themselves are composed of different organs and each of them have different type of cells. This trends continues until molecular level. While there are many different processes at multiple length scales responsible for this increase in the complexity and emergence of hierarchy of life, there are a few events in the history of life that explain the majority of changes known as major evolutionary transitions (METs). Example of such transitions are: origin of life, emergence of prokaryotes, formation of multicellular organisms, and evolution of eusociality [4]. A subset of METs are characterized by individual entities capable of replication that cooperate to form a group that is itself a new entity that can undergo Darwinian evolution. This process is known as an "Evolutionary Transition in Individuality" (ETI)[7]. One of the most notable examples of an ETI is the evolution of multicellularity from unicellular life, which is the focus of this thesis.

While there is general agreement about benefits of multicellularity, such as avoiding

predation, protection against toxins, and division labor [8, 9], the processes by which this transition has happened are still unknown, and there are many open questions on this topic. In this thesis we focus on two problems in two different stages of the transition to multicellularity. First we focus on the first steps of an ETI where individuals form groups. For these groups to be themselves individuals, they need to go through the cycle of reproduction, variation, and selection (i.e., the Darwinian algorithm). It is possible for an individual to be under selection pressure if it has heritable traits (phenotypes) that can be selected for. While these newly formed groups consist of individuals with heritable traits, group-level traits are not necessarily heritable as well.

In the first part of this thesis, through system-agnostic mathematical modeling and computer simulations, we show how heritability of group-level traits can emerge as groups are forming. We tested some of the predictions of our analysis using snowflake yeast model system.

In the second part, through a long term evolution experiment we show that the size of a nascent multicellular organism can increase multiple orders of magnitude via biophysical changes by selection for larger size over a year, and we subsequently explore the underlying physical principles that enable this change. This work shows that large size in multicellular organisms can evolve without first evolving complex developmental traits.

1.2 Multicellularity

1.2.1 Background

Few events in the history of life have had more profound effects as the transition from unicellularity to multicellularity. Once only composed of unicellular life, today multicellular organisms account for most of the biomass on Earth. Plants alone represent $\sim 80\%$ of biomass on the planet [10]. This transition has happened at least 25 times across all three domains of life [11] in many different forms and has two main modes. First, unrelated cells come together and form groups; this process is known as aggregative multicellularity and

is limited to terrestrial and semi-terrestrial micro-organism[12, 13]. The second method is when cells stay together after reproduction and form a group with a uniform genetic background. If this process involves a mechanism to ensure the genetic uniformity for the following multicellular generation, it results in clonal development[14, 15]. The majority of complex multicellular organisms, organisms with 3D structure and genetically predetermined developmental program [8], that have sophisticated developmental networks and internal structure have some form of clonal development [8, 16, 17].

The first step in the transition to multicellularity before evolving complex traits was forming new groups [4, 18]. For these groups to be considered individuals there must be a shift in selection from cell-level traits to group-level traits [19]. However, for this shift to happen group traits have to be heritable[20, 21]. These emergent phenotypes are functions of cell−level phenotypes unless one believe in phenotypes at the group−level are autonomous from underlying cell traits, a philosophical position tantamount to mysticism [22]. The function that relates cell-level traits and group-level traits could be very complicated and may not have a closed analytical form; nonetheless, there is a relationship between these two levels of traits. After a new level of selection is established, the next step is evolving larger size. Most of the benefits of multicellularity, such as avoiding predation [23, 24], extra−cellular cooperation [25, 26] and protection against hostile environment [27, 28], are correlated with higher number of cells per group. It is believed that nascent multicellular organisms needed some level of developmental network and complex traits such as division of labor for the maintenance of large size [8]. However, large size is also considered a prerequisite to evolving complex traits and structures [12, 11]. This poses a chicken and egg problem for the development of early multicellular organisms. The main consensus is that some of the phenotypes required to support large size preceded the evolution of large size [8], but the idea that large size can evolve first has not been refuted.

Directly studying “how” and “why” multicellularity emerged in the nature is almost impossible since the last transition to multicellularity happened million of years ago [12]

and we have a limited number of fossils from the early stages of this transition [8]. Complementary methods such as comparing extant multicellular taxa to their relatives using phylogenetic mapping as a genomic route to study this question [29, 30] but the biggest drawback of this method is the lack of information about ecological factors, our large uncertainty in the timing of events [31], and missing genomes of extinct organisms.

1.2.2 Experimental evolution of multicellularity

In addition to the above retrospective approach, experimental evolution of multicellularity provides a perspective method for studying this transition which has the advantage of tractability in both phenotype and genome level. While it is impossible to replicate the exact conditions and details of the early stages of our multicellular ancestors in the lab, it is possible to study the general properties of this phenomena through experimental evolution of a model system [32, 33, 34]. Since this method lacks some disadvantages of the other methods, combining all approaches can provide a more complete image of this transition. For example phylogenetic analysis of Volvocine green algae supported experimental evolution have shown multiple origination events followed by reverting to unicellular form in their history [35, 35, 36].

One of approach to study *de novo* evolution of multicellularity is to subject unicellular *Saccharomyces cerevisiae,* (baker's yeast) to selection under gravity for rapid settling in a tube. After two months of daily selection, clonal clusters of yeast called "Snowflake yeast" reported in 10 independent populations [32]. These clusters are formed because of mutations in *ACE2* transcription factor which halt production of chitinase enzyme in cells. In the absence of this enzyme when mother and daughter cells stay together because they cannot digest the chitin ring that connects them. This process results in a tree like structure in which every cell is only connected to their mother and their direct offspring. If a single cell−cell bond fails the cluster fractures into two smaller clusters (Figure 1.1) [32, 34, 37].

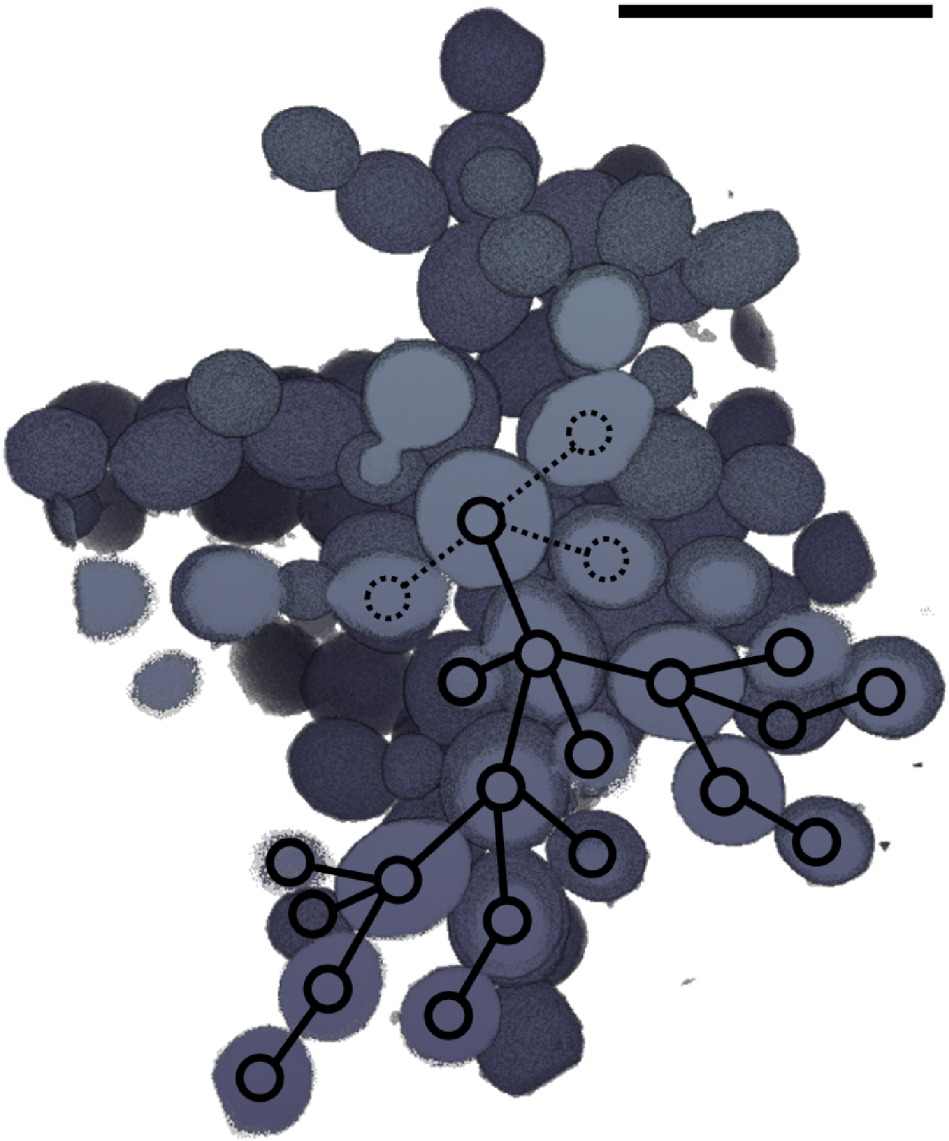

Figure 1.1: Serial block-face scanning electron microscopy of snowflake yeast clusters reveals the tree like structure of the cluster. Removing each node from the cluster can result in fracture. Black circles and lines illusterate the parental relationshop between different cells. Scale bar= $10.\mu m$

Upon emergence, snowflake yeast clusters have all of the properties of an Darwinian individual and can be treated as a new level of selection. They have a characteristic size at which they fracture, which acts a mechanism for group-level reproduction [37]. They have heritable group-level traits that can be selected for [32]. Finally, because of their structure

and clonality, different clusters have different genetic backgrounds [38]. These properties combined with the tractability and simplicity of this particular approach to experimental evolution have created an exceptional opportunity to study the early stages of the transition from unicellularity to multicellularity.

1.3 Heritability and Transition to Multicellularity

One key to explaining life's hierarchy and biological complexity is the ability to understand how a new group emerges from the interactions between existing individuals to become itself an individual capable of undergoing Darwinian evolution? In this process, the fundamental level of evolution transfers from the lower-level unit to the higher-level unit [4]. One such area of particular interest is the transition from single-celled to multicellular organisms. For this transition to happen a two-step process is needed: first, individuals evolve to form a robust collective [7, 39], and then the level at which selection acts shifts from individuals to groups. Here we focus on groups that their members are have the same genotype also known as a colony. These colonies have traits that did not exist in the unicellular population, for example colony diameter, colony shape, and number of cells per colony. These traits are potentially subject to natural selection. How effective such selection will be in changing group-level traits depends on the heritability of the trait.

To be considered an individual, the new group should be able to go through the cycle of reproduction, variation, and selection (one cycle of the Darwinian algorithm). Natural selection requires heritable variation in traits that affect fitness at the level at which selection happens [40]. The breeder's equation ($R = h^2 S$, where R equals the change in the mean trait value in the population, h^2 is the narrow sense heritability, the proportion of trait variation explained by additive genetic variation, and S is the strength of selection) model selection pressure and heritability contribute equally to the adaptive response [41](Figure 2.3). For simplicity, we consider asexual populations, for which the relevant measure of heritability is broad-sense heritability, H^2, the proportion of phenotypic variation ex-

plained by all genetic variation [41]. The response to selection in an asexual population, then, is $R = H^2S$. When selection acts on a trait, that trait's heritability determines the extent of the response in the population. Hence, multicellular heritability is crucial for shifting adaptation from unicellularity (lower level) to multicellularity (higher level) [42, 32].

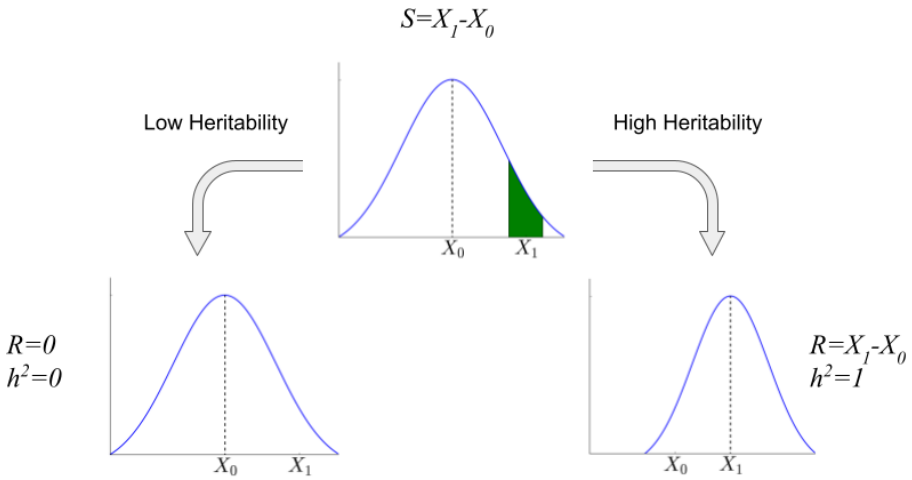

Figure 1.2: Relationship between selection, heritability and the response to selection. Top middle shows an distribution of a trait in an initial population with mean X_0. The individuals in the green area with mean X_1 are selected to reproduce (selection pressure $S = X_1 - X_0$. If the trait is not heritable (h^2) the new generation has the same mean as the parent population (bottom left). If the trait has a very high heritability in the given condition then the mean of the trait for the new generation is X_1.

It should be noted that heritability is not an intrinsic feature of individual organisms but rather a statistical property of the population at a given time that depends on many factors, such as structure of the population and the background environment [43]. Hence, estimates of heritability for a trait in one population can be very different from another population of the same organism [14, 21] depending on the environment and the genetic background. Here, we looked at the ratio of heritability of cell-level traits to group-level traits across a wide range of variables.

There has been a great body of work trying to understand the selective pressures that

could have created the right conditions for the emergence of multicellularity [24, 44, 25, 45]. However, according to the breeder's equation, heritability is just as important as the selection pressure for predicting the outcome of evolutionary processes. However, heritability has largely been ignored in the literature [46, 20], or taken to be artificially high (e.g., 1 for microbial communities) [47, 48, 49, 50, 51, 52, 53, 54, 55]. In this thesis, we explore the emergence of heritability of newly formed groups and its relationship to the underlying cell-level traits through a combination of analytical modeling, computer simulations, and experiments with snowflake yeast as a proxy for nascent multicellular organisms. Although here we are focusing on the transition to multicellularity, our results are likely valid for any two adjacent levels of individuality that have similar relation to what we have investigated here.

1.4 Evolution of Macroscopic Size in nascent multicellular organisms

Life started on earth at the molecular level and has explored many different niches including increased in both size and complexity through evolution by natural selection [56, 57, 58]. Today, there is 22 orders of magnitude difference in size between a typical bacteria and blue whale the largest known animal [59]. If we classify viruses as organisms and consider clonal colonies such as Pando (a male male *Populus tremuloides* [60]) as a single organism then there will be 30 orders of magnitude difference between them. It is widely believe that the difference in size correlates changes in shape and structure [8]. To illustrate this point Bonner gives the example of commissioning an engineer to build two bridges one over Hudson river and another over a narrow creek. Because of the sheer difference in size, these two bridges are likely going to be built with different designs and materials [58]. The same principle applies to living organisms. For an egg to a mature human our shape and structure change significantly [57, 61].

This change in structure usually manifests itself as an increase in complexity [9, 57, 8]. According to the size-complexity "rule", the number of cell types in an organism (as

a proxy for organismal complexity) increases with the notional number of cells in that organism [57] Figure 1.3. This rule generally holds up on almost all different level of hierarchy of life: There is strong positive correlation between genome size and cell length in most kingdoms of eukaryotes [62, 63] but interestingly they are independent for bacteria or archaea [64]. On the level of eusocial organisms, phylogenetic comparative analysis and empirical studies have shown that colony size is a predictor of both reproductive and non-reproductive division of labor in ants [65, 66]. The same pattern have been observed in bees [67]. Finally number of occupations in a society has increases as the population and physical size of cities grow [68]. Of course like almost any other "rule" or "law" in biology there are many exception to this rule to and there can be changes in size without any change in the complexity or even decreasing it [69].

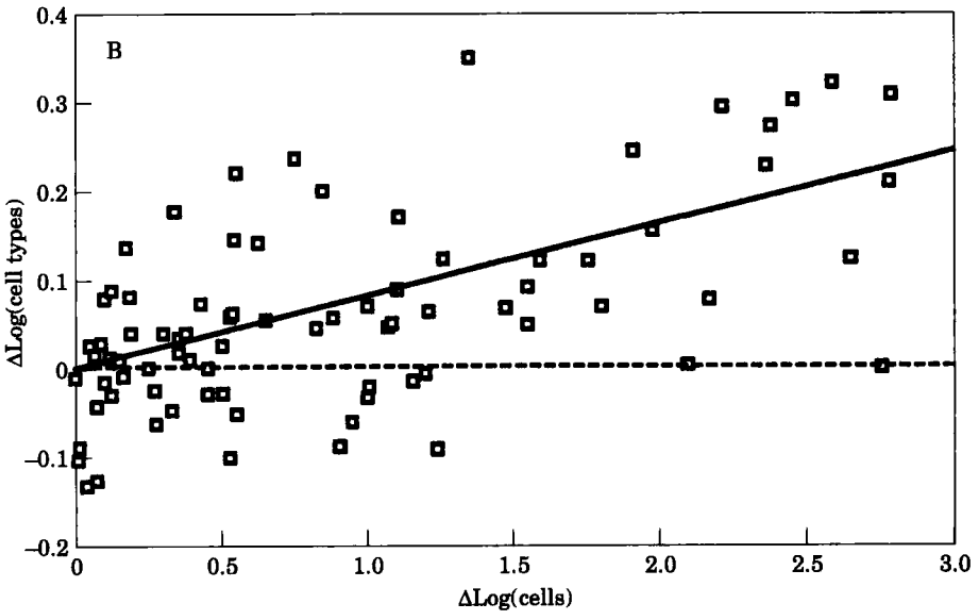

Figure 1.3: number of cell type is generally increasing with the number of cells per organism [56].

Here we focus primarily on the evolution of large size in nascent multicellular organisms. It is believed that the same evolutionary force that led to the emergence of first multicellular organisms also favored larger size in the early stages of this transition [32, 39, 70]. One example of such a selection pressure is predation, which has long been considered

as an ecologically plausible cause for increase in size [57, 71, 72]. The green alga *Chlorella vulgaris* evolved a small stable colonies after being subjected to predation by the fagellate *Ochromonas vallescia* [24]. In a more recent study, Herron and colleagues exposed cultures of the unicellular green alga *Chlamydomonas reinhardtii* to selection by the filter-feeding predator *Paramecium tetraurelia*, a unicellular eukaryote. They reported *De nove* evolution of multicellular structures in two out of five population subject to this selection regime, and none of the unselected control populations within 750 asexual generations [73].

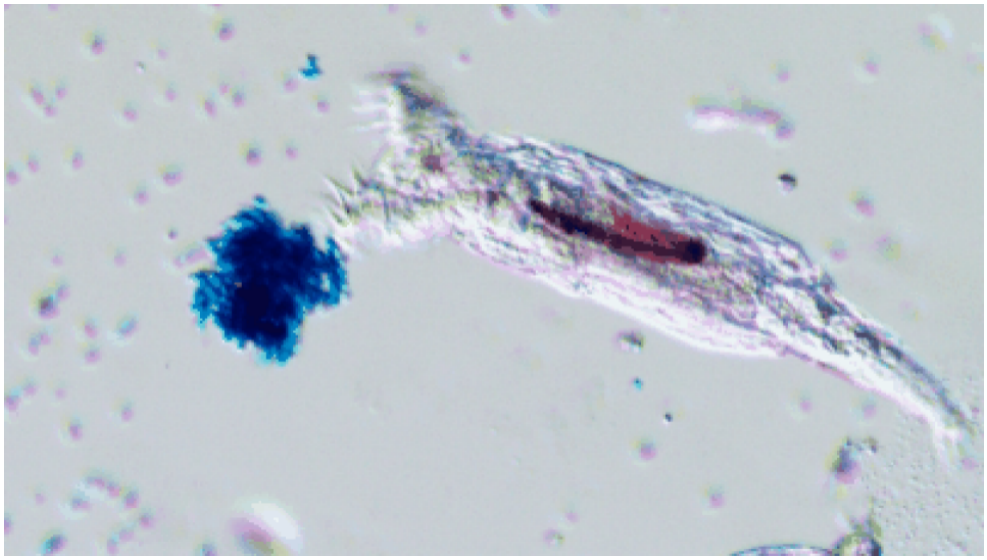

Figure 1.4: Larger size that be advantages against predation. A filter-feeder rotifer is fed both uni (labeled red) and multicellular (labeled blue)yeast. The multicellular yeast is too big and can't be eaten hence the stomach of the predator is completely red. [33]

Another factor that could have played a role in the evolution of multicellularity is co-operation [74]. For example, budding yeast, *Saccharomyces cerevisiae*, cannot directly metabolize sucrose, a disaccharide, so they need to first break it down to two monosaccharides by secreting invertase and then importing the products into the cell. Because sucrose is broken down extracellularly, in low sugar density environments, single cells can not capture enough sugar to grow. Koschwanez and colleagues, through experimental evolution, showed that yeast cells can overcome this by forming clonal clusters while increasing invertase expression. This strategy allows them to produce a large quantity of this public good,

while also ensuring that cheaters that do not make invertase do not invade the group since the cluster is clonal [45, 25]. Another type of cooperation is coming together to over come a physical constraint. An example of this type of cooperation is seen in Volvocalean Green Algae. Single cells are negatively buoyant and use their flagellar to avoid sinking [75]. Some genuses of this order like *Gonium* and *Volvox* form groups wherein cells arrange on the surface of a spherical extracellular matrix and beat their flagellar together to swim more efficiently. This cooperation enables them to stay near the water's surface, where there is more light and CO2 [76].

All the aforementioned examples are focused on the origins of simple multicellular organisms, while the evolution of complex multicellularity have been mostly overlooked. It is widely believed that relatively large size is a necessary precursor for the evolution of complex multicellular traits and an increase in the number of cells, with its concomitant increase in group size, can confer several advantages, such as division of labor and specialization [57, 77, 8, 78]. But to support large three-dimensional size, new mechanisms are necessary to transport oxygen and nutrients to the interior and to remove waste [8]. To solve this chicken and egg problem, Knoll and Hewitt hypothesize that large size, cell differentiation, and metabolism together create a positive feedback loop [79]. As nascent multicellular organisms emerge, simple innovations like gap junctions, that directly connect the cytoplasm of two cells, can allow gradual increase in size and thickness which consequently increases the difference between interior and exterior environment. This difference between surface and interior can promote cell differentiation in a way that helps transferring nutrients and oxygen from the surface inward [56].

We used the snowflake yeast model system to study the evolution of macroscopic body size in nascent multicellular organisms. Previous studies have shown how oxygen can limit the size of the clusters [80]. Here we report the emergence of a new phenotype in snowflake yeast that is orders of magnitude larger than its ancestor clusters. To the best of our knowledge this is the first time that a macroscopic nascent multicellular organism has

evolved in the lab from a microscopic ancestor. We show that these macroscopic clusters can resist macroscopic forces and do not fracture when a single cell-cell bound fails, as their snowflake yeast ancestors do, allowing them to change their material properties significantly by just sheer force of evolution. While this work does not attempt to claim a generality of its results nonetheless it shows that in contrast to conventional wisdom it is possible to evolve macroscopic three-dimensional bodies without very complicated structures such as vascular systems to support it.

CHAPTER 2

EMERGENCE OF TRAIT HERITABILITY IN MAJOR TRANSITIONS

2.1 Summary

The evolution of multicellularity was vital step in both increasing the complexity of life and providing immense potential for life to explore new scales. A crucial component of this paradigm is that after the transition in complexity or organization, adaptation occurs primarily at the level of the new, higher−level unit. For group-level adaptations to occur, though, group −level traits—properties of the group, such as group size-must be heritable. Since group−level trait values are functions of lower−level trait values, group−level heritability is related to lower level heritability. However, the nature of this relationship has rarely been explored in the context of major transitions. We examine relationships between cell−level heritability and group−level heritability for several functions that express group−level trait values in terms of cell−level trait values. For clonal populations, when a group-level trait value is a linear function of cell−level trait values and the number of cells per group is fixed, the heritability of a group−level trait is never less than that of the corresponding cell-level trait and is higher under most conditions. For more complicated functions, group-level heritability is higher under most conditions, but can be lower when the environment experienced by groups is heterogeneous. Within-genotype variation in group size reduces group-level heritability, but it can still exceed cell-level heritability when phenotypic variance among cells within groups is large. These results hold for a diverse sample of biologically relevant traits. Rather than being an impediment to major transitions, we show that, under a wide range of conditions, the heritability of group−level traits is actually higher than that of the corresponding cell−level traits. High levels of group−level trait heritability thus arise "for free," with important implications not only for

major transitions but for multilevel selection in general.

2.2 Introduction

Major transitions, or evolutionary transitions in individuality, are a framework for understanding the origins of life's hierarchy and of biological complexity [9]. During such a transition, a new unit of evolution emerges from interactions among previously existing units. This new unit, or group, has traits not present before the transition and distinct from those of the units that comprise it (e.g. cells). These group-level traits can potentially be under selection. Over the course of the transition, the primary level of selection shifts from the cell (lower-level unit) to the groups (higher-level unit), for example, from cells to multicellular organisms or from individual insects to eusocial societies.

As we showed in the previous chapter, the breeder's equation of quantitative genetics dictates that heritability and strength of selection contribute equally to the adaptive response. Hence, Evolution by natural selection requires heritable variation in phenotypes that affect fitness at the level at which selection occurs [81]. When a group-level trait is exposed to selection, it is group-level heritability (the heritability of the group-level trait) that determines the magnitude of the response. Group-level heritability of traits is thus necessary for group-level adaptations, but the emergence of group-level heritability during a major transition has often been assumed to be difficult. For example, Michod considers the emergence of group-level heritability through conflict mediation a crucial step in major transitions [21, 44, 61]. Simpson says that "From the view of some standard theory, these transitions are impossible," in part because cell-level heritability greatly exceeds group-level heritability [8].

Major transitions can be conceptualized as a shift from MLS1 to MLS2, in the sense of Damuth and Heisler [81], as in Okasha [82] (see also Godfrey-Smith [20], Shelton and Michod [83]). In MLS1, properties of the cells are under selection; in MLS2, it is the properties of the groups. Although our biological analogies are presented in terms of cells

as cells and multicellular organisms as groups, our model is system agnostic and could be extended to any pair of levels. Whether or not collective-level fitness in MLS2 is a function of particle-level fitness is a matter of some disagreement (for example, Rainey and Kerr say no [84]). However, group-level phenotypes must be functions of cell-level trait phenotypes. The function may be complex and involve cell-cell communication, feedbacks, environmental influences, etc., but it is still a function that is, in principle, predictable from cell-level trait values.

According to Michod [85], "...the challenge of ETI [evolutionary transitions in individuality] theory is to explain how fitness at the group level in the sense of MLS2 emerges out of fitness at the group level in the sense of MLS1." But fitness, or selection, is only half of the breeder's equation. Predicting the response to selection requires an estimate of heritability.

The relationship between the heritability of cell-level traits and that of group-level traits has rarely been considered in the context of major transitions, leading Okasha [86] to wonder, "Does variance at the cell level necessarily give rise to variance at the group level? Does the heritability of a group character depend somehow on the heritability of cell characters? The literature on multi-level selection has rarely tackled these questions explicitly, but they are crucial." Similarly, Goodnight [87] says, "...we really do not have a good understanding of what contributes to group heritability, how to measure it, or even how to define it."

While the role of selection has often been considered in the context of major transitions, the role of trait heritability has been relatively neglected. We examine relationships between cell-level heritability and group-level heritability for several functions that express group-level trait values in terms of cell-level trait values. For the simplest (linear) function, we derive an analytical solution for the relationship. For more complex functions, we employ a simulation model to explore some biologically relevant relationship over a range of conditions.

2.3 Analytical Model

2.3.1 Cell Level Heritability

We assume that the population is reproducing asexually at both levels, so broad-sense heritability (H^2) is the proper measure of heritability and is defined as the proportion of phenotypic variation explained by all genetic variation. Based on this definition we can define heritability as the correlation coefficient between phenotype values of parents and offspring (Fisher, 1918):

$$H^2 \equiv Corr(P, P') = \frac{E[(P - \overline{P})(P' - \overline{P'})]}{Var(P)} \tag{2.1}$$

We can define P and P' as phenotypic values that are a sum of three terms: a purely genetic part (G with mean $\overline{G}$ and variance σ_G^2), an environmental part (E with mean 0 and variance σ_E^2), and developmental noise (S with mean 0 and variance σ_S^2):

$$P = G + E + S \tag{2.2}$$

$$P' = G + E' + S' \tag{2.3}$$

Here we assume that the mutation rate is zero; hence parent and offspring have the same genetic value (G) and cells reproduce asexually. If there is no temporal correlation except for the same genotype between offspring and parents then $\overline{P} = \overline{P'}$ and we can rewrite the numerator of heritability as:

$$E[(P - \overline{P})(P' - \overline{P})] = E[PP'] - \overline{P}^2 = \sigma_G^2 \tag{2.4}$$

So the heritability of the cells is equal too:

$$H_c^2 = \frac{\sigma_G^2}{\sigma_G^2 + \sigma_S^2 + \sigma_E^2} \tag{2.5}$$

2.3.2 Group Level Heritability

For a clonal group like snowflake yeast and that parents and off springs have the same genotype we :

$$Y = \sum_{i=1}^{N} P_i \tag{2.6}$$

$$Y' = \sum_{i=1}^{N'} P'_i \tag{2.7}$$

Here N is the number of cells in a group (with mean N and variance $\sigma_N^2 = N \times CV_N$ where CV_N is the coefficient of variation for the number of cells per group in the population).Here we assume that N is independent of size of cell in the group and all cells within each group are experiencing the same environmental effect. Since all cells within a group have the same genotype we can rewrite the relationship between group level and cell level phenotype as:

$$Y = NG + NE + \Sigma_{i=1}^{N} S_i \tag{2.8}$$

$$Y' = N'G + N'E + \Sigma_{i=1}^{N} S'_i \tag{2.9}$$

All random variables are independent so for $Var(Y)$ we will have:

$$Var(Y) = E[Y^2] - E[Y]^2 \tag{2.10}$$

We can also write that as:

$$Var(Y) = Var(NG) + Var(NE) + Var(\Sigma_{i=1}^{N} S_i) \tag{2.11}$$

The first term on the r.h.s is equal to:

$$Var(NG) = E[(NG)^2] - E[NG]^2 \tag{2.12}$$

Because N and G are independent we can write:

$$Var(NG) = E[N^2]E[G^2] - \overline{N}^2\overline{G}^2 \tag{2.13}$$

We also know that for a random variable X we have $\sigma_X^2 = E[X^2] - \overline{X}^2$. So, we can rewrite (6) as:

$$Var(NG) = (\sigma_N^2 + \overline{N}^2)(\sigma_G^2 + \overline{G}^2) - \overline{N}^2\overline{G}^2 \tag{2.14}$$

$$= \overline{N}^2[(1 + CV_N^2)\sigma_G^2 + CV_N^2\overline{G}^2] \tag{2.15}$$

For the $Var(NE)$ we can write the same thing. The only difference is that $\overline{E} = 0$ so we have:

$$Var(NE) = \overline{N}^2(1 + CV_N^2)\sigma_E^2 \tag{2.16}$$

The third one is different from the last two since it's the sum of N identical, independent random variables when N itself is a random variable. So we have:

$$Var(\Sigma_{i=1}^N S_i) = \Sigma_{n=1}^\infty P(N = n) \int dsP(\Sigma_{i=1}^n S_i = s)(\Sigma_{i=1}^n S_i)^2 \tag{2.17}$$

The integral part is the variance of n independent random variables which is equal to $n\sigma_S^2$:

$$Var(\Sigma_{i=1}^{N} S_i) = \Sigma_{n=1}^{\infty} P(N=n) n\sigma_S^2 \tag{2.18}$$

$$= \sigma_S^2 \Sigma_{n=1}^{\infty} P(N=n) n \tag{2.19}$$

$$= \overline{N}\sigma_S^2 \tag{2.20}$$

So in total for $Var(Y)$ we have:

$$Var(Y) = \overline{N}^2[(1+CV_N^2)(\sigma_G^2+\sigma_E^2) + CV_N^2\overline{G}^2] + \overline{N}\sigma_S^2 \tag{2.21}$$

First we calculate group level heritability using coefficient of correlation:

$$E[(Y-\overline{Y})(Y'-\overline{Y}] = E[YY'] - \overline{Y}^2 \tag{2.22}$$

$$= E[(NG+NE+\Sigma_{i=1}^{N} S_i)(N'G+N'E'+\Sigma_{i=1}^{N'} S_i')] - E^2[NG+NE+\Sigma_{i=1}^{N} S_i] \tag{2.23}$$

$$= E[NN'G^2] - E^2[NG] \tag{2.24}$$

Assuming that N and G are independent we can write:

$$E[(Y-\overline{Y})(Y'-\overline{Y}] = E^2[N]E[G^2] - E^2[N]E^2[G] \tag{2.25}$$

$$= E^2[N](E[G^2] - E^2[G]) \tag{2.26}$$

$$= \overline{N}^2\sigma_G^2 \tag{2.27}$$

Hence the group level heritability is equal to:

$$H_g^2 = \frac{\overline{N}^2\sigma_G^2}{\overline{N}^2[(1+CV_N^2)(\sigma_G^2+\sigma_E^2) + CV_N^2\overline{G}^2] + \overline{N}\sigma_S^2} \tag{2.28}$$

Which for the large $\overline{N}$ will approach:

$$\lim_{\overline{N}\to\infty} H_g^2 = \frac{\sigma_G^2}{(1+CV_N^2)(\sigma_G^2+\sigma_E^2)+CV_N^2\overline{G}^2} \tag{2.29}$$

Therefore, the ratio of group to cell heritability in the limit of large $\overline{N}$ is:

$$\lim_{\overline{N}\to\infty} \frac{H_g^2}{H_c^2} = \frac{\sigma_G^2+\sigma_E^2+\sigma_S^2}{(1+CV_N^2)(\sigma_G^2+\sigma_E^2)+CV_N^2\overline{G}^2} \tag{2.30}$$

Note that if the variation in the number of cells per group is very small ($CV_N^2 = 0$), the group-level heritability is always higher than the cell-level heritability. Stochastic variation in cell traits around the group's genetic mean reduces the heritability of lower-level individuals by increasing phenotypic variation. By averaging across the all cells in a group, we subdue the effects of the variation in trait values. This decreases the phenotypic variation at the group level, hence increasing the group-level heritability relative to individuals. Also, in Equation 2.28 both σ_E^2 and σ_G^2 have the same coefficients and power so their effect on the relative heritability is identical.

2.4 Simulation Model

For most biologically interesting traits, the relationship between cellular-level and multicellular-level trait values is more complicated than a linear sum. We simulate more complicated phenotype relationships using a numerical simulation. In our model, cells grow in clonal groups, which reproduce by forming two new groups with the same genetic mean but different number of cells per each group. For the sake of simplicity, we have assumed that the number of cells in each group in the population is sampled from a normal discrete distribution with mean N and coefficient of variation of CV_N. The initial population is founded by ten genetically distinct clones, each with a different genetic mean for cell size. Each clone contains ten identical groups.

We examine the consequences of three different sources of variation affecting the relative heritability of group- and cell-level traits. The first and the most fundamental one is intrinsic reproductive noise that has a normal distribution with standard deviation σ_S^2. Stochastic variation in cell traits around the genetic mean reduces the heritability of lower-level individuals and higher-level groups by increasing phenotypic variation. By averaging across multiple cells, however, groups subdue the effects of the variation in trait values and take advantage of the fact that the noise is random. This increases their relative heritability compared to individuals. The second source of noise is environmental variation. We assumed that all cells in a group are experiencing the same environmental noise, so we modified the phenotype of cells in each group with a random number that is drawn from a normal distribution with mean 0 and standard deviation σ_E^2. This modifier is the same for all cells in a group but different for each group. The last source of variation is the number of cells per group, N. This variable doesn't affect the phenotype of the cells; however, since the phenotype of the group depends on N, it affects the final relative heritability. Like the other two variables, N is drawn from a normal distribution with a mean that is the same for every group during the simulation and coefficient of variation CV_N^2.

First, we examine the effect of developmental noise and environmental variation independently for the example of cells within nascent multicellular organisms. For a linear relationship, group size is simply the sum of the sizes of cells within the group. For both cells and groups, heritability is assessed by calculating the slope of a linear regression on parent and offspring phenotype[88]. In this simple case, mean group-level heritability is always greater than or equal to cell-level heritability. Only when $\sigma_s = 0$ (i.e., when all cells within a group have identical phenotype) are cell- and group-level heritability equal, in agreement with the analytical model. Greater developmental instability for cell size increases the advantage of group-level heritability over cell-level heritability Figure 2.1a. Larger groups, which average out cellular stochasticity more effectively, experience a greater increase in heritability than smaller groups Figure 2.1a. Note that the simulations run in Figure 2.1a

reflect a patchy environment in which environmental effects on cell size within groups are large ($\sigma_E = 0.25$). While our model is not explicitly spatial, when σ_E is high, different groups experience different environmental effects on their mean cell size, simulating the effects of a patchy environment. Increasing the magnitude of these environmental effects on cell size diminishes the difference in heritability between groups and cells, but mean group-level heritability is still greater than cell-level heritability for all parameter combinations (Figure 2.1b).

The volume of the cellular group, which is simply the sum of the cell volumes within it, represents the simplest function mapping cellular to multicellular trait values. We now consider more complicated nonlinear functions relating cellular to multicellular trait values, some of which have biological relevance to the evolution of multicellularity. The first nonlinear group−level trait we consider is its diameter. Large size is thought to provide a key benefit to nascent multicellular groups when they become too big to be consumed by gape−limited predators [89, 89, 73]. For a group that is approximately spherical, the trait that actually determines the likelihood of being eaten is diameter, which is therefore an important component of fitness. For geometric simplicity, we assume that the cells within the group are pressed tightly together into a sphere. group volume (Figure 2.2a) and diameter (Figure 2.2b) exhibit similar dynamics, with group-level heritability always exceeding cell-level heritability and being maximized under conditions of strong cell size stochasticity (high σ_S) and no environmental heterogeneity (low σ_E).

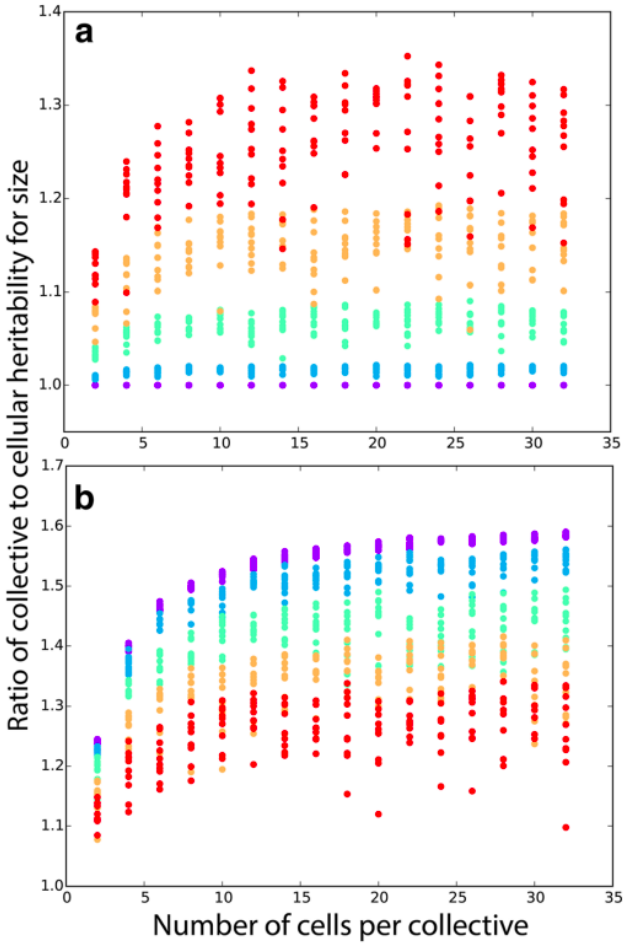

Figure 2.1: Group−level heritability of size is greater than cell level heritability for size. In **a**, we hold the effect of the environment fixed (standard deviation $\sigma_E = 0.25$) and vary the degree of developmental instability for cell size σ_S : 10^{-4} (purple), 0.0625 (blue), 0.125 (green),0.1875 (yellow), 0.25 (red). In the absence of developmental instability for size, group and cell−level heritabilities are identical. Greater developmental instability increases relative group−level heritability. **b** Here, we hold developmental instability fixed at $\sigma_S = 0.25$, an vary between group environmental effects on cell size from σ_E^2 : 10^{-4} (purple) to 0.25 (red). When developmental instability is nonzero, larger groups improve group level heritability. We ran ten replicates of each parameter combination and simulated populations for nine generations of growth.

Next, we consider swimming speed as a function of cell radius. We based this simulation on the hydrodynamics model of volvocine green algae derived by Solari et al[76]. For simplicity, we modeled 32-celled, undifferentiated groups (GS colonies in [76]), which would be similar to extant algae in the genus Eudorina. In this model, the swimming force of cells is independent of cell size, so, as cells get larger, the group will become heavier (more negatively buoyant) without a corresponding increase in total swimming force, and therefore, its upward swimming speed will decrease. Thus, upward swimming speed is a monotonically declining function of cell radius (Figure 2.2c inset), unlike the functions for volume and diameter (Figure 2.2a, b insets), both of which are monotonically increasing. Nevertheless, the general behavior of heritability is very similar to the previous ones, and for a wide range of parameter values, the group-level trait has a higher heritability than the cell−level trait (Figure 2.2c)

Next, we consider a function describing a group's survival rate in the presence of a predator that can only consume groups below a certain size. We calculated the survival rate as a logistic function of the group's radius, effectively assuming that predation efficiency drops off quickly when groups reach a threshold size (Figure 2.2d inset). As with the previous functions (Figure 2.2a–c), group-level heritability is greater than cell-level heritability for much of the trait space and is maximized under conditions of high cellular stochasticity (σ_S) and low environmental heterogeneity (σ_E; Figure 2.2d).

Finally, we consider the case in which the simplifying assumption of constant cell number does not hold. Instead, the number of cells per group at maturation fluctuates around the genetic mean $\overline{N}$. In this case, each group reproduces two new groups, but the number of cells in each new group before they reproduce is a random variable drawn from a normal distribution with mean $\overline{N}$ and coefficient of variation CV_N (the coefficient of variation for a normal distribution is the ratio of standard deviation to the mean). We chose to represent variation in the number of cells per group as CV_N instead of standard deviation so that the scale of variation would not change with the size of the groups.

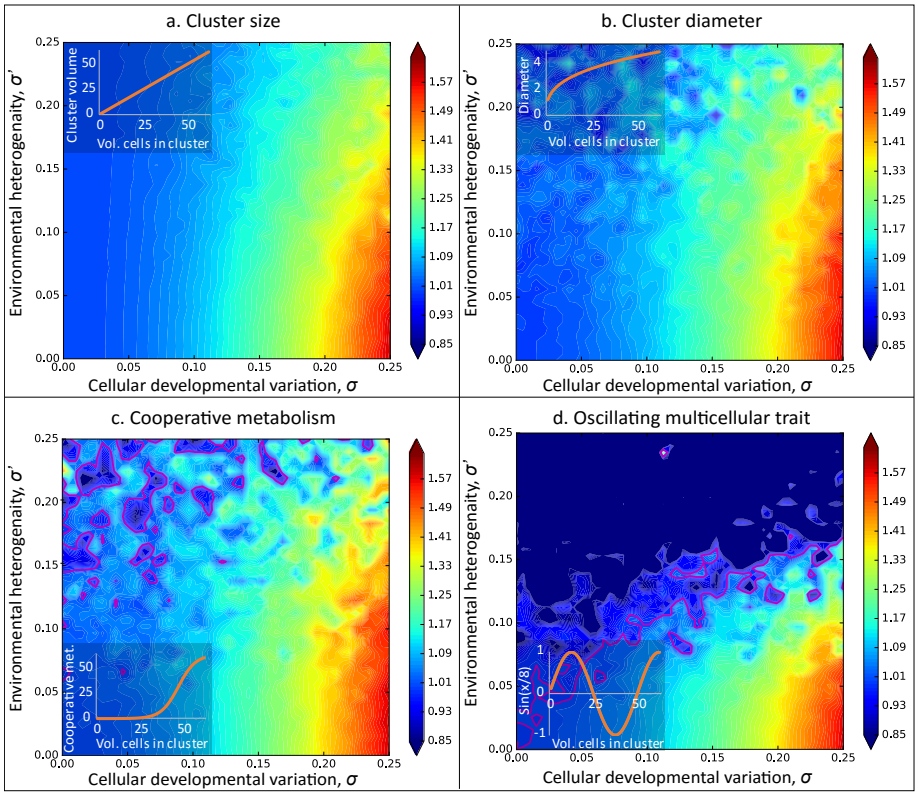

Figure 2.2: Relative heritability of various group−level traits to cell−level heritability for different mapping functions. Here, we examine the heritability of four multicellular traits that depend on the size of their constituent cells, relative to cellular heritability for size. The relationship between the size of the cells within groups and the multicellular trait are shown as insets. We consider three biologically significant traits with different functions mapping the size of cells within the group onto group phenotype. The heritability of group size (**a**) and diameter (**b**) is always higher than cell−level heritability for size and is maximized when cellular developmental noise is greatest and among−group environmental effects are smallest (lower right corner). We modeled swimming speed (**c**) based on the model of Solari et al[76]. for volvocine green algae. We also considered survival rate under predation as a logistic function of radius (**d**). Like **a** and **b**, group−level heritability is highest relative to cell−level heritability when environmental heterogeneity is minimal. Pink contours denote relative heritability of 1. In these simulations, we consider 32 cell groups grown for seven generations. The colormap denotes group−level heritability divided by cell−level heritability for size across 1024 σ_S, σ_E combinations.

Unlike the developmental and the environmental variation, variation in cell number affects the heritability of groups-level traits but not the heritability of cells-level traits. Therefore, we expected that increasing CV_N would decrease the ratio of group-level to cell-level heritability. For the simplest case, we consider the size of the groups and its relation to

the size of the cells in the group and test the effect of each factor on the relative heritability comparing the groups to the cells. According to equation 5, when developmental and environmental noise are fixed, groups demonstrate higher heritability compared to cells for low values of CV_N but lower heritability compared to cells for higher values of CV_N. To test this effect, we calculated the relative heritability of size (volume) for groups and cells across 1024 combinations of σ_S^2 and CV_N ranging from 0 to 0.25. The simulation shows that the CV_N has a strong effect on group-level heritability (Figure 2.3). The purple line in Figure 2.3 represents the inflation line and it is a line with constant slope and intercept zero. This result is in agreement with the theoretical inflation line (black dash line). By equating the r.h.s of Equation 2.30 to 1, we have:

$$CV_N = \frac{\sigma_S^2}{\sqrt{\sigma_E^2 + \sigma_G^2 + \overline{G}^2}} \tag{2.31}$$

2.5 Discussion

When unicellular organisms form a colony, traits inevitably come into being that previously did not exist. Regardless of the nature of that trait there should be a relation between this newly emerged traits and traits of individuals that formed the group. This relation can be as simple as sum of lower-level traits like size of a group is the aggregate of the size of the individuals in the groups or it could be very complicated and involving feedback loops and non-analytical functions. According to the breeder's equation these new traits' response to selection depends on their heritability. Here we showed that one can calculate that heritability if they know two things: the heritability of underlying cell-level traits and the function that maps the cell-level traits to the group-level trait. Estimating the former is straightforward; if we can define the latter, we can in principle predict the efficacy of selection on the new trait.

We derived an analytical formula for the simplest for a clonal group where the group-

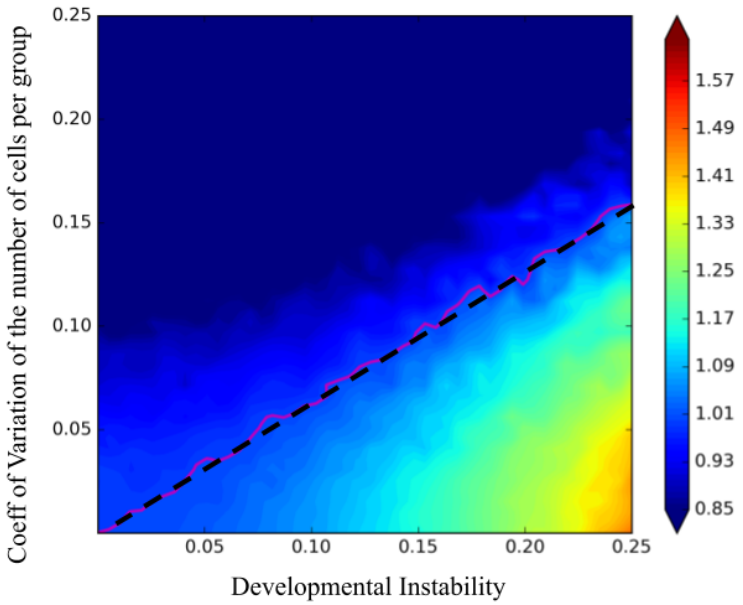

Figure 2.3: Relative heritability of group size to cell size when the number of cells per group varies. When the coefficient of variation for cell number per group (CV_N) is low, group-level heritability is always higher than cell-level heritability, but this advantage is undercut by increased variation in cell number. The ratio of group to cell-level heritability is maximized when developmental instability in cell size (σ_S^2) is large and variation in the number of cells per group is low. The purple contour denotes a ratio of group-level to cell-level heritability of 1 (inflation line). In these simulations, we consider group with a genetic mean of 32 cells grown for 7 generations. The colormap denotes group-level heritability divided by cell-level heritability for size across 1024 σ_S^2, CV_N combinations. The dash line is the theoretical inflation line.

level trait is the sum of underlying cell-level traits (like size). When cell number is constant and the group-level trait value is a linear function of the cell-level trait values, the organismal heritability turns out to be a simple function of the cell-level heritability. In contrast to claims that cell-level heritability is always higher than group-level heritability [46] we have shown that for a wide range of analytical functions the group-level heritability is higher than the corresponding cell-level trait heritability.

This analytical result is a step toward understanding the relationship between heritabilities at two adjacent hierarchical levels, but the assumptions of constant particle number and linear function are restrictive. The simulation model shows that the results are somewhat dependent on the function relating the trait values at the two levels. However, these func-

tions were chosen to be diverse, and the behavior of the relative heritabilities is nevertheless qualitatively similar, increasing with cellular developmental variation (σ_S), decreasing with environmental heterogeneity (σ_E), and exceeding 1 for most of the parameter space.

Although, we have not (and cannot) comprehensively test the universe of all possible functions mapping group-level traits to particle-level traits, we have explored a small number of biologically relevant functions, ranging from extremely simple (volume) to somewhat more complex (swimming speed, survival under predation). We do not claim that the high heritabilities estimated for these group-level traits would apply to all such traits, and a full accounting of possible functions is beyond the scope of this study. Rather, we have shown that for at least some such functions, the resulting group-level traits can have higher heritability than their cell-level trait counterpart, and thus be altered by selection, early in an evolutionary transition in individuality.

All four of the group-level traits in the simulation models are potentially biologically relevant. Volume and diameter are both aspects of size, which can be an important component of fitness both in evolutionary transitions in individuality [76] and in life history evolution [57]. Swimming speed is a measure of motility, which has selective consequences for a wide range of organisms, including many animals and microbes. For planktonic organisms, a positive upward swimming speed provides active control of depth, allowing some control over light intensity (for autotrophs) and prey abundance (for heterotrophs). Survival under predation obviously has important fitness implications for many organisms, and both theoretical and experimental evidence implicate predation as a possible selective pressure driving the evolution of multicellularity. Kirk, for example, suggests that a "predation threshold" above which algae are safe from many filter feeders may have driven the evolution of multicellularity in the volvocine algae [90]. Microbial evolution experiments in the algae *Chlorella* and *Chlamydomonas* have shown that predation can drive the evolution of undifferentiated multicellular clusters [73, 91, 92, 91].

In our simulations, we examined the effects of three independent sources of phenotypic

variation affecting the relative heritability of particle and group-level traits. Stochastic variation in cell size around the clone's genetic mean reduces the absolute heritability of cells and groups by introducing non-heritable phenotypic variation. By averaging across multiple cells, however, groups reduce the effects of this phenotypic variation, providing them with a relative heritability advantage over cells.

We also considered the effect of environmental heterogeneity in which all of the cells within a groups are affected in the same manner (σ_E). Groups are disproportionately affected: each group is assessed a different size modifier, but all of the cells within these groups are affected in the same manner. As a result, groups experience n-fold more stochastic events (where n is the number of cells per group), which reduces their heritability relative to cells. The influence of these sources of variation is evident in the contour plots of Figure 2.2: the relative heritability of groups to cells is maximized when the cellular stochastic variation is high and environmental heterogeneity low (lower right corner of the plots).

Finally, we considered variation in the number of particles per group. Such variation substantially reduces the heritability of a group-level trait. Even with reasonably large variation in group size, though, the group-level trait retains most of the heritability of the particle-level trait on which it is based (for example, 55% at a CV_N in particle number of 0.25).

A large number of previous studies have addressed heritability in the context of multilevel or group selection. Heritability above the individual level has been called group heritability (e.g., [93]), populational heritability (e.g., [94]), community heritability (e.g., [95]), and heritability of the family mean [88]. These prior treatments differ from ours in one or more of the following respects: they are concerned with the evolution of individual-level traits rather than group level traits (particle- rather than group-level in our terminology), are based on MLS1 rather than MLS2 models, and are focused on narrow-sense rather than broad-sense heritability. Furthermore, few previous studies have addressed these questions

in the context of the major transitions. Without attempting a comprehensive review, we summarize several such studies, and important differences from our own, below.

Queller [93] presents a useful reformulation of the Price equation for selection at two levels:

$$\Delta\overline{X} = S_b h_b^2 + S_w h_w^2 \tag{2.32}$$

in which $\Delta\overline{X}$ is the change in average trait value, S_b and S_w are the selection differentials between groups and within groups, respectively, and h_b^2 and h_w^2 are the heritabilities of the group-level and individual-level traits, respectively. This formulation partitions the response to selection on a particle-level trait into withinand among-group change, but the focus is still on particle-level traits. Our focus is on the evolution of group-level traits. In the terminology of Damuth and Heisler [19], our focus is on MLS2, while Queller's is on MLS1. In addition, Queller makes no attempt to derive the relationship between group-level heritability and cell-level heritability.

Michod and Roze [44] have previously modeled the relationship between particle-evel and group-level heritability of fitness during a major transition. However, as Okasha [86] points out, the heritability of fitness only ensures that mean population fitness will increase over time. For selection to result in directional phenotypic change, it is phenotypes that must be heritable. Furthermore, Michod and Roze focused on within-organism genetic change. Our models assume that such change is negligible, as is likely to be true early in a transition, when groups (e.g., nascent multicellular organisms) presumably include a small number of clonally replicating particles (e.g., cells).

Okasha [95] considers heritability in MLS1 (which he refers to as group selection 2) and MLS2 (his group selection 1) but does not attempt to derive a relationship between heritabilities at two levels. Knowing the ratio of heritabilities is necessary, though not

sufficient, to predict the outcome of opposing selection at two levels and so has important implications for group-level traits that arise from cooperation among cells. The presumed higher heritability of the cell-level traits has been seen as a problem for the evolution of cooperation that benefits the group []. Our results show that this problem does not always exist, though we would need to know not only the relative heritabilities but also the relative strengths of selection to predict the outcome of opposing selection at two adjacent levels.

Several previous papers have shown that group-level heritability (group-level heritability in our terminology) exists and can be substantial. Slatkin [], for example, showed that one measure of group-level heritability, fraction of total variance between lines, is substantial both in an analytical model and in the Tribolium experiments of Wade and McCauley [40][]. Under some conditions, the between-line variance of a linear trait such as the one we consider in our analytical model exceeds the within-line variance.

Bijma et al. [41, 42] and Wade et al. [43] showed that variance in the total breeding value of a population can be increased, even to the point of exceeding phenotypic variance, by interactions among individuals. Our model does not consider (or require) interactions among individuals. Further, their model and empirical example are exclusively concerned with individual-level traits (particle-level traits in our terminology), for example, survival days in chickens. They do not estimate group heritability as such and judge that "it is unclear how this parameter should be defined or estimated."

Goodnight [96] addresses the effect of environmental variance at two scales on the responses to individual and group selection in *Arabidopsis thaliana*. Although Goodnight's study focused on an individual-level trait (leaf area, thus an MLS1 scenario) of an obligately sexual organism (thus narrow-sense heritability), our results (shown in Fig. 3) showed analogous effects. In both cases, environmental variation at a fine scale (analogous to our σ_S) increased the efficacy of group selection relative to individual selection, while environmental variation among demes (analogous to our σ_E) had the opposite effect. Wade [97] examines a similar case from a theoretical perspective and finds that increased relative

efficacy of group selection results from environmental variation among particles decreasing particle-level heritability.

Goodnight [87] considers the ratio of group-level heritability to individual-level heritability (in the narrow sense) using contextual analysis. Although this paper does not provide a formula to calculate this ratio, its inequality 5 sets a minimum bound (with the assumption that selection at the two levels is in opposition). As in our analyses, Goodnight shows that group-level heritability can exceed individual-level heritability in some circumstances.

Several simplifying assumptions underlie our models, most importantly the genetic identity of particles within groups. This condition only applies to a subset of the major transitions. Queller recognized two subcategories within Maynard Smith and Szathmáry's [4] list of transitions, which he called "egalitarian" and "fraternal" transitions [46]. Briefly, egalitarian transitions involve particles that may be genetically distinct, or even from different species, such as the alliance of a bacterium with an Archaean that gave rise to the eukaryotic cell. Fraternal transitions are those in which the particles are genetically similar or identical, such as the origins of eusociality and of most multicellular lineages.

Because of our assumptions of asexual reproduction and genetic identity among particles, we cannot generalize our results to all types of major transitions. Egalitarian transitions will not normally meet this criterion. A possible exception is aggregative multicellularity, as seen in cellular slime molds and myxobacteria, when assortment is so high that fruiting bodies are genetically uniform. This is probably uncommon [98], but it does happen [99]. Transitions in which reproduction of particles is obligately sexual, such as the origins of eusociality, also violate this assumption.

A better fit for our models is clonal multicellularity, which is probably the most common type of major transition. An incomplete list of independent origins of clonal multicellularity includes animals; streptophytes; chytrid, ascomycete, and basidiomycete fungi; florideophyte and bangiophyte red algae; brown algae; peritrich ciliates; ulvophyte green

algae; several clades of chlorophyte green algae; and filamentous cyanobacteria [50–53]. In most cases, the early stages in these transitions probably violated the assumption of uniform particle number per group, but our simulations show that our main results are robust to reasonable violations of this assumption.

One example that does approximate all of our assumptions is that of the volvocine green algae, an important model system for understanding the evolution of multicellularity. Volvocine algae undergo clonal reproduction only occasionally punctuated by sex, are small enough that within-group mutation probably has negligible phenotypic effects, and have cell numbers that are under tight genetic control.

2.6 Conclusion

A great deal of work has gone into understanding the selective pressures that may have driven major evolutionary transitions. However, heritability is just as important as the strength of selection in predicting evolutionary outcomes. We have shown that, given some simplifying assumptions, heritability of group-level traits comes "for free;" that is, it emerges as an inevitable consequence of group formation. Qualitatively, this result holds across a wide range of parameters and for a diverse sample of biologically relevant traits. group-level heritability is maximized (relative to particle-level heritability) when phenotypic variation among particles is high and when environmental heterogeneity and variation in group size are low. Understanding the emergence of trait heritability at higher levels is necessary to model any process involving multilevel selection, so our results are relevant to a variety of other problems.

CHAPTER 3
NASCENT MULTICELLULAR ORGANISMS POSSESS NOVEL TRAITS SUBJECT TO ADAPTATIVE EVOLUTION

3.1 Summary

The existence of multicellular organisms is an outcome of evolutionary processes operating on populations of unicellular organisms [100]. Dozens of unicellular lineages from all three domains of life have independently evolved multicellularity [11, 8], leading in each case to the emergence of multicellular-level traits that did not exist before the transition [101]. For these traits to evolve through natural selection, some of their phenotypic variation must be due to genetic variation, i.e. they must have non-zero heritability [102]. The necessity of heritability for adaptive evolution has been seen as a problem for evolutionary transitions to multicellular life [46, 103, 104, 105, 42, 85]: a reorganization subsequent to the origin of multicellularity is presumed necessary to explain the emergence of heritability at the multicellular level. Here we show that an ecologically relevant, emergent trait in a nascent multicellular organism has higher heritability across a range of conditions than the unicellular-level trait on which it is based. These results suggest that nascent multicellular organisms are Darwinian individuals capable of adaptive evolution [20], possessing heritable variation in traits that are likely to affect fitness [40]. Thus the formation of multicellular structures as such generates novel traits that are subject to evolution by natural selection.

3.2 Introduction

Life on Earth has been, predominantly unicellular. At various times, particular unicellular populations have evolved multicellular structures, bodies, or thalli. In some cases, these

now multicellular populations massively diversified, giving rise to the major radiations of multicellular life: plants, animals, fungi, and various groups of seaweeds. In other cases, they left few descendants, or none.

Our focus here is on the first steps in the transition to multicellular life: the evolution of multicellularity *per se* and the early evolution of nascent multicellular populations. A necessary early step in the transition from unicellular to multicellular life is the evolution of a mechanism of cell to cell adhesion [106, 107, 70]. In some cases, the population may have already expressed a multicellular phenotype plastically, as is known to happen in some algae and choanoflagellates, and the transition in question is from facultative to obligate multicellularity. In other cases, the multicellular phenotype may be entirely novel, resulting in a transition from a purely unicellular population to an obligately multicellular one. Both processes have been observed in microbial evolution experiments in which a selective pressure was applied to unicellular laboratory populations [32, 33, 108, 73].

The resulting populations consist of clusters of related cells, or colonies. These colonies have traits that did not exist in the unicellular population, for example colony diameter, colony shape, and number of cells per colony. These traits are potentially subject to natural selection. How effective such selection will be in changing the trait value depends on the heritability of the trait.

The breeder's equation of quantitative genetics shows that a trait's response to selection (R) is the product of the selective coefficient (S) and the heritability of the trait under selection (h^2): $R = h^2 S$. Heritability in this formulation is the narrow-sense heritability, the proportion of phenotypic variation explained by additive genetic variation, and this formulation predicts the response to a given strength of selection in an obligately sexual population [41]. For simplicity, we consider asexual populations, for which the relevant measure of heritability is broad-sense heritability, H^2, the proportion of phenotypic variation explained by all genetic variation [41]. The response to selection in an asexual population, then, is $R = H^2 S$ [41].

Thus we could, in principle, predict the response of a nascent multicellular population to a given strength of selection if we could predict H^2. Doing so is not trivial, though. Heritability is not an inherent property of organisms or species. Rather, it is a population-level statistical measure that applies only to a particular trait in a particular population at a particular time.

Our approach to estimating the heritability of traits in a nascent multicellular population relies on the relationship of colony-level traits to cell-level traits. All colony-level traits can, in principle, be expressed as functions of cell-level traits, though in many cases these functions will be so complex as to be intractable [102]. They may, for example, include cell-cell communication, complex feedbacks, and interactions with the environment, such that cell-level phenotype is only one of several arguments. Our focus is on an emergent colony-level trait the value of which is a function of a single cell-level trait.

In multicellular 'snowflake' yeast, colony size (number of cells per cluster) is a simple function of cell aspect ratio. Through a combination of analytical models, simulations, and experimental manipulations, we show that heritability of colony size exceeds that of cell aspect ratio across a wide range of conditions.

3.3 Results

3.3.1 Analytical model.

Prior work examining experimentally-evolved multicelluar 'snowflake' yeast have shown that there is a linear relationship between the size to which clusters grow before they divide and cellular aspect ratio [37, 109]. Specifically, more elongate cells increase the size to which clusters can grow by reducing cellular crowing within the cluster interior, slowing the rate of stress accumulation that ultimately causes the group to fracture. Using this relationship as a starting point, we developed a theoretical model for describing the relationship between the heritability of cellular aspect ratio, which is directly affected by mutations, and that of number of cells at division, which is an emergent property of aspect ratio.

First, we calculate broad sense heritability as the correlation coefficient between parental phenotype α (cellular aspect ratio) and offspring phenotype α' for cellular aspect ratio, partitioning the phenotype into its key components [110]:

$$H^2 \equiv Corr(\alpha, \alpha') = \frac{E[(\alpha - \overline{\alpha})(\alpha' - \overline{\alpha'})]}{Var(\alpha)} \tag{3.1}$$

Where:

$$\alpha = G + E + S \quad \alpha' = G + E' + S' \tag{3.2}$$

In this equation G is the genetic mean of aspect ratio, E are environmental effects, and S is developmental noise. Here we assume that S is a white noise, with mean zero and variance (σ_S^2).

If there is no temporal correlation except for the same genotype between offspring and parents, then $\overline{\alpha} = \overline{\alpha'}$ and we can rewrite the numerator as:

$$E[(\alpha - \overline{\alpha})(\alpha' - \overline{\alpha})] = E[\alpha\alpha'] - \overline{\alpha}^2 = \sigma_G^2 \tag{3.3}$$

So the heritability of aspect ratio is equal to:

$$H_\alpha^2 = \frac{\sigma_G^2}{\sigma_G^2 + \sigma_S^2 + \sigma_E^2} \tag{3.4}$$

If N is a linear function of the mean of cellular aspect ratio, then N will also a linear function of G, because all the cells in a clonal cluster will have the same genetic mean value for aspect ratio. But because developmental noise S is random and different for each cell, its expected value for all the cells in a cluster is zero. We also consider developmental noise at the cluster level, ϵ, which accounts for internally-generated (i.e., not environmental) vari-

ation in cluster phenotype. So for N we have: $N = a(G+E+\epsilon), \quad \overline{N} = a\overline{G}, \quad Var(N) = a^2(\sigma_G^2 + \sigma_E^2 + \sigma_\epsilon^2)$. Given these equations, the heritability of the number of cells at division in the simplest form is equal to:

$$H_N^2 = \frac{\sigma_G^2}{\sigma_\epsilon^2 + \sigma_E^2 + \sigma_G^2} \tag{3.5}$$

so the ratio of the heritability of the number of cells per cluster and cell size is equal to:

$$\frac{H_N^2}{H_\alpha^2} = \frac{\sigma_S^2 + \sigma_E^2 + \sigma_G^2}{\sigma_\epsilon^2 + \sigma_E^2 + \sigma_G^2} \tag{3.6}$$

Thus, in principle, an emergent multicellular trait (cluster size at division) can be more heritable than the underlying cellular trait, as long as $\sigma_\epsilon^2 > \sigma_S^2$ (Figure 3.1).

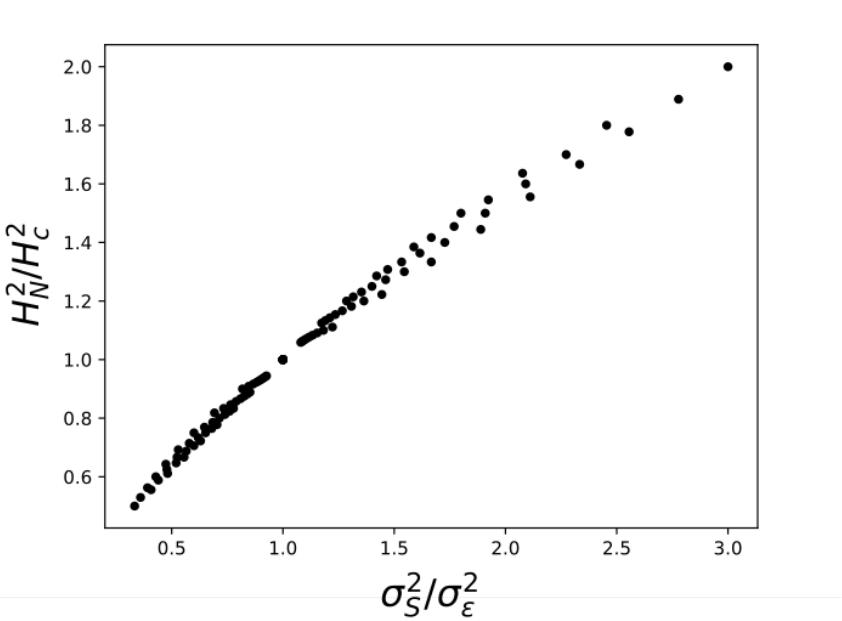

Figure 3.1: Heritability of number of cells at fracture (H_N^2) is higher than that of cellular aspect ratio (H_c^2) whenever cellular developmental noise (σ_S^2)is higher than collective level developmental noise (σ_ϵ^2).

3.3.2 Experimental setup

We experimentally examined the relative heritability of mutations affecting both a cellular trait (cellular aspect ratio) and an emergent multicellular trait (number of cells in the cluster at division) using the snowflake yeast model system [32]. We deleted three cell cycle regulatory genes (*AKR1, ARP8, CLB2*, generating a range of mutants that varied in their mean cellular aspect ratio. In each case, we generated otherwise isogenic unicellular and multicellular versions of these strains by leaving *ACE2* functional, or deleting the *ACE2* open reading frame, respectively [34] (Figure 3.1a).

In both unicellular and multicellular isolates, we measured the cellular aspect ratio of cells that were only a single division old, ensuring that we did not introduce phenotypic variation due to varying cell age. Whether or not *ACE2* was active did not significantly affect cellular aspect ratio in any of our genotypes (Figure 3.2b, $t = -0.96$, $p = 0.33$ for wild type, $t = 1.12$, $p = 0.26$ for Δ*ARP8*, $t = -.69$, $p = 0.49$ for Δ*AKR1*, $t = -0.29$, $p = 0.76$ for Δ*CLB2*; two-tail t-tests).

To measure the number of cells at fracture we first measured the packing fraction (ϕ) of each genotype and their size at fracture ($V_c l$) using time-lapse microscopy. We also measured the volume of cells ($v_c e$)for each genotype and using the formula $\phi = N v_c e / V_c l$ calculated number of cells at fracture (Figure 3.3a). These results are in agreement with the computer simulation (Figure 3.3d) and previous studies [109]. This agreement suggests that our genetic manipulation only changes one phenotype that is relevant for the number of cells at fracture. It may very well cause other phenotypic changes at the cell level but they don't have any noticeable effect on the cluster-level phenotype that we are interested in.

3.3.3 Simulation population

A trait's heritability is a statistical feature of a population, not an inherent property of an organism, and is highly sensitive to population composition ([43]). We used a variance

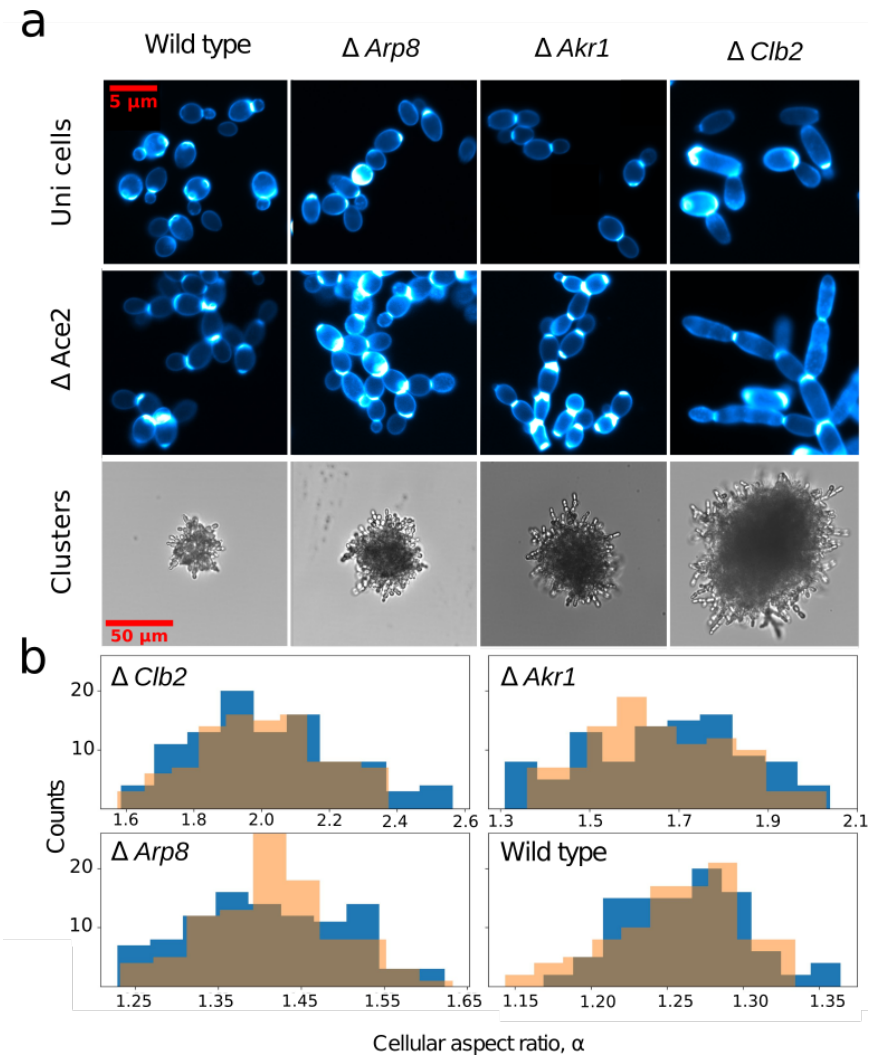

Figure 3.2: Yeast genotypes used in this study. **a**) yeast genotypes in combination with functional (top row) or nonfunctional (second row) ACE2. Bottom row shows bright−field images of ACE2 knockouts. **b**) distribution of cell aspect ratio for each genotype with ACE2 (yellow bars) and without ACE2 (blue bars).

partitioning approach to calculate the heritability of cellular aspect ratio and group size at division from our experimental data (see supplementary material). Because each genotype has a different genetic mean cellular aspect ratio, heritability depends on the frequency of each genotype in the population (Equation 3.6). For example, at equal frequencies, a population that consists of wild type snowflake yeast and the $\Delta Akr1$ mutant has a lower genetic variation compared to a population of wild type and the $\Delta Clb2$ mutant. Therefore, we measured the heritability of both cellular aspect ratio and cluster size at division

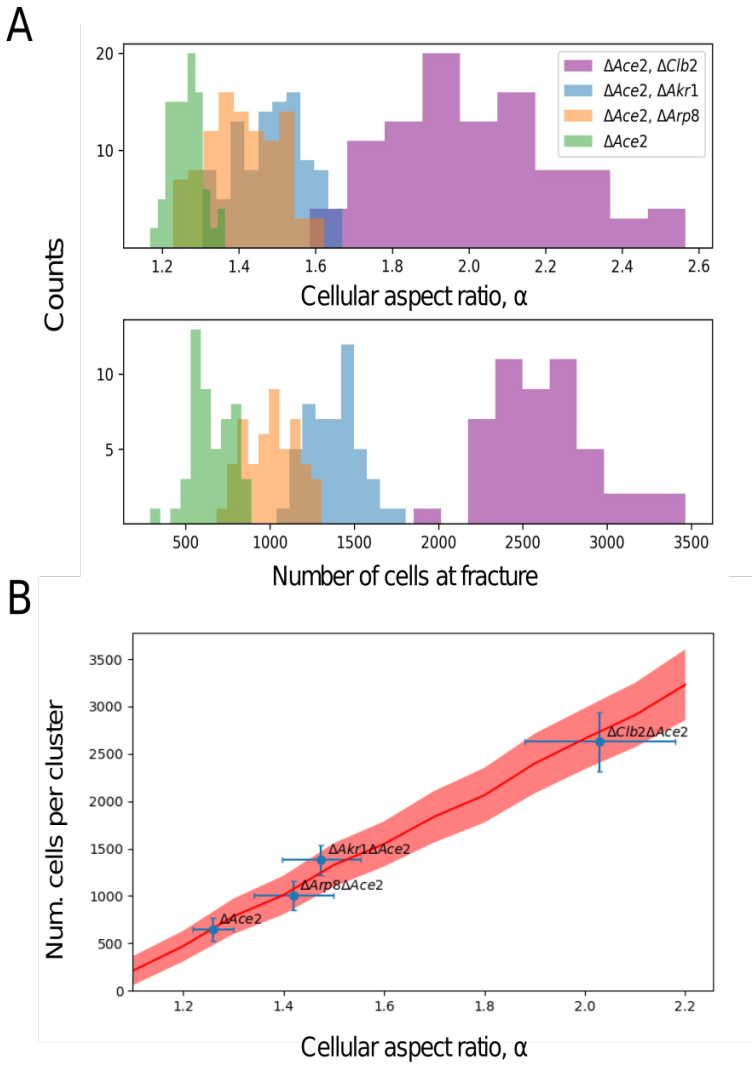

Figure 3.3: A)distribution of cell aspect ratio (top) and number of cells at fracture (bottom) for ACE2 knockout genotypes. B) relationship between cellular aspect ratio and number of cells per cluster in ACE2 knock outs. Empirical measurements (blue dots) are shown with standard deviations. The lines how simulation results with the shaded area representing one standard deviation area around the mean for each value. Experimental results are in good agreement with simulations, and both show strong linear relation between the two parameters ($r^2 = 0.99$, $y = 2718.05 * x - 2780.83$ for simulation and $r^2 = 0.96$, $y = 2549.83 * x - 2526.60$ for experimental results.

by simulating all possible hypothetical populations by bootstrapping (up to an N = 1000) without replacement from our experimental data (Figure 3). To avoid uniform populations first we fixed one genotype's frequency f_1 at 5%. Then we looked at all different possible populations composed of three remaining genotypes with the condition that sum of their

frequencies is equal to 95% ($f_2 + f_3 + f_4 = 95\%$). In nearly all possible populations, the multicellular trait, cell number at division, is more heritable than the underlying cell-level trait, cellular aspect ratio, despite the fact that aspect ratio is the only trait being modified via mutation.

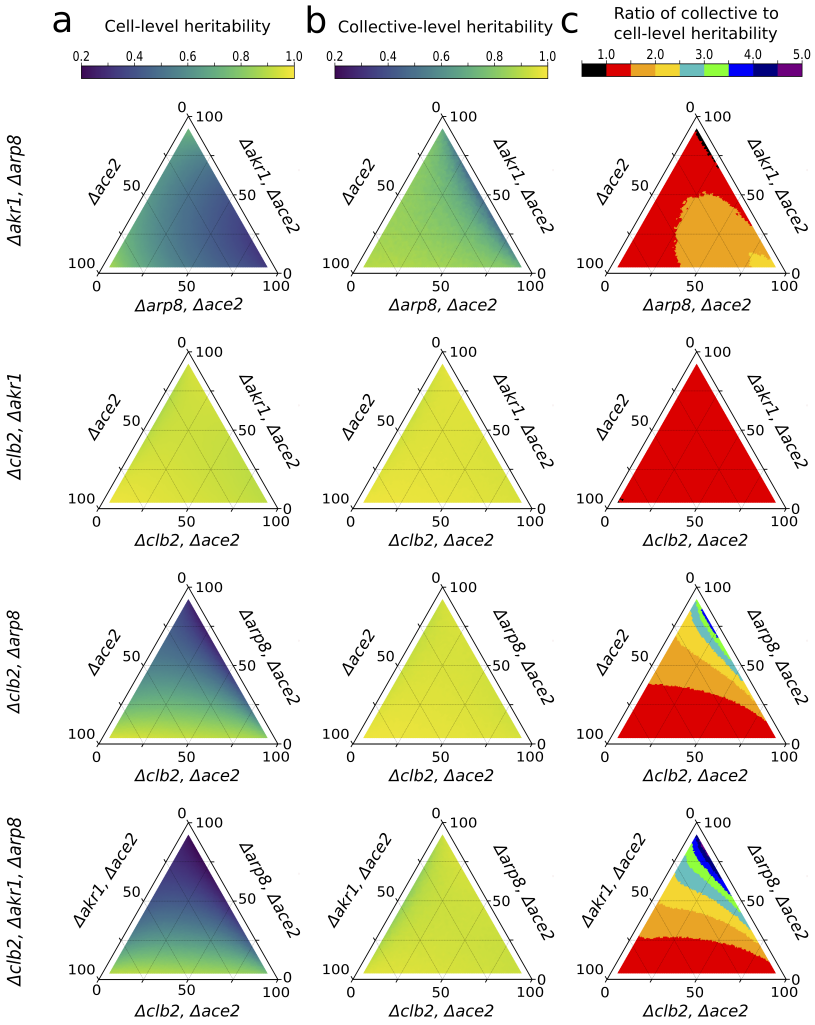

Figure 3.4: Heritability of a colony-level trait exceeds that of the corresponding cell-level trait over a wide range of simulated populations. Each triangle plot represents one type of heritability for a possible 3-way combination of the four genotypes at different frequencies (fourth genotype held constant at 5% in each case). a) Cell-level heritability for all possible 3-way combinations of genotypes. b) Collective-level heritability for all for example possible 3-way combination of genotypes. c) Ratio of two heritabilities for all possible 3-way combinations of genotypes.

Discussion

We have shown that an emergent multicellular trait, group size at division, is a linear function of a cell-level trait, cell aspect ratio, in snowflake yeast. Furthermore, the value of the cell-level trait is independent of whether or not the cell is in a multicellular body. Taken together, this means that the multicellular trait value can be predicted from the cell-level trait value, even before the population has become multicellular.

In agreement with a previous analytical model [102], we have shown that the heritability of the multicellular trait is generally higher than the underlying cellular trait. Although the ratio of the two heritabilities depends on the proportion of each genotype in the population, it is in nearly all cases greater than one. While it might seem surprising that an emergent multicellular trait can be more heritable than a cell-level trait directly encoded for by genes, multicellular groups possess a powerful advantage over isolated cells: the ability to average out stochastic variation in cellular phenotype.

Although it is routinely estimated and widely recognized as useful in predicting responses to selection in clonally reproducing multicellular organisms [47, 48, 49, 50, 51, 52, 53, 54, 55], H^2 is typically assumed to be 1 in asexually reproducing microbes [111, 112, 113, 114, 115, 116]. This assumption is so widespread that the concept of heritability is rarely addressed in discussions of microbial evolution; rather, the response to selection is simply assumed equal to the strength of selection ($R = S$). However, H^2 is **never** 1 for a continuously varying trait in a real population. Because broad-sense heritability is defined as the ratio of genetic variance to total phenotypic variance, which includes genetic variance, the only way for H^2 to equal 1 is for there to be zero non-genetic variance.

In reality, phenotypic heterogeneity is widespread even among genetically identical individuals reared in carefully controlled environments. This phenomenon is well documented among microbes, but it is also true for diverse plants, fungi and animals [117] and for traits as diverse as gene expression [118, 119], antibiotic [120] and formaldehyde

[121] resistance, motility [122] and phototaxis [123], cell number [124], predator evasion behavior [125], and number of sense organs [126].

3.4 Conclusion

While the emergence of multicellular heredity is widely regarded as a major challenge in this major evolutionary transition [95, 82, 127], we show that multicellular heredity may in fact arise "for free", without any additional evolutionary change required. This has several implications. First, it means that, immediately after formation, simple multicellular groups like snowflake yeast will be capable of multicellular adaptation, assuming that selection acts on the emergent multicellular traits. Second, high multicellluar heritability facilitates multicellular responses to selection. This may be especially important in cases where selection on cell-level fitness and multicellular fitness are acting in opposite directions. For example, recent work [80] has shown that mutations in *ARP5* and *GIN4* arise during snowflake yeast experimental evolution, increasing group size but decreasing cellular growth rate by 6.2 and 10.2%, respectively. Over time, the accumulation of mutations like these which decrease cell-level fitness may act as an evolutionary 'ratchet', limiting opportunities for evolutionary reversion to unicellularity and thereby entrenching the lineage in a multicellular state [42]. These results provide mechanistic context for the emerging context that the transition to multicellularity is less constrained than previously thought [44, 46].

CHAPTER 4

DE NOVO EVOLUTION OF MACROSCOPIC MULTICELLULARITY

4.1 Summary

The evolution of large size is fundamentally important for multicellularity, creating novel ecological opportunities and driving the origin of increased organismal complexity. Yet little is known about how readily large size evolves, particularly in nascent multicellular organisms that lack genetically-regulated multicellular development. Here we examine the interplay between biological, biophysical, and environmental drivers of macroscopic multicellularity using long-term experimental evolution. Over 600 daily transfers (3,000 generations), multicellular snowflake yeast evolved macroscopic size, becoming more than 19,000 times larger while still remaining clonal. This happened through sustained biophysical adaptation, evolving increasingly elongate cells that initially reduced the strain of cellular packing, then facilitated branch entanglement so that fracture would require breaking many cellular bonds. As a result, individual multicellular yeast became over a million times more biophysically tough. 4/5 replicate populations show evidence of directional selection, with mutations becoming significantly enriched in genes affecting the cell cycle and budding processes. Macroscopic size only evolved in a treatment incapable of aerobic metabolism, demonstrating how limiting oxygen can constrain the evolution of larger size. Taken together, this work shows how selection acting on the emergent properties of simple multicellular groups can drive sustained biophysical adaptation, an early step in the evolution of increasingly complex multicellular organisms.

4.2 Introduction

Complex multicellularity has independently evolved in five eukaryotic lineages (animals, plants, fungi, red algae and brown algae), increasing organismal size by up to multiple orders of magnitude [8, 128, 129]. Size plays a fundamental role in the evolution of multicellularity, allowing organisms to explore novel ecological niches [12], affords protection from the external environment [74, 130], and underlies the evolution of cellular differentiation [56, 57, 77, 131, 132]. The evolution of macroscopic size has been hypothesized to be a key driver of increased organismal complexity, creating a selective incentive to solve challenges of nutrient and oxygen transportation that are otherwise inescapable consequences of diffusion limitations [8, 58]. However, little is known about how simple clusters of cells evolve macroscopic size, and whether selection for size itself can be a driver of multicellular innovation.

The evolution of macroscopic size presents a fundamental challenge to nascent multicellular organisms, requiring the evolution of biophysical solutions to evolutionarily novel stresses that act over previously-unseen multicellular length scales [133, 134, 135, 37]. Indeed, while prior work with yeast and algae have shown that novel multicellularity is relatively easy to evolve *in vitro*, these organisms remain microscopic, typically growing to a maximum size of tens to hundreds of cells [91, 45, 32, 33, 73]. Extant multicellular organisms, which have been under selection for size for hundreds of millions of years, have evolved a number of developmentally-regulated mechanisms for increasing biophysical toughness, or reducing the rate at which stress accumulates [136, 137, 138]. In the absence of genetically-regulated multicellular development, however, we do not know how, or even whether, nascent multicellular organisms can evolve the increased biophysical toughness required for the evolution of macroscopic size.

Here we examine the interplay between biological, biophysical, and environmental drivers of macroscopic multicellularity using long-term experimental evolution. We subject

snowflake yeast, a model of undifferentiated multicellularity, to 600 rounds (3,000 generations) of daily selection for increased size. Because oxygen is thought to have played a key role in the evolution of macroscopic multicellularity, we evolved snowflake yeast with either anaerobic or aerobic metabolism. All five of our anaerobic replicate populations evolved macroscopic size, while all aerobic populations remained microscopic through the duration of the experiment. Macroscopic size evolved through two sequential steps in all five replicate populations. First, snowflake yeast increased the length of their constituent cells, which delays fracture caused by packing-induced strain [37]. Next, they evolved to entangle branches of connected cells such that a single cell-cell separation no longer causes multicellular fracture. Together these adaptations increased the toughness of individual clusters by more than a million-fold, increasing average size by more than 19,000-fold. Sequencing reveals evidence for directional selection, with mutations occurring at especially high frequency in genes affecting the cell cycle (which affects cellular aspect ratio) and budding processes.

4.3 Results

All five populations of anaerobic snowflake yeast evolved macroscopic size, with individual clusters visible to the naked eye (Figure 4.1a). In contrast, snowflake yeast capable of metabolizing oxygen remained relatively small, likely due to competition for limiting O2 [80]. The evolved populations increased their mean cluster radius from 16 μm to 434 μm (Figure 4.1b, $p < 0.0001, F5, 13321 = 2100$, Dunnett's test in one-way ANOVA-stats), a $> 19,000$-fold increase in volume. In cellular terms, this corresponds to an average increase from 100 to $450,000$ cells per cluster. The maximum size of evolved macroscopic snowflake yeast was 1.1 mm, which is comparable to the size of an adult *Drosophila* [139]. In this paper we focus on the anaerobic populations, examining the biophysical and genetic mechanisms underlying the evolution of macroscopic size.

The evolution of macroscopic multicellularity occurred via two distinct phases (Fig-

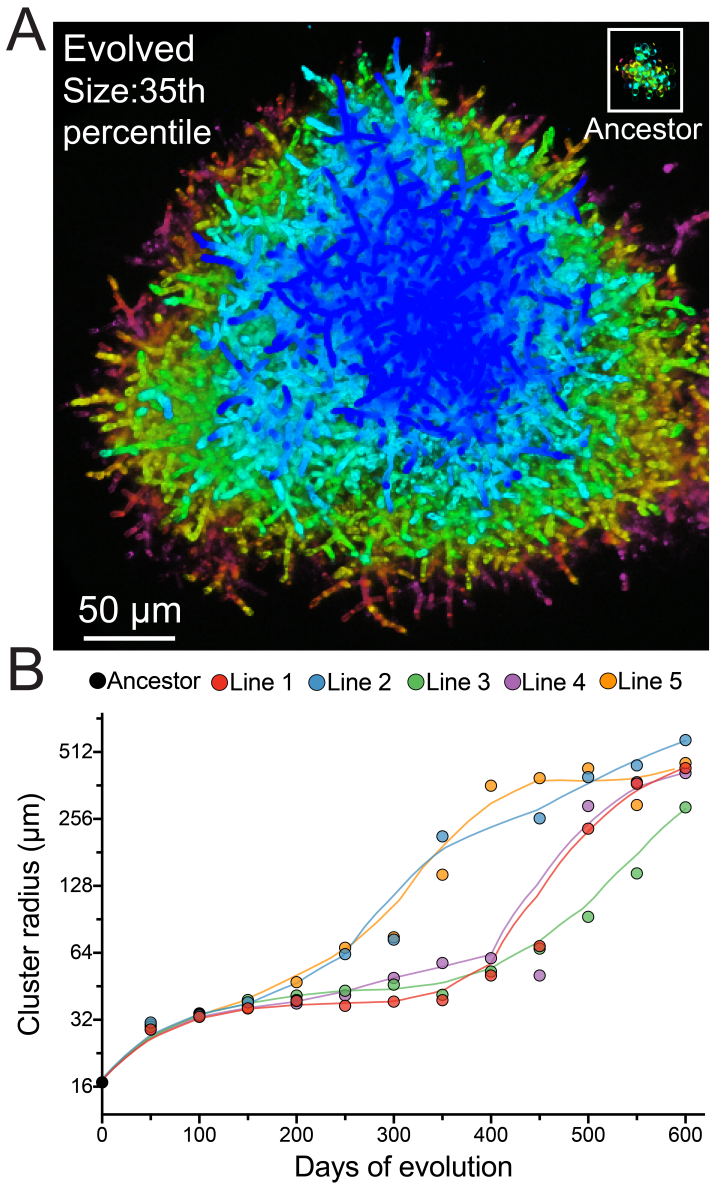

Figure 4.1: Increase in size in experimental evolution of macroscopic multicellularity in 5 independent population of snowflake yeast populations.

ure 4.1B). Over the first 100 days of evolution, we saw remarkable parallelism- all five replicate populations evolved a 2-fold increase in radius (from $16.7\mu m$ to $33.6\mu m$; $p < 0.0001$, $F5, 27005 = 4518$, Tukey's HSD, one-way ANOVA) with no significant difference only minimal among-replicates variance (range in pairwise difference of mean is $0.11 - 0.53\mu m$ stats). At this point, they entered a period of stasis, waiting anywhere from 50 days in population L5 to 300 days in population L1 before rapidly evolving fur-

ther size increases. Such stasis is a classical outcome of the stochastic nature of evolution, and is expected when phenotypic variation is mutationally limited [71]. The wide among-population variance in the duration of evolutionary stasis suggests that the evolution of macroscopic size was more challenging than the initial evolution of increased size, which was highly parallel.

The evolution of macroscopic multicellularity is fundamentally a biophysical challenge. Throughout the experiment, snowflake yeast cells evolve to be more elongate, increasing in average aspect ratio from 1.2 to 2.7 (Figure 4.2ab; $p < 0.0001$, $F5, 1993 = 206.2$, Dunnett's test in one-way ANOVA). Initially, this increases cluster size by reducing cell-cell strain caused by cellular packing [37]. Indeed, prior to the evolution of macroscopic size, cluster size was a roughly linear function of aspect ratio (Figure 4.2b; $R^2 = 0.72, \quad p < 0.0001, \quad Y = 41.12 * X - 27.77$), but this relationship is discontinuous upon the evolution of macroscopic size (Figure 4.2b). Using a 3D biophysical simulation of growth and fracture in the ancestor [109], we find that increasing cellular aspect ratio should decrease the cluster's packing fraction (proportion of the cluster's volume that is occupied by cells; Figure 4.2d), which should increase size by by avoiding cell-cell collisions. Experimentally, we found remarkable concordance with theoretical expectations, but only for early timepoints (Figure 4.2e). Initially, as our yeast evolved more elongated cells, they also formed less densely packed clusters, but around aspect ratio 2 experimental results began to diverge from our simulation. Indeed, the relationship between cellular aspect ratio and cluster packing fraction was reversed, with increasingly elongated cells driving more densely packed clusters (up to a packing fraction of 0.45 in Line 2 at 600 days, Figure 4.2e). While the initial evolution of increased size closely matches our prior biophysical models [37, 109], the divergence we see concordant with the evolution of macroscopic size suggests that snowflake yeast have evolved a novel biophysical mechanism for increased cluster toughness.

To determine if macroscopic yeast are simply aggregates of multiple clusters, we la-

beled a single-strain isolate of macroscopic snowflake yeast taken from Line 2, t600 (henceforth referred to as GOB1413-600) with either GFP or RFP. After 24h of co-culture, all multicellular clusters remained monoclonal, excluding aggregation as a potential mechanism (Figure C.8). We excluded flocculation as a mechanism by demonstrating that GOB1413-600 was insensitive to proteinase K, a protease that cleaves extracellular flocculation proteins that can prevent yeast cells from aggregation [140](see Figure C.10).

To examine the possibility that macroscopic snowflake yeast are growing large while remaining as a single, topologically-connected component, we imaged yeast via Serial Block Face Scanning Electron Microscopy (SBF-SEM). This technique allows us to image the interior of clusters that is impossible to image with light-based microscopy, ultimately allowing us to map their internal architecture with nanometer precision [141]. Surprisingly, individual macroscopic snowflake yeast were composed of multiple disconnected 'branches' of connected cells. For example, the connections to the tan and olive cellular branches shown in Figure 4.3 are severed, but they remain within the interior of the cluster. This is a sharp contrast with the ancestral growth form, in which clusters form a single connected component. Within macroscopic clusters, separate branches contact, intercalate, and even wrap around each other (Figure 4.3a). As these clusters are densely packed, moving one component would require moving many other components as well. Based on these observations, we hypothesized that branches are entangled, in a manner reminiscent of physical gels [142] and entangled granular materials [143]. Entanglement provides a mechanism for branches of cells to remain in the same, densely packed group after cell-cell bonds break.

To test whether branch entanglement underlies the evolution of macroscopic size, we must first formally define entanglement. Inspired by string knotting analysis [144, 143] we constructed the convex hull of each connected component, which denotes the smallest convex polyhedron that can fit the connected component (see Figure C.9). If two convex hulls overlap, then the connected components are entangled. Two connected components belong to the same entangled component if there is a path from one to the other that only

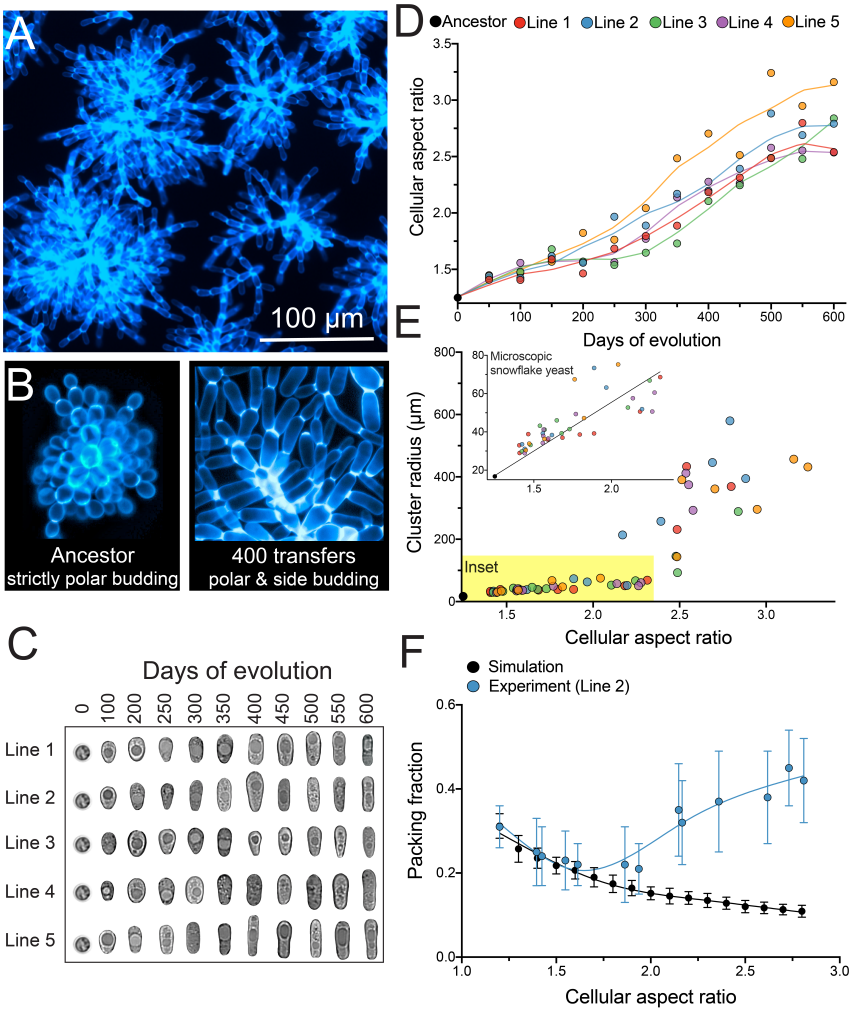

Figure 4.2: Cell-level phenotypic changes generate a shift in biophysical organization in snowflake yeast. A) Individual clusters of these macroscopic snowflake yeast adopt a modular growth form in which the group is composed of thousands of snowflake-shaped modules. Time-lapse microscopy and fluorescence tagging experiments demonstrate that these do not aggregate to form a group, but like their ancestor, grow clonally from cells that are within a propagule. B) While the ancestor had a strictly polar budding pattern, large clusters evolved to branch from their sides. C and D) show the parallel evolution of elongated cell shape, resulting in an increase in average aspect ratio from 1.2 to 2.7 ($p < 0.0001$, $F_{5,1993} = 206.2$, Dunnett's test in one-way ANOVA). E) Early in their evolution (aspect ratio 1-2.3), cluster size is an approximately linear function of cellular aspect ratio (Inset; $p < 0.0001$, $y = 41.1x - 27.8$, $r^2 = 0.72$). This relationship does not hold for higher aspect ratios. F) Volume fraction changes for the line 2 and simulation as a function of cellular aspect ratio. The experiment diverges from the simulation at around aspect ratio of 2.

moves along entangled components (Figure 4.3b).

For entanglement to underlie macroscopic size, the largest entangled component must

be able to resist mechanical stress, meaning that there must be an entangled component that spans the majority of the cluster [145]. In analyses of 10 randomly selected subvolumes from different macroscopic snowflake yeast clusters, we found that the largest entangled component contains $93\% +/- 2\%$ of all connected components. This observation supports the hypothesis that entanglement between cell branches can prevent cluster fracture in the event that a cell-cell bond fails.

As a further check, we investigated the mechanics of macroscopic snowflake yeast. Strain stiffening is a signature of entangled chains [146, 147, 143, 148]. When entangled chains are compressed, their effective stiffness increases with increased strain. This enables entangled materials to withstand stress orders-of-magnitude greater than their non-entangled counterparts, a property necessary for achieving macroscopic size [143]. Conversely, as the ancestor is not entangled, it is not expected to exhibit strain-stiffening behavior. We measured the stress response of 10 macroscopic snowflake yeast clusters under uniaxial compression using a macroscopic mechanical tester (Zwick Roell Universal Testing Machine). We repeated the same experiment for the ancestral snowflake yeast clusters using an atomic force microscope (AFM Workshop LS-AFM). While the stress-strain plot for the ancestor is linear ($r^2 = 0.97 +/- 0.2$ average of 10 samples) (Figure 4.3c inset), macroscopic snowflake yeast clusters have a convex stress-strain curve (Figure 4.3c) and can support stresses as large as 7 MPa without failing. Thus, entanglement both enables separate branches within macroscopic snowflake yeast to stay together and allows them to endure the large stresses necessary for growth to macroscopic size.

In addition to changes in cellular shape, macroscopic snowflake yeast have evolved significant changes in the geometry of budding. Rather than budding being completely restricted to distal cellular poles, as it was in the ancestor, it now also occurs at the cells' sides, creating right-angled branches (Figure 4.2 e&f). Side branching may promote entanglement by increasing the angle of budding, allowing recursive growth such that branches reenter the cluster interior.

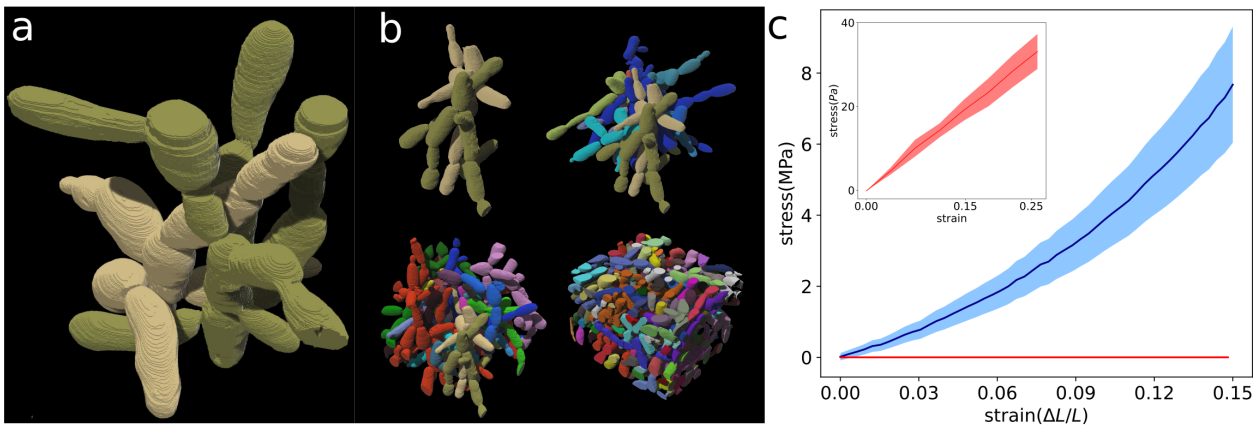

Figure 4.3: (a) Example of two entangled connected components inside a sub volume of a microscopic snowflake yeast rendered from the SBF-SEM images. (b) Progressive build of a sub-volume by many entangled connected components in four steps. (c) Stress vs strain for macroscopic snowflake yeast clusters in blue and the ancestor in red. The shaded area shows 1 standard deviation based on 10 repeated measurements. Macroscopic snowflakes experience strain stiffening. Inset: Stress strain plot for the ancestor. The shaded area shows 1 standard deviation based on 10 repeated measurements. Unlike the macroscopic snowflakes, the ancestor's curve is linear without any strain stiffening.

To uncover the genomic basis of multicellular adaptation, we sequenced the genomes of a single strain from each of the five populations to independently evolve macroscopic multicellularity after 600 transfers (Figure 4.4 a&b). 4/5 populations had a dN/dS ratio > 1.0 for potentially fixed mutations (Figure 4.4c), indicating that directional (or positive) selection has played a major role in allele frequency changes in these populations. The one population with a dN/dS ratio below 1, population 3, also evolved macroscopic multicellularity considerably later than the other replicate populations, suggesting a potential connection between the evolution of macroscopic size and directional selection.

The evolution of elongated cells is primarily driven by non-silent mutations affecting cell cycle progression, as this significantly enriched Gene Ontology (GO) category contains the largest number of genes (21 genes,$p = 4.68e - 10$). In *S. cerevisiae*, delays in the progression of the cell-cycle result in more elongated cells . Furthermore, the evolution of elongated cell shape seems to be driven by mutations within the 'filamentous growth' GO category (9 genes, $p = 0.01$). In parallel to variants affecting cellular elongation, we find

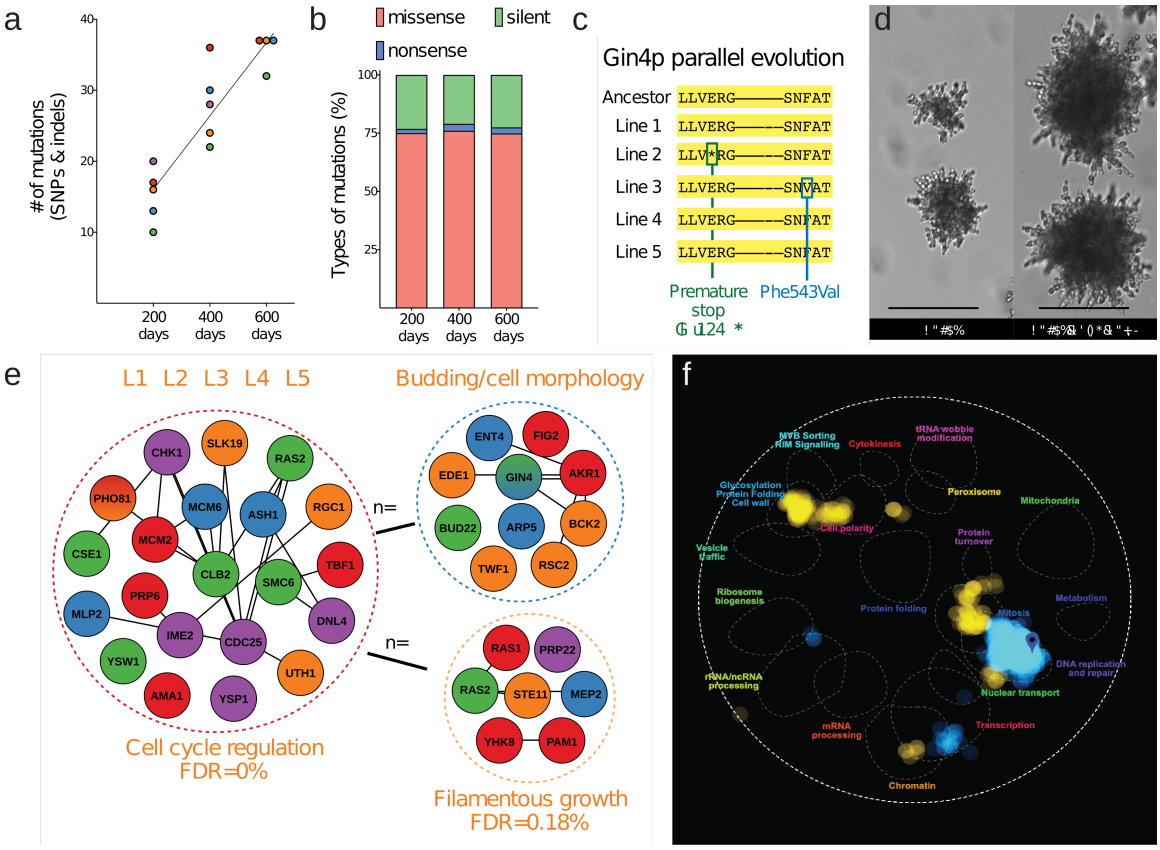

Figure 4.4: Whole-genome sequencing reveals the dynamics of molecular evolution and the genetic basis of cell-level changes. (a) and (b) show the number and types of mutations in evolved single strains from each population. (c) GIN4, a kinase controlling the size of cellular bud necks with a potential strengthening effect on connections between cells, is mutated in two independent populations. (d) Genetic engineering of cell lengthening (i.e., AKR1 and ARP5) and bud-scar strengthening (i.e., GIN4) mutations in the ancestral (i.e., bottom left) background increased multicellular size. (e) The list of non-silent mutations is significantly enriched for genes controlling cell-cycle progression (23 genes, $p = 4.68e - 10$) and filamentous growth (6 genes, $p = 0.0103$). Mutation on both is known to result in the formation of elongated cell shape in yeast []. Outside of these searchable GO-term categories, there is a substantial enrichment for genes with potential effects on the budding index, random budding pattern, and larger bud neck size (15 out of 41 genes with non-silent mutations). (f) Spatial analysis of functional enrichment [149] of non-silent mutations show enrichment for mitosis ($p = 1.11E - 06$) and cell polarity pathway ($p = 1.74E - 05$). Co-clustering of mutations in these genetic networks implies adaptive changes in the shape of cells or the direction of the bud site.

many nonsynonymous mutations in genes with known roles on cellular budding. Among these, four genes increase budding index (CDC25, CLB2, FAT3, YCF1), and four genes generate random budding in yeast (BUD22, EDE1, RPS18B, SLA1), which may play a

role in the evolution of the side-budding phenotype. Moreover, we see mutations in eight genes that have previously been shown to increase the size of buds (AKR1, ARP5, CLB2, GIN4, PRO2, RPA49, RSC2, PHO81), two of which are mutated in two independent populations, indicating parallelism (i.e., PHO81 and GIN4) [150, 151]. All else equal, larger bud necks should increase the amount of cell wall shared between mother and daughter cells, increasing the strength of the cell-cell connection.

4.4 Discussion

Nascent multicellular organisms face a distinct biophysical challenge, encountering physical forces acting on evolutionarily novel length scales that threaten to disrupt this new level of biological individuality. Here we show that snowflake yeast, a model system of undifferentiated multicellularity, were capable of evolving macroscopic size over 600 days of directed evolution. Macroscopic snowflake yeast are readily visible to the naked eye, containing hundreds of thousands of clonal cells. They evolved this remarkable increase in size via two distinct biophysical innovations. First, they evolved more elongate cells, increasing cluster size by reducing the density of cellular packing (and thus the rate at which strain accumulates) within the cluster. Next, they evolved branch entanglement, which allows multicellular groups to remain physically attached even when individual cellular connections are severed. This critical innovation increased the physical strength of multicellular groups one million-fold. Genetics summary.

To our knowledge, this is the first long-term evolution experiment to directly show how simple multicellular organisms evolve increased complexity. Snowflake yeast do not possess evolved systems of developmental control over multicellular morphology- they were synthetically created from a unicellular ancestor at the start of this experiment by deleting the $ace2$ transcription factor, and have had little prior opportunity to gain multicellular adaptations. Instead, they demonstrate how, prior to the evolution of development, novel, heritable multicellular traits can arise as an emergent property of changes in the traits of

constituent cells. Two cell-level innovations appear to have played a key role in the evolution of macroscopic size: elongate cells and side-budding. Increased cell length initially reduces strain generated from cellular packing, which is the primary manner in which size increased early in the experiment, and subsequently facilitates entanglement by reducing the number of cells that are required to make a loop. This process may be accelerated by side budding.

Our results depend on the fact that snowflake yeast grow as topologically-structured groups with permanent cellular bonds, and we would not necessarily expect similar biophysical exaptation in organisms with alternative means of group formation. These features, however, make it well suited as a model system for the lineages that have ultimately evolved complex multicellularity. Of the five lineages that independently evolved complex multicellularity (animals, plants, red algae, brown algae, and fungi), all but animals possess permanent cell-cell bonds, and early multicellular lineages are inferred to have been topologically structured [152]. While animals do not currently have permanent cell-cell bonds, little is known about their ancestral mode of cellular adhesion. Indeed, their closest living relatives, the choanoflagellates, form topologically structured multicellular groups with permanent cell-cell bonds [153, 154].

Despite daily selection for increased size, macroscopic multicellularity only evolved in our anaerobic, rather than aerobic lineages. This is further evidence that oxygen, rather than acting to promote the evolution of macroscopic multicellularity, may in fact act as a powerful constraint on the evolution of large size. Oxygen can increase cellular growth by increasing ATP yield from metabolism [155], and allowing growth on non-fermentable carbon [156]. When oxygen availability within an organism is limited by diffusion, large size can be maladaptive by reducing the ability of interior cells to utilize this valuable resource [80]- this is a constraint that anaerobic organisms simply do not face. The positive effect of oxygen on multicellular size [8] may only be realized when it reaches high levels, as happened around 0.6 Ga [157].

4.5 Conclusion

Broadly speaking, our results demonstrate that rapid multicellular innovation is possible, even in the absence of genetically-regulated multicellular development. The evolution of macroscopic size required the evolution of new physical mechanisms increasing organismal toughness, which itself required fundamental changes in the shape and behavior of the cells within the organism. Selection acting on the emergent properties of multicellular groups thus created ample opportunity for sustained adaptive evolution underlying the origin of novel multicellular phenotypes, providing the first in vitro experimental demonstration of how selection for larger size can itself be a powerful driver of increased organismal complexity.

CHAPTER 5
CONCLUSION

5.1 Summary of Findings

Understanding how a new group capable of undergoing Darwinian evolution emerges from the interactions between existing individuals is essential to understand emergence of complexity and hierarchy in life. In this process, the fundamental level of evolution transfers from the lower-level unit to the higher-level unit [4, 21, 87]. There has been many studies about the relationship between the fitness of the higher- and lower-level. However, for selection and adaptation to happen, heritability is as important as selective pressure. Here, we focused on the emergence of multicellularity from unicellular life forms and looked at two problems related to this: First the heritability of group level traits, and second the emergence of macroscopic size in nascent multicellular organisms.

The outcome of a selection process depends on both the strength of the selection and the heritability of the trait of interest. However the role of heritability of group-level traits and its relationship to heritability of cell-level traits was unclear. Here, through a combination of analytical models, computer simulations, and experiments we examined this relationship. First, we showed that heritability of group-level traits emerges as the groups form. Second, for a wide range of variables and for different ecologically relevant traits, heritability of group-level traits is higher than the heritability of cell-level traits, as group traits emerge from an average over individual cell level traits, minimizing the effect of random noise at the individual cell level.

On the second project, we used the snowflake yeast model system to study the evolution of large group size in nascent multicellular organisms. We observed the emergence of macroscopic-sized clusters in five out of five populations of anaerobic snowflake yeasts.

Although different populations reached macroscopic size at different times, they followed similar general patterns of increasing size over time. Moreover, they reach macroscopic size without any visible sign of evolving developmental structures that are ubiquitous in present complex organisms such as vascular system [8, 79]. We demonstrated that physics played an important role in their formation. If any cell-cell connection fails in the ancestor clusters they fracture into two smaller clusters. However, branches of cells inside the macroscopic clusters are physically entangled, and as a result clusters do not fracture when a single bond between cells breaks. Furthermore, entanglement makes the cluster much tougher than their ancestors, enabling them to endure large mechanical stresses.

Although these results are not generalizable to every incident of the evolution of complex multicellular organisms, nonetheless they provide a proof of concept for: first, evolution of large size without extensive genetic and developmental innovation in very short time in evolutionary time scale; second, how early multicellular organisms could have used simple mechanisms to resist forces much greater than those relevant to their unicellular ancestor.

5.2 Future Work

One possible direction to take is to understand how nonlinear relationships between cell-level and group-level traits impact heritability. Understanding heritability is as important as the magnitude of selective pressure in a major transition in individuality. We have shown that the heritability of group traits, under certain conditions, emerges from the heritability of cell level traits as a consequence of averaging over the developmental noise. Here, we only studied the interplay between σ_S , σ_E and CV_N for the simplest case of size, both theoretically and experimentally. But the relationship between group traits and cellular traits are not always simple linear functions. For more complex functions we presented only the simulation results for the case of no variation in the cell numbers per group. It is neither practically possible to test all possible analytical functions nor have we made such

a claim. What we have shown here is that for a wide range of functions relating group traits to cellular traits the group level heritability is higher than the cell-level heritability and can be altered by selection at the group-level.

Bourrat [158, 159] has claimed in a recent analytical study that when group-level traits are nonlinear functions of cell-level traits the group-level heritability is lower than cell-level heritability. This result is in contradiction to our simulation results. So, one natural direction for this project is to develop a theoretical framework to consider nonlinear functions which is essential for understanding the emergence of more complex higher-level trait heritability.

Our preliminary simulations and model carry assumptions that limit their generalizability to more complex systems: they assume asexual reproduction at both the cell and group levels, zero mutation, no selection, clonal groups, and that heritability of a trait doesn't change from one generation to the next. Because of these assumptions, the current model is a statistical model rather than a full-fledged evolutionary model. Therefore, I plan to develop an analytical model and a computer simulation to look at the changes in heritability across multiple generations and track its changes in the presence of mutation and selection. The next step would be to add sexual reproduction to the model. This would set the stage for expanding the scope of the model to accommodate the evolution of eusociality in insects such as ants or bees.

Our experimental evolution results demonstrate that innovation at the multicellular level is possible even without genetically-regulated developments that are usually considered prerequisites for increasing size. However, there are still many unanswered questions about the dynamics of evolution of macroscopic size. While we showed that entanglement is responsible for increased size, we don't know how clusters avoid fracturing before reaching entanglement since entanglement requires higher packing fraction than has been seen before in granular chain materials [143]. Moreover, the shape and geometry of cells and budding scars have changed continuously over the run time of the experiment. We need to

answer a few fundamental questions: how are cells able to create these knots and what key innovations make knot formation possible? Do they grow large because of side budding or in spite of it?

Another important direction is to continue the evolution experiments that are underutilized tools for studying the transition to multicellularity. Nature is full of surprises and can often find ways that we would not have thought about beforehand. For example, the main goal of this experiment when it started was to investigate the role of oxygen in the evolution of early multicellularity [80]. However, it led to surprising results that unveiled the role of physics in emergence of macroscopic size. There many questions that could be answered with this experiment such as: What are limits of size that this clusters can reach and what are the liming factors? Would they evolve division of labor between outer cells and cells near the surface of the clusters?

Appendices

APPENDIX A

TRAIT HERITABILITY IN MAJOR TRANSITIONS

A.1 One way ANOVA to calculate heritability in populations with different genotypes

Let's assume that we have N clonal lineages and each has n_i members where i is from 1 and N. For the simplest case we can assume a linear model for the phenotype of each individual:

$$x_{ij} = \mu + f_i + \epsilon_{ij} \tag{A.1}$$

x_{ij}: The phenotype of the jth member of the ith family.

f_i: The effect of the ith family where: $f_i \sim \mathcal{N}(0, \sigma_f^2)$

ϵ_{ij}: The residual and random effect dues to all other variables: $\epsilon_{ij} \sim \mathcal{N}(0, \sigma_\epsilon^2)$ From which we have:

$$\sigma_x^2 = \sigma_f^2 + \sigma_\epsilon^2 \tag{A.2}$$

We can partition the total variation on phenotype in the population into the sum of variance of contributing factors by using a one-way ANOVA. We define heritability as:

$$H^2 = \frac{\sigma_f^2}{\sigma_f^2 + \sigma_\epsilon^2} \tag{A.3}$$

The denominator of equation 8 is the total phenotypic variation in the population while the numerator is the part of variation that's due to the genetic variation in the population. Our goal is to estimate the numerator (σ_f^2) from experimental data by using a one way ANOVA.

Now we estimate the heritability of a quantitative trait for a collection of clonal organisms that has N different genotypes and each genotype has n_i member for i from 1 to N (unbalanced clonal population). For ANOVA for the some of squares for among genotype variation we have:

$$SS_f = \sum_{i=1}^{N} n_i(\overline{x}_i - \overline{x})^2 = \sum_{i=1}^{N} \frac{1}{n_i} x_{i\bullet}^2 - \frac{1}{T}^2 x_{\bullet\bullet} \tag{A.4}$$

Not that $T = \sum n_i$ is the total number of organisms; $x_{i\bullet}$ is the average phenotypic value of the genotype i and $x_{\bullet\bullet}$ is the mean phenotype value of the whole population. Because we have N different genotype the degree of freedom is $(N-1)$. Hence for the means squares we get:

$$MS_f = SS_f/(N-1) \tag{A.5}$$

The expected value is the mean squares then is:

$$E[MS_f] = \frac{1}{N-1}(E[\sum_{i=1}^{N} \frac{1}{n_i} x_{i\bullet}^2] - \frac{1}{T} E[x_{\bullet\bullet}^2] \tag{A.6}$$

$$= \frac{1}{N-1}(T\mu^2 + T\sigma_f^2 + N\sigma_\epsilon^2 - T\mu^2 - \frac{1}{T}\sum n_i^2 - \sigma_\epsilon^2 \tag{A.7}$$

$$= \frac{1}{N-1}(T - \frac{1}{T}\sum_{i=1}^{N} n_i^2)\sigma_f^2 + \sigma_\epsilon^2 \tag{A.8}$$

Now we calculate within-genotype variation:

$$SS_w = \sum_{i=1}^{N}\sum_{j=1}^{n_i}(x_{ij} - x_{i\bullet})^2 = \sum_{i=1}^{N}\sum^{n_i} x_{ij}^2 - \sum \frac{1}{n_i} x_{i\bullet}^2 \tag{A.9}$$

The degree of freedom here is $T - N$. Hence for the expected value of mean square we have:

$$E[MS_w] = \frac{1}{T-N}(E[\sum_{i=1}^{N}\sum^{n_i} x_{ij}^2] - E[\sum \frac{1}{n_i} x_{i\bullet}^2]) \tag{A.10}$$

$$= \frac{1}{T-N}(T\mu^2 + T\sigma_f^2 + T\sigma_\epsilon^2 - T\mu^2 - T\sigma_f^2 - N\sigma_\epsilon^2) \tag{A.11}$$

$$= \sigma_\epsilon^2 \tag{A.12}$$

Combining the results of equations 13 and 17, we can drive an expression of σ_f^2:

$$\sigma_f^2 = (MS_f - MS_w)\frac{N-1}{T - \sum \frac{n_i^2}{T}} \tag{A.13}$$

Hence the heritability is equal too:

$$H^2 = \frac{(MS_f - MS_w)\frac{N-1}{T-\sum \frac{n_i^2}{T}}}{(MS_f - MS_w)\frac{N-1}{T-\sum \frac{n_i^2}{T}} + MS_w} \tag{A.14}$$

A.1.1 Strain Construction.

All yeast strains were produced from a Y55 strain background made homozygous at all loci via sporulation and selfing, as previously described by the Ratcliff laboratory[34]. All strains were based on the GOB8 strain bearing a homozygous deletion of the ACE2 open reading frame with the KanMX cassette resulting in an $ace2\Delta :: KANMX/ace2\Delta :: KANMX$, producing small constitutively multicellular snowflake yeast.

Cell-lengthening mutations were chosen from previous work showing that disruption of CLB2 results in an alteration of filamentous growth[160], and screens of genes known to alter the aspect ratio or filamentous growth form of yeast cells[161]

Strains were produced via standard yeast genetics protocols. Cells were transformed via standard yeast lithium acetate + polyethylene glycol transformation protocols[162]. All deleted genes were deleted via transformation using PCR products of plasmid pYM25[163], creating ends-out gene deletion cassettes bearing the hygromycin-resistance hphNTI gene with 50 base pairs of flanking sequence just outside of each reading frame. Sequences can be seen in Table Table A.1. Upon selection of heterozygous deletion strains on YPD + hygromycin plates, colonies heterozygous for lengthener mutations were sporulated and tetrads dissected onto YPD + hygromycin plates, and spores allowed to self-mate before single-colony purification for analysis.

A.1.2 Measuring packing fraction of clusters:

To measure the packing fraction of each genotype, we took $1mL$ of each cell culture and stained them with Dapi using the following protocol: First we transferred $500\mu L$ of each cell culture to 1.5 ml Eppendorf tubes and replaced the YEPD media with $500\mu L$ of 70% ethanol. Then we shake the tubes at $1300rpm$ for 5 minutes at $25°C$ and washed the ethanol. Then added 1% PBS solution to the tubes and $1\mu L$ of Dapi for each $1mL$ of the PBS solution and vortexed vigorously. Then incubes the tubes for 5 minutes Then incubes the tubes for 5 minutes at $25°C$. After that we transferred $100\mu L$ of each tube to a new

Table A.1: Oligonucleotides used for strain construction

Oligo	Sequence
clb2Δ F	CCAAGAAGCCTTTTATTGATTACCCCCTCTCTCTCTTCATTGATCTT ATAGatcgatgaattcgagctcg
clb2Δ R	GGACATTTATCGATTATCGTTTTAGATATTTTAAGCATCTGCCCCTC TTCgacatggaggcccagaatac
akr1Δ F	TCCGTTTCGTCTAGATAAAAAAACACTTCTTTGTTCAGAGTAGCTAA TTGatcgatgaattcgagctcg
akr1Δ R	TGATAAAAGGCTAAAATATACAGTTTCTCCTAATGAAAACAACAAAA TTTgacatggaggcccagaatac
arp8Δ F	TAAATTACTAGTCAATAGTACATAAATACAGGGATACAATCGCACCT AACatcgatgaattcgagctcg
arp8Δ R	TGCAAAGACCTTTCAGAAAAAAAGATAACAAAAACTTCCATATGCAT ATCgacatggaggcccagaatac

tube and diluted it with $1mL$ of 1% PBS solution. Then we carefully pipted one cluster on a slide and imaged it in bright field (Figure A.1a) to calculate the area of the clusters. From this we calulated the effective raduis of cluster as:

$$r_{eff} = \sqrt{\frac{Area}{\pi}} \tag{A.15}$$

We approximated volume of clusters by calculating the volume of a sphere with $R = r_{eff}$. Then we put a cover on top of it and pressured it until we reached a cell monolayer (Figure A.1b) and imaged the nuleus of each cell (Figure A.1c) so we can count the number of cells in each cluster (N_{cell}). We approximate the volume of cells (V_{cell}) for each genotype by calculating the volume of a prolate ellipsoid that its minor and major axis are equal to short and long axis of a cell respectively. Using these information and the formula:

$$\phi = \frac{N_{cell} * V_{cell}}{V_{cluster}} \tag{A.16}$$

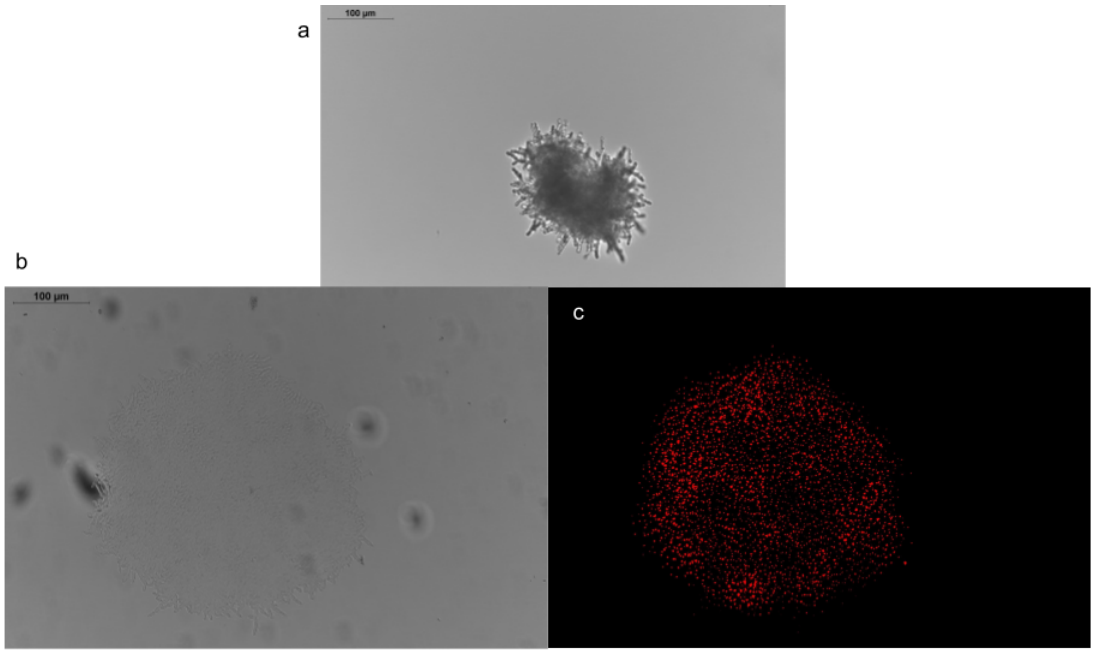

Figure A.1: a) Bright field image of a cluster. b) bright field image of a crushed cluster until it is a cell monolayer. c) Image of cell's nucleus.

APPENDIX B

LONG TERM EVOLUTION EXPERIMENT

Long-term experimental evolution. In order to generate our ancestral snowflake yeast for the long-term evolution experiment, we started with a unicellular diploid yeast strain (Y55). In this yeast, we replaced both copies of ACE2 transcription factor using a KANMX resistance marker (ace2::KANMX/ace2::KANMX) and obtained a snowflake yeast clone (SuppTable_ primers). From this Δ ace2 snowflake yeast, we selected a randomly reproduced 'petite' (p-) mutant. Due to a large deletion in its mitochondrial DNA, this snowflake yeast is unable to respire its carbon, and therefore metabolically 'anaerobic'. Starting with this isogenic ancestral clone (p-), we evolved five independent replicate populations. Snowflake yeast were grown in 10 ml YEPD (1% yeast extract, 2% peptone, 2% dextrose) in $25x150$ mm culture tubes for 24 hours at 30°C with 225 rpm shaking. To apply selection for large size, we performed settling selection at the end of every 24-hour growth period. We transferred 1.5 ml of daily culture into eppendorf tubes, let them settle by gravity for 3 minutes, discarded the top 1.45 mL of the culture, and only transferred the bottom $50\mu l$ of the settlement into a fresh culture for the next round of growth and settling selection. All the pipetting is done using wide bore filtered pipette tips (Thermo ScientificTM). In total, we applied 600 rounds (days) of growth and settling selection. By inoculating a portion of each daily culture in YEP-Gly (1% yeast extract, 2% peptone, 2% glycerol) for every 10-15 days, we made sure that our snowflake yeast populations were not contaminated by facultatively aerobic yeast, and only after that we prepared frozen glycerol stocks and archived them at -80°C.

Measuring and analyzing multicellular size data. In order to measure multicellular size over 600 days of evolution, we used a standard visualization protocol for each sample. Since variation in size of all populations from all time points spans a 4-orders of magnitude

range, we used a camera with a 5X objective allowing us to measure the area of clusters larger than $200\mu m$. To prepare populations for imaging, we revived evolved frozen cultures from 12 time points with 50 days of intervals. We then inoculated each sample recapitulating their daily growth conditions experienced during the experimental evolution. After 5 rounds of growth, we transferred $1ml$ of each culture to $1.5ml$ eppendorf tubes. We added $1ml$ of sterile water to each well of 12-well culture plates. We gently vortexed each culture and diluted them in the water. Each plate was gently shaken so that an even spread of cells covered the bottom of the well. We placed a small piece of wire in the bottom of each well as a calibration standard. We took images of each population using a Nikon camera using the following settings:a 5X lens, and 200 for ISO, and 5.6 aperture. To suspend the camera, we used a tripod and oriented straight down over the culture plate using the level on the tripod. The lens zoom was kept consistent at 5X magnification, and we made small adjustments to the height of the tripod to control focus. Finally, we set the self-timer function to minimize vibrations from touching the camera while taking the images.

Next, we analyzed the size data in each image by measuring the two-dimensional area of each cluster. The images were opened in [NIS-Elements AR] and exported to .tiff file format for manipulation using a combination of Photoshop (V.20) and ImageJ. We measured the width of the wire in pixels systematically for each picture in Photoshop. Then in ImageJ, the wire width in pixels was set to a standard-length of 1000 units using the 'Set Scale' function. Once the scale was set, we used an imageJ Macro script to calculate the two-dimensional area of each individual cluster in the picture. We finally converted the standard arbitrary units of area measurements to microns (μm) using a specific conversion ratio calculated using the wire in each image.

Testing aggregative vs. clonal development. To rule out the possibility of aggregative growth in our macroscopic snowflake yeast populations, we tagged macroscopic single strain isolates from 600 days evolved frozen populations with a red or green fluorescence

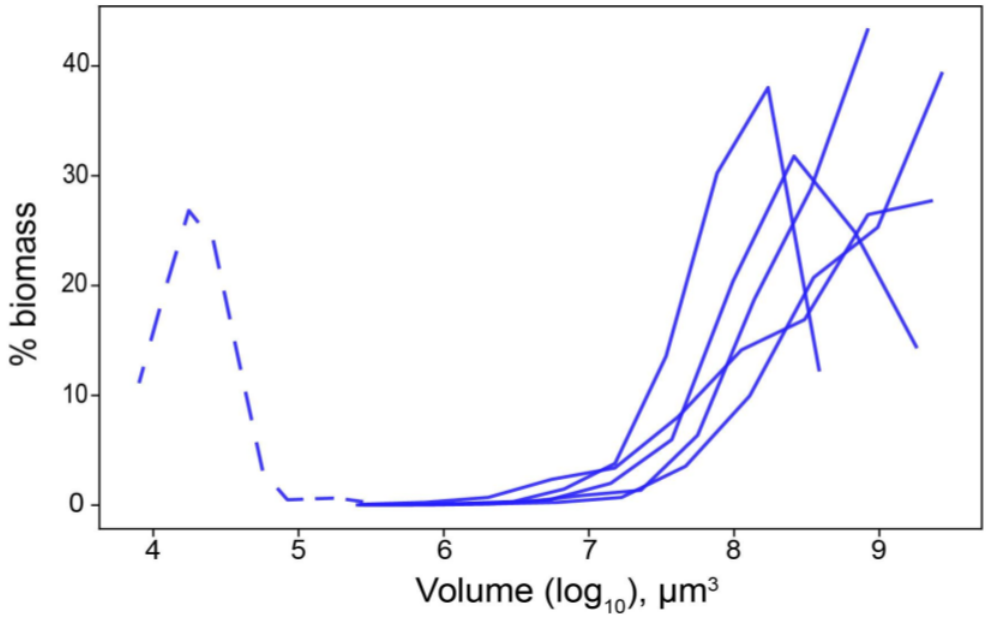

Figure B.1: A representative size distribution plot for ancestral (dotted line) and 600 days evolved populations.

protein. To do that, we amplified prTEF_GFPN_ATMX construct from pFA6a-eGFP plasmid and prTEF_dTOMATO_NATMX construct from pFA6a-tdTomato plasmid. We then separately replaced URA3 open reading frame with GFP or dTOMATO constructs in an isogenic single strain isolate by following the LiAc transformation protocol (primers, and strains are listed in SuppFileX). We selected transformants on Nourseothricin Sulfate (Gold Biotechnology Inc., U.S.) YEPD plates and confirmed green or red fluorescent protein activity of transformed macroscopic clusters by visualizing them under a Nikon Eclipse Ti inverted microscope. In order to test whether they develop through clonal or aggregative growth, we first inoculated GFP or dTOMATO expressing clones individually for overnight. We then mixed the two cultures in equal volume and diluted 100-fold into a 10 ml fresh culture. We grew five replicates of mixed-cultures for five consecutive days of growth. Finally, we washed each culture in 1ml sterile water, and visualized 50 individual clusters from each replicate under both red and green fluorescent channels. After overlaying images taken at both fluorescent channels, we counted the number of macroscopic

clusters that are green or red or a mixture of both colors.

Aspect ratio data collection and analysis. To measure cellular aspect ratio of all five populations with 50 days of intervals that is spanning 600 days of experimental evolution, we first inoculated 61 samples for overnight at 30°C (1 ancestor + 5 replicates at 12 time points). Following the same growth protocols as in our cluster size measurements, we grew these samples for five consecutive days. At the final day, we transferred 200 µl of each culture into tubes with fresh YEPD and grew them for 12 hours. Next, we stained samples in calcofluor-white and imaged and analyzed them as explained earlier. For each sample on average, we analyzed 453 number of individual cells.

DNA extraction and genome sequencing. In order to extract DNA for whole-genome sequencing, we isolated single clones from our ancestral strain and each of the evolved replicate population from three different time-points (i.e. 200, 400, and 600 days). We inoculated these 16 samples in YEPD for 12 hours and extracted their genomic DNA using a commercially available kit (Amresco, Inc. VWR USA). We measured DNA concentration using a Qubit fluorometer (Thermo Fisher Scientific, Inc.). We prepared genomic DNA library for 16 samples using NEBNext Ultra DNA Library Prep Kit for Illumina (New England Biolabs, Inc). We quantified the quality of genomic DNA library using the Agilent 2100 Bioanalyzer system that is located at the Genome Analysis Core Laboratories at Georgia Institute of Technology (Agilent Technologies, Inc). Finally, whole-genomes were sequenced using the HiSeq 2500 platform (Illumina, Inc) by the Genome Analysis Core Center located in the Petit Institute, Georgia Tech. As a result, we obtained 150 paired-end (R1 & R2) FASTQ reads from two lanes (L1 & L2).

Bioinformatic analysis. For our bioinformatics analysis. We used the 'bash command-line interface' on a Linux platform. To identify de novo mutations (single nucleotide changes, or 'SNPs', and small insertion / deletions, or 'indels') in the ancestral and evolved genomes, we first filtered out low quality reads using a sliding window approach on Trimmomatic (v0.39). We aligned reads to the yeast reference genome (S288C, SGD) using

an algorithm in the BWA software package (i.e. BWA-MEM). Next we used the genome analysis toolkit (GATK) to obtain and manipulate .bam files (Broad Institute). Duplicate reads were marked using the Picard - Tools (MarkSuplicates v2.18.3). We called SNPs using two different tools, i.e. GATK4 HaplotypeCaller (v4.0.3.0) and FreeBayes (v1.2.0). We validated SNP calls by comparing results obtain by two independent tools. For indels, we simply used the output from HaplotypeCaller. To filter variants according to their quality and depth scores and to generate an overview of statistical outcome of the variant calling step, we used the latest version of VCFTOOLS (). Finally, after manually checking each variant call by visualizing SAM files and VCF files on Integrative Genomics Viewer (IGV), we extracted de novo variants by making a pairwise comparison of each VCF file of evolved samples against the VCF file of the ancestral genome by using bcftools-isec (v1.10). Lastly, we annotated evolved mutations using SnpEff (v4.3T).

APPENDIX C

SERIAL BLOCK-FACE SCANNING ELECTRON MICROSCOPY

Specimen preparation for SBF-SEM. We first fixed samples 2% formaldehyde (fresh from paraformaldehyde (EMS)) with 2mM calcium chloride at 35°C for 5 minutes. Then we removed them and fixed them for an additional 2-3 hours on ice in the same solution. Then we incubated the sample in a solution of 3% potassium ferrocyanide + 0.3M CB + 4mM CaCl2 added to equal vol of 4% aqueous osmium tetroxide (OsT) on ice for an hour under vacuum. Then we washed them and incubate them at room temperature in thiocarbohydrazide (THC) and ddH2O solution followed by en bloc uranyl acetate and lead aspartate staining (Deerinck et al., 2010, Ngo et al., 2016, Williams et al., 2011).

Serial block-face imaging. We did the imaging using a Zeiss Sigma VP 3View. This system has Gatan 3View SBF microtome installed inside a Gemini SEM column. For this work, clusters that were embedded in resin were typically imaged at 2.5 keV, using 50-100 nm cutting intervals, 50 nm pixel size, beam dwell time of 0.5-1 μsec and a high vacuum chamber.

SEM Image analysis. The initial format of images was dm3 which then converted to tiff using GMS3 software. Then we cleaned them and pass them through a gaussian filter in Python. Using interactive learning and segmentation toolkit (ilastik) we segmented images into 3 parts: live cells, dead debris, and the background. We then imported segmented HDF5 files in python. First, we identified connected cells using the nearest neighbor algorithm to identify connected cells. We call a set of connected cell inside a subvolume, a connected component. Then using a 3D extention of gift-wrapping algorithm we extracted the convex hull of each connected components.

Visualization of SEM images. We repeated all the steps mentioned in the previous section until we get the cleaned segmented files. Then instead of running the nearest neigh-

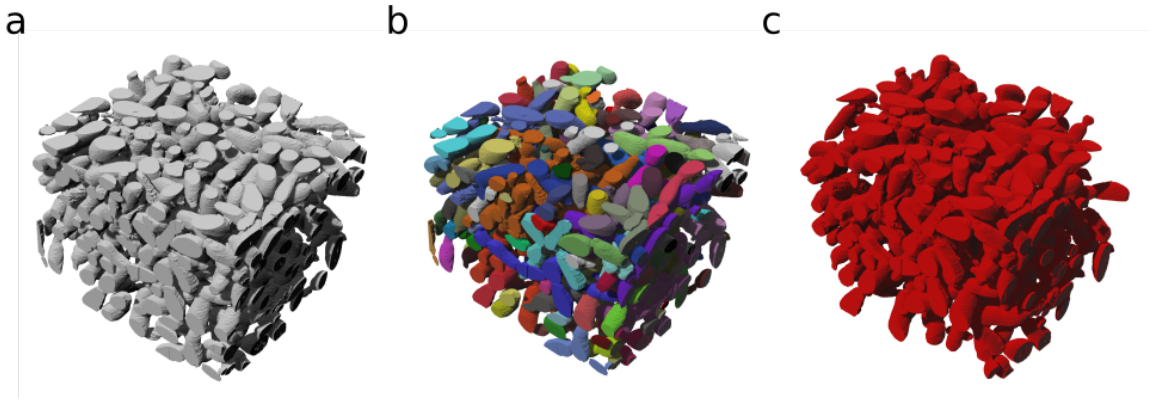

Figure C.1: a) a rendered view of subvolume of a macroscopic snowflake yeast cluster. b) Each connected component inside that cube has been colored differently. c) All connected components that belong to the largest entangled component are red and everything else has been deleted.

bor algorithm we dilate them so we could get each individually that steps is necessary so we could create a mesh of individual cells using Mathematica's Mesh tool. After creating the surface mesh of each individual cell we imported a whole subvolume in Rhino6. Then we manually identified cell to cell connections and colored each connected component differently.

Protol for teating yeast cell with Proteinase K: We put five of the cluster culture in $200\mu L$ buffer ($10mM$ Tris-HCl; $2.5mM$ MgCl2; $0.5mM$ CaCl2) only as a control. We put five more cluster culture in 190 L buffer with $10\mu L$ Proteinase K (stock 20 mg/mL), and incubated at 37 degrees. After 24 hours there was no visible difference between control and test.

C.1 List of mutations in long term evolution experiment

Time point	CHROM	POS	ID	REF	ALT
200	chrII	70494	.	T	C
200	chrIV	1030371	.	G	A
200	chrIV	1072032	.	C	A
200	chrIV	1491567	.	C	T

200	chrVI	241348	.	G	A
200	chrIX	264825	.	C	T
200	chrX	647857	.	C	T
200	chrXI	129811	.	A	T
200	chrXII	136624	.	G	A
200	chrXII	300286	.	T	C
200	chrXII	358973	.	T	A
200	chrXII	1034858	.	C	A
200	chrXII	1049381	.	C	T
200	chrXIII	497151	.	G	A
200	chrXV	12943	.	A	G,T
200	chrXVI	657408	.	T	C
400	chrII	175966	.	C	T
400	chrII	345533	.	G	T
400	chrII	510383	.	G	A
400	chrII	753615	.	C	T
400	chrIII	32815	.	C	G
400	chrIII	180899	.	C	T
400	chrIII	270040	.	T	G
400	chrIII	302884	.	G	C
400	chrIV	962144	.	A	G
400	chrIV	996345	.	G	A
400	chrIV	1366870	.	T	A
400	chrIV	1491567	.	C	T
400	chrV	290178	.	C	T
400	chrV	311445	.	A	G
400	chrVII	440719	.	G	A

400	chrVII	947016	.	GT	G
400	chrVII	957744	.	T	C
400	chrVIII	35684	.	G	T
400	chrVIII	206068	.	G	A
400	chrVIII	331646	.	G	C
400	chrVIII	395918	.	A	G
400	chrIX	245658	.	G	GT
400	chrX	356756	.	G	A
400	chrX	647857	.	C	T
400	chrXI	95688	.	C	T
400	chrXI	326897	.	G	A
400	chrXII	38567	.	G	A
400	chrXII	358973	.	T	A
400	chrXII	846594	.	T	C
400	chrXIII	41404	.	C	T
400	chrXIII	599761	.	T	C
400	chrXIII	877410	.	T	G
400	chrXIV	312963	.	A	G
400	chrXIV	441767	.	G	A
400	chrXV	515311	.	A	T
400	chrXVI	119171	.	A	G
600	chrII	175966	.	C	T
600	chrII	345533	.	G	T
600	chrII	510383	.	G	A
600	chrII	753615	.	C	T
600	chrIII	180899	.	C	T
600	chrIII	270040	.	T	G

600	chrIII	302884	.	G	C
600	chrIV	76906	.	CT	C
600	chrIV	76913	.	T	C
600	chrIV	962144	.	A	G
600	chrIV	996345	.	G	A
600	chrIV	1366870	.	T	A
600	chrIV	1491567	.	C	T
600	chrV	311445	.	A	G
600	chrV	435871	.	G	T
600	chrVII	440719	.	G	A
600	chrVII	947016	.	GT	G
600	chrVII	957744	.	T	C
600	chrVIII	35684	.	G	T
600	chrVIII	206068	.	G	A
600	chrIX	419497	.	G	A
600	chrX	356756	.	G	A
600	chrX	647857	.	C	T
600	chrXI	37223	.	G	C
600	chrXI	95688	.	C	T
600	chrXI	326897	.	G	A
600	chrXII	846594	.	T	C
600	chrXIII	23985	.	G	T
600	chrXIII	41404	.	C	T
600	chrXIII	192219	.	C	A
600	chrXIII	540385	.	G	T
600	chrXIII	873863	.	C	T
600	chrXIV	312963	.	A	G

600	chrXV	515311	.	A	T
600	chrXV	922197	.	C	T
600	chrXVI	306976	.	C	G
600	chrXVI	824288	.	G	A

Table C.1: List of mutations of lane 1

time point	CHROM	POS	ID	REF	ALT
200	chrII	240583	.	T	C
200	chrII	269323	.	C	T
200	chrII	316449	.	G	T
200	chrII	396491	.	T	C
200	chrIV	196814	.	C	T
200	chrVI	39330	.	T	A
200	chrVII	827598	.	G	C
200	chrVII	957729	.	G	T
200	chrX	97522	.	C	T
200	chrX	531865	.	C	A
200	chrXII	760972	.	G	C
200	chrXIII	270186	.	A	T
200	chrXVI	261622	.	G	T
400	chrI	174689	.	C	T
400	chrII	316449	.	G	T
400	chrIV	196814	.	C	T
400	chrIV	727219	.	C	A
400	chrIV	798775	.	G	T
400	chrIV	1352513	.	C	A
400	chrIV	1465417	.	C	A

400	chrV	511671	.	G	T
400	chrVI	44136	.	C	A
400	chrVI	106610	.	C	G
400	chrVII	118671	.	A	G
400	chrVIII	166245	.	C	A
400	chrIX	63538	.	C	T
400	chrIX	177398	.	C	A
400	chrX	97522	.	C	T
400	chrX	727311	.	G	A
400	chrXI	421775	.	C	T
400	chrXII	232533	.	C	T
400	chrXII	613034	.	G	A
400	chrXII	846614	.	G	C
400	chrXIII	20340	.	A	G
400	chrXIII	770418	.	C	G
400	chrXIV	126725	.	A	T
400	chrXIV	358252	.	C	T
400	chrXV	183069	.	G	T
400	chrXV	253030	.	A	G
400	chrXV	774188	.	T	TA
400	chrXV	1020658	.	G	C
400	chrXVI	148716	.	GACAGCACCAACC	G
400	chrXVI	778763	.	G	A
600	chrI	174689	.	C	T
600	chrII	316449	.	G	T
600	chrIV	17952	.	T	C
600	chrIV	17955	.	C	T

600	chrIV	196814	.	C	T
600	chrIV	384185	.	G	T
600	chrIV	395622	.	A	T
600	chrIV	727219	.	C	A
600	chrIV	896107	.	A	G
600	chrIV	1352513	.	C	A
600	chrIV	1465417	.	C	A
600	chrV	289356	.	A	G
600	chrV	419511	.	T	G
600	chrV	511671	.	G	T
600	chrVI	44136	.	C	A
600	chrVI	106610	.	C	G
600	chrVII	118671	.	A	G
600	chrIX	63538	.	C	T
600	chrIX	177398	.	C	A
600	chrX	97522	.	C	T
600	chrX	149239	.	G	C
600	chrXI	421775	.	C	T
600	chrXII	66331	.	C	G
600	chrXII	232533	.	C	T
600	chrXII	613034	.	G	A
600	chrXIII	20340	.	A	G
600	chrXIII	770418	.	C	G
600	chrXIV	126725	.	A	T
600	chrXIV	181556	.	G	T
600	chrXIV	358252	.	C	T
600	chrXIV	513315	.	C	T

600	chrXV	183069	.	G	T
600	chrXV	253030	.	A	G
600	chrXV	774188	.	T	TA
600	chrXV	1020658	.	G	C
600	chrXVI	148716	.	GACAGCACCAACC	G
600	chrXVI	778763	.	G	A

Table C.2: List of mutations of lane 2

Time point	CHROM	POS	ID	REF	ALT
200	chrII	316464	.	C	G
200	chrV	319276	.	T	TAAGAACAAAAAG
200	chrVII	783134	.	C	G
200	chrIX	164271	.	C	T
200	chrX	568812	.	G	C
200	chrXI	176362	.	G	A
200	chrXI	513913	.	C	A
200	chrXIV	440500	.	G	A
200	chrXV	962650	.	A	G
200	chrXVI	797232	.	C	A
400	#CHROM	POS	ID	REF	ALT
400	chrII	316464	.	C	G
400	chrII	732905	.	C	A
400	chrIV	91153	.	T	C
400	chrIV	119927	.	C	T
400	chrIV	1464160	.	A	C
400	chrV	319276	.	T	TAAGAACAAAAAG
400	chrVII	609913	.	C	A

400	chrVII	783134	.	C	G
400	chrVIII	325431	.	G	A
400	chrX	300724	.	C	A
400	chrXI	45164	.	C	A
400	chrXI	144474	.	C	A
400	chrXI	176362	.	G	A
400	chrXII	175255	.	A	G
400	chrXII	269373	.	A	C
400	chrXIII	58614	.	G	T
400	chrXIII	299580	.	G	A
400	chrXIII	481828	.	A	C
400	chrXIV	440500	.	G	A
400	chrXIV	685594	.	T	C
400	chrXVI	773079	.	C	A
400	chrXVI	797232	.	C	A
600	#CHROM	POS	ID	REF	ALT
600	chrII	46915	.	T	G
600	chrII	216219	.	C	T
600	chrII	316464	.	C	G
600	chrII	539550	.	T	C
600	chrIV	91153	.	T	C
600	chrIV	119927	.	C	T
600	chrIV	1464160	.	A	C
600	chrV	152031	.	T	A
600	chrV	300896	.	G	A
600	chrV	319276	.	T	TAAGAACAAAAAG
600	chrV	440250	.	C	A

600	chrVI	193319	.	A	G
600	chrVII	50653	.	G	T
600	chrVII	609913	.	C	A
600	chrVII	783134	.	C	G
600	chrVII	1003344	.	T	C
600	chrXI	176362	.	G	A
600	chrXI	664249	.	G	A
600	chrXII	887984	.	G	T
600	chrXIII	58614	.	G	T
600	chrXIII	223185	.	G	A
600	chrXIII	299580	.	G	A
600	chrXIII	481828	.	A	C
600	chrXIII	581107	.	G	A
600	chrXIV	440500	.	G	A
600	chrXIV	634759	.	G	A
600	chrXIV	685594	.	T	C
600	chrXV	330038	.	G	A
600	chrXV	552901	.	A	G
600	chrXV	962650	.	A	G
600	chrXVI	773079	.	C	A
600	chrXVI	797232	.	C	A

Table C.3: List of mutations of lane 3

Time point	CHROM	POS	ID	REF	ALT
200	chrII	143658	.	C	T
200	chrII	749620	.	AC	A
200	chrIV	446557	.	C	A

200	chrIV	694712	.	C	A
200	chrV	565447	.	C	A
200	chrVII	926037	.	A	T
200	chrVIII	352802	.	C	T
200	chrX	222679	.	G	T
200	chrX	648651	.	G	A
200	chrXI	238416	.	G	A
200	chrXI	340719	.	A	C
200	chrXI	535395	.	C	T
200	chrXII	752787	.	C	T
200	chrXIII	633706	.	C	A
200	chrXIII	885896	.	T	G
200	chrXIV	602464	.	G	A
200	chrXV	171754	.	C	A
200	chrXV	334739	.	C	G
200	chrXV	416132	.	A	C
200	chrXVI	324770	.	T	C
400	chrII	749620	.	AC	A
400	chrIV	446557	.	C	A
400	chrIV	575880	.	A	C
400	chrV	180969	.	T	G
400	chrV	230025	.	G	A
400	chrVII	225455	.	G	T
400	chrVIII	408357	.	C	T
400	chrX	64825	.	A	T
400	chrX	222679	.	G	T
400	chrX	545912	.	C	T

400	chrX	648651	.	G	A
400	chrXI	52153	.	G	A
400	chrXI	73457	.	G	A
400	chrXI	89753	.	G	A
400	chrXI	89754	.	C	A
400	chrXI	238416	.	G	A
400	chrXI	506585	.	T	A
400	chrXI	535395	.	C	T
400	chrXII	752787	.	C	T
400	chrXIII	633706	.	C	A
400	chrXIV	602464	.	G	A
400	chrXV	135575	.	A	G
400	chrXV	334739	.	C	G
400	chrXV	727817	.	C	T
400	chrXVI	21259	.	C	T
400	chrXVI	324770	.	T	C
400	chrXVI	379696	.	G	A
400	chrXVI	892348	.	C	A

Table C.4: List of mutations of lane 4

Time point	CHROM	POS	ID	REF	ALT
200 days	#CHROM	POS	ID	REF	ALT
200	chrI	87619	.	T	G
200	chrIV	751898	.	T	C
200	chrIV	1074350	.	G	A
200	chrV	86402	.	G	T
200	chrIX	256210	.	G	A

200	chrXII	240259	.	G	T
200	chrXV	884102	.	A	G
400	chrII	173895	.	G	A
400	chrII	427526	.	A	G
400	chrIV	88043	.	G	A
400	chrIV	198682	.	C	A
400	chrIV	451353	.	TACC	T
400	chrV	83112	.	C	A
400	chrV	519003	.	C	T
400	chrVI	221444	.	G	A
400	chrVII	185682	.	A	T
400	chrVII	642643	.	G	A
400	chrVII	749093	.	C	G
400	chrVII	808461	.	A	G
400	chrVII	955515	.	G	A
400	chrVIII	40034	.	G	C
400	chrX	282015	.	C	A
400	chrX	648705	.	G	T
400	chrX	715727	.	C	T
400	chrXI	143509	.	C	T
400	chrXI	520188	.	G	A
400	chrXII	850697	.	A	G
400	chrXII	886620	.	C	T
400	chrXIV	224748	.	G	T
400	chrXV	324488	.	T	TA
400	chrXVI	897565	.	C	T
600	chrI	37165	.	G	T

600	chrII	91979	.	G	C
600	chrII	129347	.	G	T
600	chrII	427526	.	A	G
600	chrII	765986	.	A	T
600	chrIII	68202	.	G	A
600	chrIV	88043	.	G	A
600	chrIV	376607	.	C	A
600	chrIV	451353	.	TACC	T
600	chrIV	757452	.	T	C
600	chrIV	757454	.	A	G
600	chrIV	1110025	.	T	C
600	chrV	443248	.	G	A
600	chrV	519003	.	C	T
600	chrVI	221444	.	G	A
600	chrVII	164451	.	G	T
600	chrVII	185682	.	A	T
600	chrVII	608931	.	C	T
600	chrVII	642643	.	G	A
600	chrVII	749381	.	C	A
600	chrVII	808461	.	A	G
600	chrVII	955515	.	G	A
600	chrVIII	311049	.	T	A
600	chrX	648705	.	G	T
600	chrXI	92279	.	A	T,AT
600	chrXI	520188	.	G	A
600	chrXII	37172	.	G	A
600	chrXII	493579	.	A	G

600	chrXII	842525	.	C	G
600	chrXII	850697	.	A	G
600	chrXIII	916665	.	G	C
600	chrXV	713872	.	C	G
600	chrXVI	111595	.	A	T
600	chrXVI	196719	.	G	T
600	chrXVI	756147	.	C	T
600	chrXVI	897565	.	C	T

Table C.5: List of mutations of lane 5

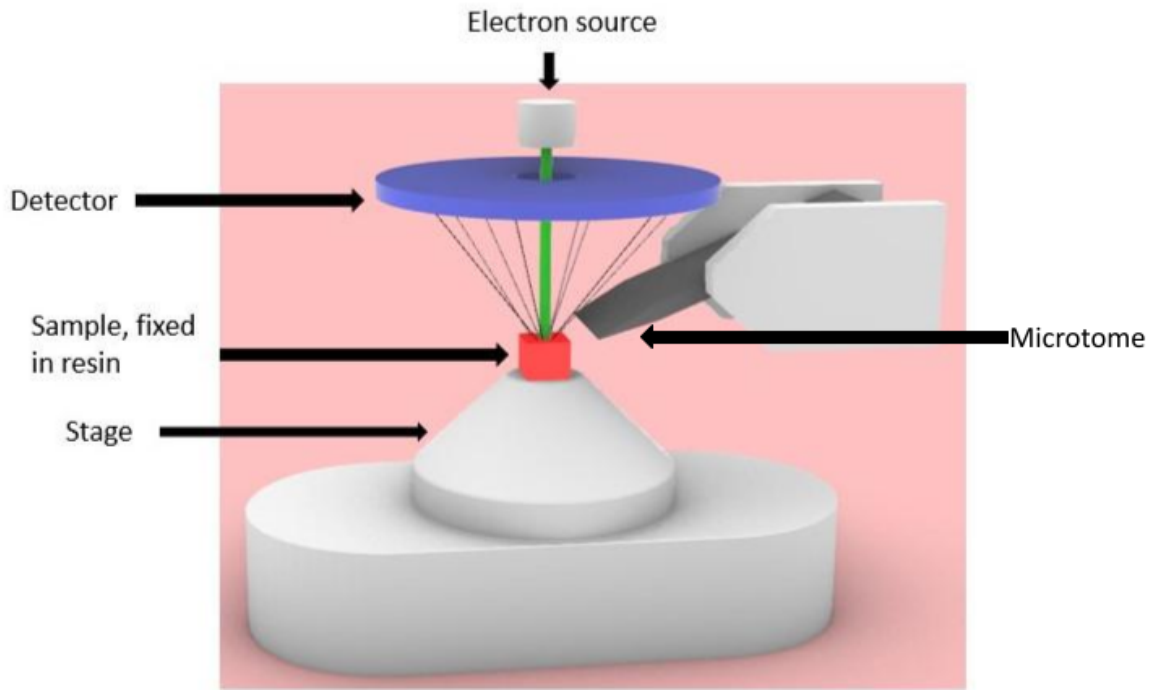

Figure C.2: Barred spiral galaxy NGC 1300 photographed by Hubble telescope. While the galaxy in the photo is not our sun, it does emit light, much like our sun. Image credit: NASA.

Figure C.3: Stained macroscopic cluster with heavy metals before embedding them in resin

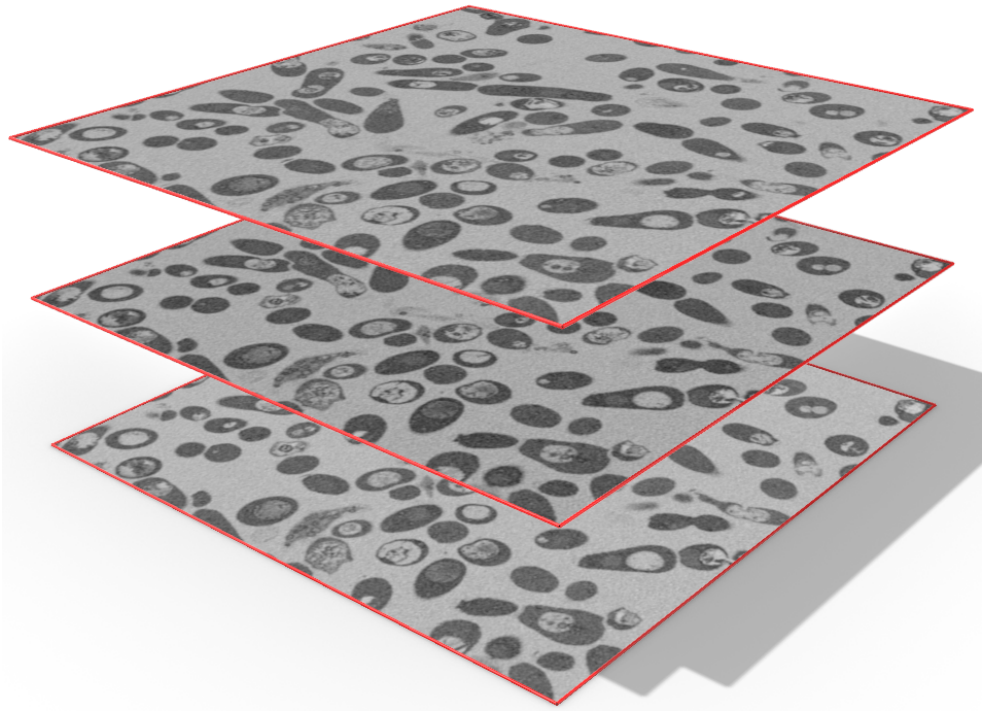

Figure C.4: Stack of SBF-SEM images

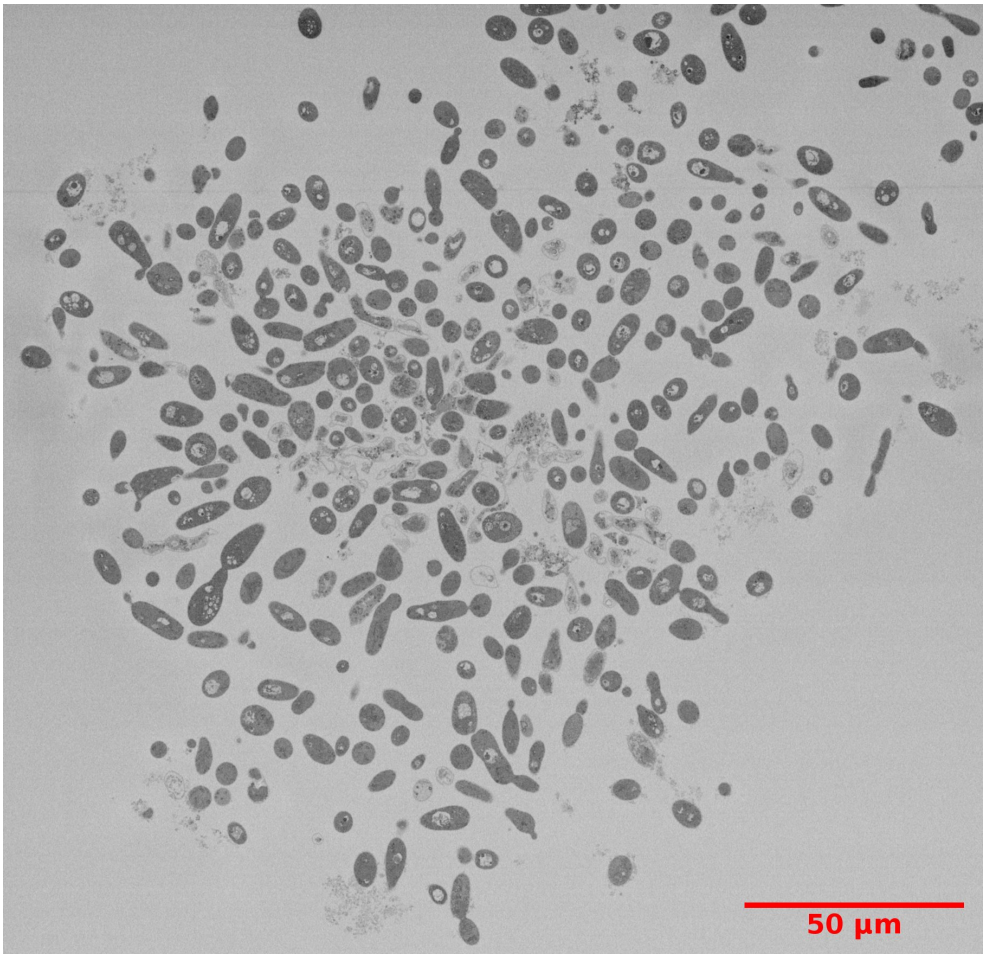

Figure C.5: Example of a raw SBF-SEM image

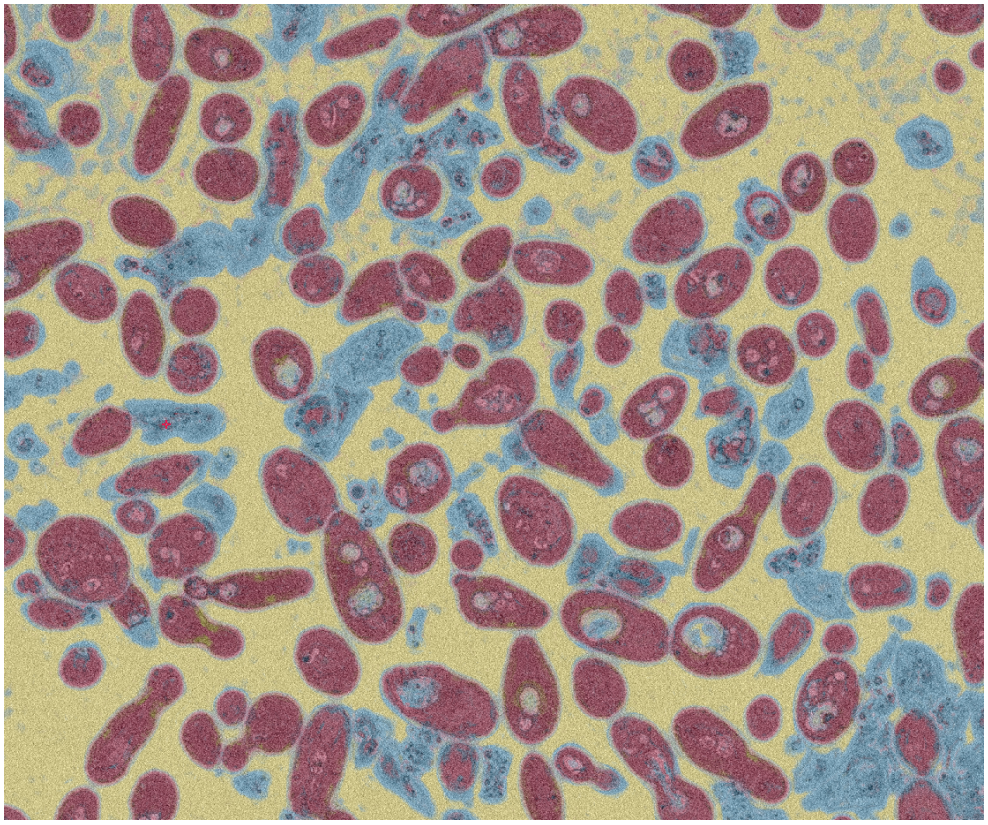

Figure C.6: Example of a segmented SBF-SEM image using ilasktik

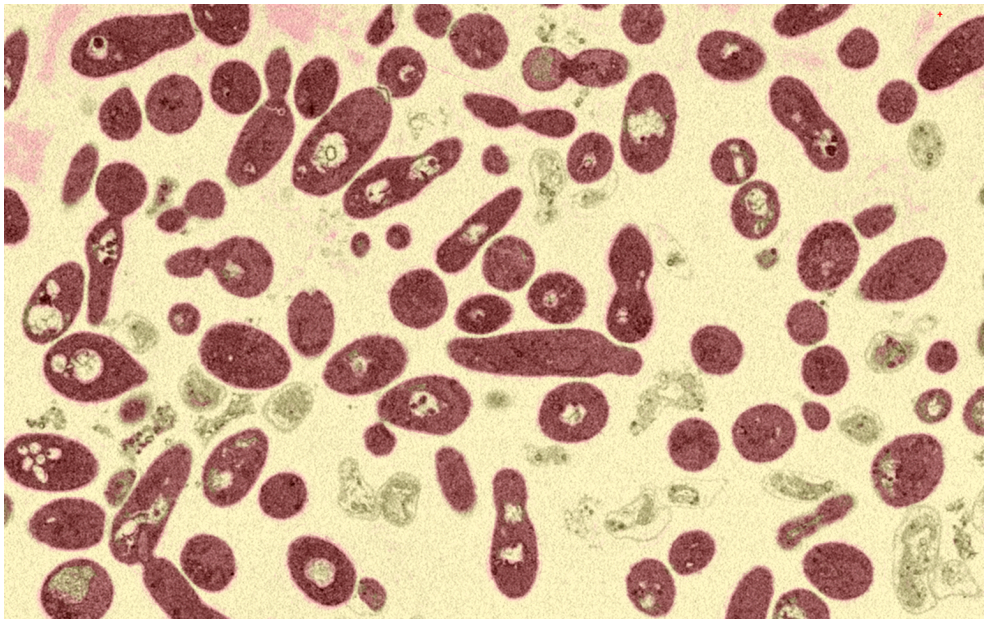

Figure C.7: Example of a segmented SBF-SEM image using ilasktik

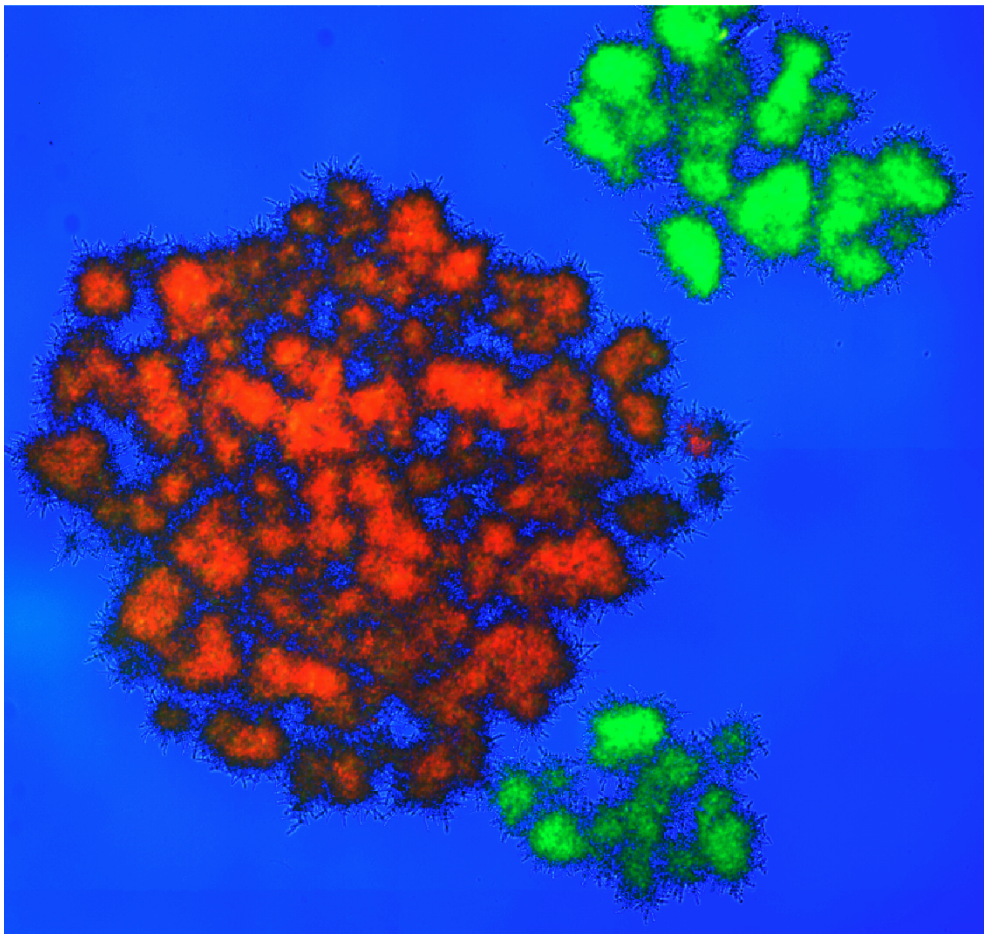

Figure C.8: To determine if macroscopic yeast are simply aggregates of multiple clusters, we labeled a single-strain isolate of macroscopic snowflake yeast taken from Line 2, t600 with either GFP or RFP. After 24h of co-culture, all multicellular clusters remained monoclonal

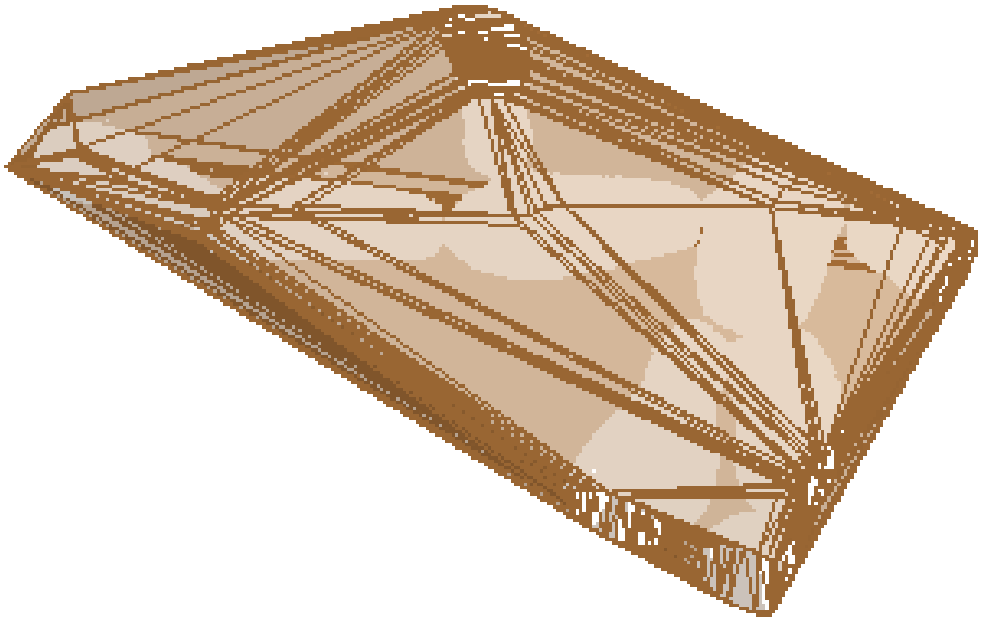

Figure C.9: Example of convex hull for a connected component inside a macroscopic snowflake yeast cluster

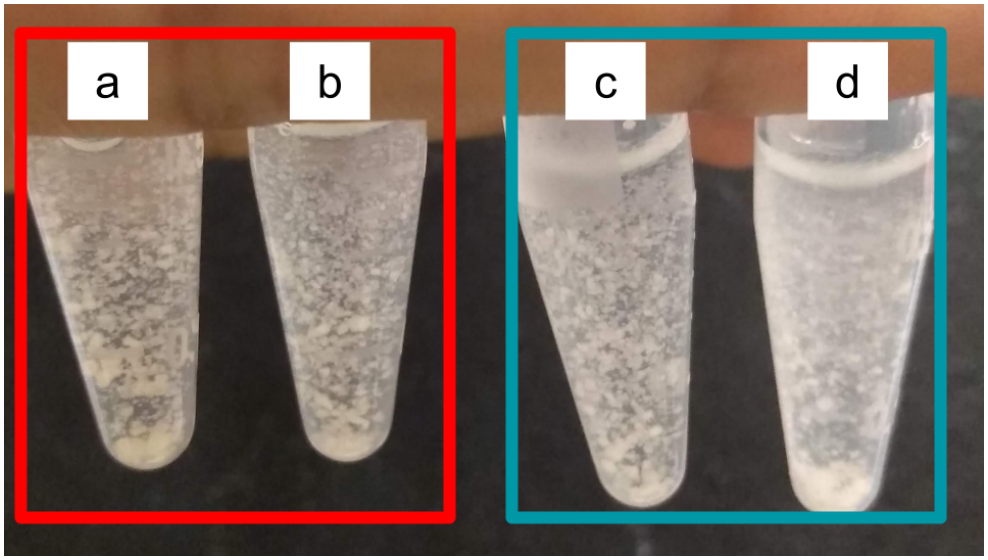

Figure C.10: Example of convex hull for a connected component inside a macroscopic snowflake yeast cluster

REFERENCES

[1] G. Wald, "The origins of life," *Proceedings of the National Academy of Sciences*, vol. 52, no. 2, p. 595, 1964.

[2] S. Arnaud-Haond, C. M. Duarte, E. Diaz-Almela, N. Marbà, T. Sintes, and E. A. Serrão, "Implications of extreme life span in clonal organisms: Millenary clones in meadows of the threatened seagrass *Posidonia oceanica*," *PloS one*, vol. 7, no. 2, e30454, 2012.

[3] T. Pievani, "The sixth mass extinction: Anthropocene and the human impact on biodiversity," *Rendiconti Lincei*, vol. 25, no. 1, pp. 85–93, 2014.

[4] E. Szathmáry and J. M. Smith, "The major evolutionary transitions," *Nature*, vol. 374, no. 6519, pp. 227–232, 1995.

[5] A. H. Van de Ven and D. N. Grazman, "Evolution in a nested hierarchy," *Variations in organization science*, pp. 185–209, 1999.

[6] M. Grene, "Hierarchies in biology," *American Scientist*, vol. 75, no. 5, pp. 504–510, 1987.

[7] S. A. West, R. M. Fisher, A. Gardner, and E. T. Kiers, "Major evolutionary transitions in individuality," *Proceedings of the National Academy of Sciences*, vol. 112, no. 33, pp. 10 112–10 119, 2015.

[8] A. H. Knoll, "The multiple origins of complex multicellularity," *Annual Review of Earth and Planetary*, vol. 39, pp. 217–239, 2011.

[9] E. Szathmáry, "Toward major evolutionary transitions theory 2.0," *Proceedings of the National Academy of Sciences*, vol. 112, no. 33, pp. 10 104–10 111, 2015.

[10] Y. M. Bar-On, R. Phillips, and R. Milo, "The biomass distribution on earth," *Proceedings of the National Academy of Sciences*, vol. 115, no. 25, pp. 6506–6511, 2018.

[11] R. K. Grosberg and R. R. Strathmann, "The evolution of multicellularity: A minor major transition?" *Annu. Rev. Ecol. Evol. Syst.*, vol. 38, pp. 621–654, 2007.

[12] J. T. Bonner, *First signals: the evolution of multicellular development*. Princeton University Press, 2007.

[13] D. Qingyou, Y. Kawabe, C. Schilde, Z.-h. Chen, and P. Schaap, "The evolution of aggregative multicellularity and cell–cell communication in the dictyostelia.," *Journal of molecular biology*, vol. 427, no. 23, pp. 3722–3733, 2015.

[14] R. M. Fisher, C. K. Cornwallis, and S. A. West, "Group formation, relatedness, and the evolution of multicellularity," *Current Biology*, vol. 23, no. 12, pp. 1120–1125, 2013.

[15] C. E. Tarnita, C. H. Taubes, and M. A. Nowak, "Evolutionary construction by staying together and coming together," *Journal of theoretical biology*, vol. 320, pp. 10–22, 2013.

[16] K. J. Niklas and S. A. Newman, "The origins of multicellular organisms," *Evolution development*, vol. 15, no. 1, pp. 41–52, 2013.

[17] T. Fagerström, D. A. Briscoe, and P. Sunnucks, "Evolution of mitotic cell-lineages in multicellular organisms," *Trends in ecology evolution*, vol. 13, no. 3, pp. 117–120, 1998.

[18] D. L. Kirk, "A twelve-step program for evolving multicellularity and a division of labor," *BioEssays*, vol. 27, no. 3, pp. 299–310, 2005.

[19] J. Damuth and I. L. Heisler, "Alternative formulations of multilevel selection," *Biology and Philosophy*, vol. 3, no. 4, pp. 407–430, 1988.

[20] P. Godfrey-Smith, *Darwinian populations and natural selection*. Oxford University Press, 2009.

[21] R. E. Michod and D. Roze, "Transitions in individuality," *Proceedings of the Royal Society of London. Series B: Biological Sciences*, vol. 264, no. 1383, pp. 853–857, 1997.

[22] M. A. Bedau, "Weak emergence," *Philosophical perspectives*, vol. 11, pp. 375–399, 1997.

[23] R. H. Kessin, G. G. Gundersen, V. Zaydfudim, and M. Grimson, "How cellular slime molds evade nematodes," *Proceedings of the National Academy of Sciences*, vol. 93, no. 10, pp. 4857–4861, 1996.

[24] M. E. Boraas, D. B. Seale, and J. E. Boxhorn, "Phagotrophy by a flagellate selects for colonial prey: A possible origin of multicellularity," *Evolutionary Ecology*, vol. 12, no. 2, pp. 153–164, 1998.

[25] J. H. Koschwanez, K. R. Foster, and A. W. Murray, "Improved use of a public good selects for the evolution of undifferentiated multicellularity," *eLife*, vol. 2, e00367, 2013.

[26] C. A. Solari, S. Ganguly, J. O. Kessler, R. E. Michod, and R. E. Goldstein, "Multicellularity and the functional interdependence of motility and molecular transport," *Proceedings of the National Academy of Sciences*, vol. 103, no. 5, pp. 1353–1358, 2006.

[27] D. A. Brock, W. É. Callison, J. E. Strassmann, and D. C. Queller, "Sentinel cells, symbiotic bacteria and toxin resistance in the social amoeba dictyostelium discoideum," *Proceedings of the Royal Society B: Biological Sciences*, vol. 283, no. 1829, p. 20 152 727, 2016.

[28] J. S. Webb, M. Givskov, and S. Kjelleberg, "Bacterial biofilms: Prokaryotic adventures in multicellularity," *Current opinion in microbiology*, vol. 6, no. 6, pp. 578–585, 2003.

[29] D. P. Anderson, D. S. Whitney, V. Hanson-Smith, A. Woznica, W. CampodonicoBurnett, and B. F. Volkman, "Evolution of an ancient protein function involved in organized multicellularity in animals," *eLife*, vol. 5, e10147, 2016.

[30] J. B. Kirkegaard, A. Bouillant, A. O. Marron, K. C. Leptos, and R. E. Goldstein, "Aerotaxis in the closest relatives of animals," *eLife*, vol. 5, e18109, 2016.

[31] M. Dos Reis, Y. Thawornwattana, K. Angelis, M. J. Telford, P. C. Donoghue, and Z. Yang, "Uncertainty in the timing of origin of animals and the limits of precision in molecular timescales," *Current biology*, vol. 25, no. 22, pp. 2939–2950, 2015.

[32] W. C. Ratcliff, D. R. Ford, M. Borrello, and M. Travisano, "Experimental evolution of multicellularity," *Proceedings of the National Academy of Sciences*, vol. 109, no. 5, pp. 1595–1600, 2012.

[33] W. C. Ratcliff, J. T. Pentz, and M. Travisano, "Tempo and mode of multicellular adaptation in experimentally evolved saccharomyces cerevisiae," *Current biology*, vol. 67, no. 6, pp. 1573–1581, 2013.

[34] W. C. Ratcliff, J. D. Fankhauser, D. W. Rogers, D. Greig, and M. Travisano, "Origins of multicellular evolvability in snowflake yeast," *Nature Communications*, vol. 6, no. 1, pp. 1–9, 2015.

[35] M. D. Herron and R. E. Michod, "Evolution of complexity in the volvocine algae: Transitions in individuality through darwin's eye," *Evolution: International Journal of Organic Evolution*, vol. 62, no. 2, pp. 436–451, 2008.

[36] M. Herron, "Origins of multicellular complexity: Volvox and the volvocine algae," *Molecular ecology*, vol. 25, no. 6, pp. 1213–1223, 2016.

[37] S. Jacobeen, J. T. Pentz, E. C. Graba, C. G. Brandys, W. C. Ratcliff, and P. J. Yunker, "Cellular packing, mechanical stress and the evolution of multicellularity," *Nature physics*, vol. 14, no. 3, pp. 286–290, 2018.

[38] E. Libby, W. Ratcliff, M. Travisano, and B. Kerr., "Geometry shapes evolution of early multicellularity," *PLoS Comput Biol*, vol. 10, no. 9, e1003803, 2014.

[39] J. T. Bonner, "The origins of multicellularity," *Integrative Biology: Issues, News, and Reviews: Published in Association with The Society for Integrative and Comparative Biology*, vol. 1, no. 1, pp. 25–36, 1998.

[40] R. C. Lewontin, "The units of selection," *Annual review of ecology and systematics*, pp. 1–18, 1970.

[41] M. Lynch and B. Walsh, *Genetics and analysis of quantitative traits*. Sinauer Sunderland, MA, 1998, vol. 1.

[42] E. Libby and P. B. Rainey, "A conceptual framework for the evolutionary origins of multicellularity," *Physical biology*, vol. 10, no. 3, p. 035 001, 2013.

[43] R. A. Fisher, "Xv.—the correlation between relatives on the supposition of mendelian inheritance.," *Earth and Environmental Science Transactions of the Royal Society of Edinburgh*, vol. 52, no. 2, pp. 399–433, 1919.

[44] R. E. Michod, "On the transfer of fitness from the cell to the multicellular organism," *Biology and Philosophy*, vol. 20, no. 5, pp. 967–987, 2005.

[45] J. H. Koschwanez, K. R. Foster, and A. W. Murray., "Sucrose utilization in budding yeast as a model for the origin of undifferentiated multicellularity," *PLoS Biol*, vol. 9, no. 8, e1001122, 2011.

[46] C. Simpson, "How many levels are there? how insights from evolutionary transitions in individuality help measure the hierarchical complexity of life," in *The Major Transitions in Evolution Revisited*, The MIT Press, 2011.

[47] G. W. Burton and d. E. Devane, "Estimating heritability in tall fescue (festuca arundinacea) from replicated clonal material 1," *Agronomy Journal*, vol. 45, no. 10, pp. 478–481, 1953.

[48] J. M. Bokmeyer, S. A. Bonos, and W. A. Meyer, "Broad-sense heritability and stability analysis of brown patch resistance in tall fescue," *HortScience*, vol. 44, no. 2, pp. 289–292, 2009.

[49] S. A. Bonos, M. D. Casler, and W. A. Meyer, "Inheritance of dollar spot resistance in creeping bentgrass," *Crop science*, vol. 43, no. 6, pp. 2189–2196, 2003.

[50] D. A. Stratton, "Life history variation within populations of an asexual plant, Erigeron annuus (Asteraceae)," *American journal of botany*, vol. 78, no. 5, pp. 723–728, 1991.

[51] J. Oard, M. Simons, *et al.*, "A growth chamber comparison of traits of aggressiveness in sexual and asexual populations of Puccinia coronata.," *Phytopathology*, vol. 73, no. 9, pp. 1226–1229, 1983.

[52] W. W. Weisser and C. Braendle, "Body colour and genetic variation in winged morph production in the pea aphid," *Entomologia experimentalis et applicata*, vol. 99, no. 2, pp. 217–223, 2001.

[53] C. Vorburger, "Positive genetic correlations among major life-history traits related to ecological success in the pea aphid Myzus perisicae," *Evolution*, vol. 59, no. 5, pp. 1006–1015, 2005.

[54] L. De Meester, "An estimation of the heritability of phototaxis in Daphnia magna Straus," *Oecologia*, vol. 78, no. 1, pp. 142–144, 1989.

[55] L. Y. Yampolsky and D. Ebert, "Variation and plasticity of biomass allocation in daphnia," *Functional Ecology*, pp. 435–440, 1994.

[56] G. Bell and A. O. Mooers, "Size and complexity among multicellular organisms," *Biological Journal of the Linnean Society*, vol. 60, no. 3, pp. 345–363, 1997.

[57] J. T. Bonner, "Perspective: The size-complexity rule," *Evolution*, vol. 58, no. 9, pp. 1883–1890, 2004.

[58] J. T. Bonner, *Why Size Matters: From Bacteria to Blue Whales*. Princeton University Press, 2011.

[59] J. M. BREIWICK, "The blue whale, balaenoptera musculus.," *Marine Fisheries Review*, vol. 46, no. 4, p. 15, 1984.

[60] J. DeWoody, C. A. Rowe, V. D. Hipkins, and K. E. Mock, "Pando lives: Molecular genetic evidence of a giant aspen clone in central utah," *Western North American Naturalist*, vol. 68, no. 4, pp. 493–497, 2008.

[61] R. E. Michod, "Evolutionary transitions in individuality: Multicellularity and sex," *The major transitions evolution revisited*, pp. 167–197, 2011.

[62] J. M. Beaulieu, I. J. Leitch, S. Patel, A. Pendharkar, and C. A. Knight, "Genome size is a strong predictor of cell size and stomatal density in angiosperms," *New Phytologist*, vol. 179, no. 4, pp. 975–986, 2008.

[63] H. A. Horner and H. C. Macgregor, "C value and cell volume: Their significance in the evolution and development of amphibians.," *Journal of Cell Science*, vol. 179, no. 4, pp. 135–146, 1983.

[64] M. Westoby, D. A. Nielsen, M. R. Gillings, E. Litchman, J. S. Madin, I. T. Paulsen, and S. G. Tetu, "Cell size, genome size, and maximum growth rate are near-independent dimensions of ecological variation across bacteria and archaea.," *Ecology and Evolution*, 2021.

[65] H. Ferguson-Gow, S. Sumner, A. F. Bourke, and K. E. Jones, "Colony size predicts division of labour in attine ants.," *Proceedings of the Royal Society B: Biological Sciences*, vol. 281, no. 1793, p. 20 141 411, 2014.

[66] C. T. Holbrook, P. M. Barden, and J. H. Fewell, "Division of labor increases with colony size in the harvester ant *Pogonomyrmex californicus*.," *Behavioral Ecology*, vol. 22, no. 5, pp. 960–966, 2011.

[67] R. Jeanson, J. H. Fewell, R. Gorelick, and S. M. Bertram, "Emergence of increased division of labor as a function of group size.," *Behavioral Ecology and Sociobiology*, vol. 62, no. 2, pp. 289–298, 2007.

[68] E. Durkheim, *The division of labor in society. Simon and Schuster*. 2014, 2000.

[69] D. W. McShea, "Perspective metazoan complexity and evolution: Is there a trend?" *Evolution*, vol. 50, no. 2, pp. 477–492, 1996.

[70] K. J. Niklas and S. A. Newman, "The origins of multicellular organisms," *Evolution & development*, vol. 15, no. 1, pp. 41–52, 2013.

[71] G. Bell, "The origin and early evolution of germ cells as illustrated by the volvocales," *The origin and evolution of sex*, vol. 7, pp. 221–256, 1985.

[72] J. T. Pentz, T. Limberg, N. Beermann, and W. C. Ratclif, "Predator escape: An ecologically realistic scenario for the evolutionary origins of multicellularity," *Education and Outreach*, vol. 8, no. 13, pp. 1–8, 2015.

[73] M. D. Herron, J. M. Borin, J. C. Boswell, J. Walker, I. K. Chen, C. A. Knox, M. Boyd, F. Rosenzweig, and W. C. Ratcliff, "De novo origins of multicellularity in response to predation," *Scientific reports*, vol. 9, no. 1, pp. 1–9, 2019.

[74] S. Smukalla, M. Caldara, N. Pochet, A. Beauvais, S. Guadagnini, C. Yan, and M. D. V. et al, "Flo1 is a variable green beard gene that drives biofilm-like cooperation in budding yeast," *Cell*, vol. 135, no. 4, pp. 726–737, 2008.

[75] V. Koufopanou, "The evolution of soma in the volvocales.," *The American Naturalist*, vol. 143, no. 5, pp. 907–931, 1994.

[76] C. A. Solari, J. O. Kessler, and R. E. Michod, "A hydrodynamics approach to the evolution of multicellularity: Flagellar motility and germ-soma differentiation in volvocalean green algae," *The American Naturalist*, vol. 167, no. 4, pp. 537–554, 2006.

[77] M. Willensdorfer, "On the evolution of differentiated multicellularity," *Evolution: International Journal of Organic Evolution*, vol. 63, no. 2, pp. 306–323, 2009.

[78] K. J. Niklas, "The evolutionary-developmental origins of multicellularity.," *American journal of botany*, vol. 101, no. 1, pp. 6–25, 2014.

[79] A. H. Knoll and D. Hewitt, "Phylogenetic, functional and geological perspectives on complex multicellularity," *The major transitions in evolution revisited*, pp. 251–270, 2011.

[80] G. O. Bozdag, E. Libby, R. Pineau, and W. C. R. Christopher T. Rienhard, "Oxygen suppression of macroscopic multicellularity," *In press*, 2021.

[81] J. Damuth and I. L. Heisler, "Alternative formulations of multilevel selection," *Biology and Philosophy*, vol. 3, no. 4, pp. 407–430, 1988.

[82] S. Okasha, "Multilevel selection and the major transitions in evolution," *Philosophy of science*, vol. 72, no. 5, pp. 1013–1025, 2013.

[83] D. E. Shelton and R. E. Michod, "Philosophical foundations for the hierarchy of life," *Biology Philosophy*, vol. 25, no. 3, pp. 391–403, 2010.

[84] P. B. Rainey and B. Kerr, "Conflicts among levels of selection as fuel for the evolution of individuality," *The major transitions in evolution revisited*, pp. 141–162, 2011.

[85] R. E. Michod, *Darwinian dynamics: evolutionary transitions in fitness and individuality*. Princeton University Press, 2000.

[86] S. Okasha, *Evolution and the levels of selection*. Oxford: Oxford University Press, 2006.

[87] C. J. Goodnight, "Multilevel selection: The evolution of cooperation in non-kin groups," *Population ecology*, vol. 47, no. 1, pp. 3–12, 2005.

[88] D. S. Falconer, *Introduction to quantitative genetics*. s. New York: Ronald Press Co, 1960.

[89] S. SM, "An ecological theory for the sudden origin of multicellular life in the late precambrian," *Proceedings of the National Academy of Sciences*, vol. 70, no. 5, pp. 1486–1489, 1973.

[90] D. Kirk, *Volvox: molecular-genetic origins of multicellularity*. Cambridge: Cambridge University Press, 1998.

[91] M. E. Boraas, D. B. Seale, and J. E. Boxhorn, "Phagotrophy by a flagellate selects for colonial prey: A possible origin of multicellularity," *Evolutionary Ecology*, vol. 12, no. 2, pp. 153–164, 1998.

[92] L. Becks, S. P. Ellner, L. E. Jones, and N. G. H. Jr, "Reduction of adaptive genetic diversity radically alters eco-evolutionary community dynamics," *Ecology letters*, vol. 13, no. 8, pp. 989–997, 2010.

[93] D. C. Queller, "Quantitative genetics, inclusive fitness, and group selection," *The American Naturalist*, vol. 139, no. 3, pp. 540–558, 1992.

[94] M. Slatkin, "Populational heritability," *Evolution*, vol. 35, pp. 859–871, 1981.

[95] S. Okasha, "The concept of group heritability," *Biology and Philosophy*, vol. 18, no. 3, pp. 445–461, 2003.

[96] C. J. Goodnight, "The influence of environmental variation on group and individual selection in a cress," *Evolution*, vol. 39, no. 3, pp. 545–558, 1985.

[97] M. Wade, *Adaptation in metapopulations: how interaction changes evolution*. Chicago: University of Chicago Press, 2016.

[98] S. Sathe, S. Kaushik, A. Lalremruata, and J. C. Ramesh K. Aggarwal, "Genetic heterogeneity in wild isolates of cellular slime mold social groups," *Microbial ecology*, vol. 60, no. 1, pp. 137–148, 2010.

[99] G. OM, F. KR, M. NJ, S. JE, and Q. DC, "High relatedness maintains multicellular cooperation in a social amoeba by controlling cheater mutants," *Proc Natl Acad Sc*, vol. 104, no. 84, pp. 3–7, 2007.

[100] L. W. Buss, *The Evolution of Individuality*. Princeton University Press, 1987.

[101] W. C. Ratcliff, M. Herron, P. L. Conlin, and E. Libby, "Nascent life cycles and the emergence of higher-level individuality," *Philosophical Transactions of the Royal Society B: Biological Sciences*, vol. 372, no. 1735, p. 20 160 420, 2017.

[102] M. D. Herron, S. A. Zamani-Dahaj, and W. C. Ratcliff, "Trait heritability in major transitions," *BMC Biology*, vol. 16, no. 1, pp. 1–12, 2018.

[103] R. A. Watson, R. Mills, C. Buckley, K. Kouvaris, A. Jackson, S. T. Powers, C. Cox, S. Tudge, A. Davies, L. Kounios, *et al.*, "Evolutionary connectionism: Algorithmic principles underlying the evolution of biological organisation in evo-devo, evo-eco and evolutionary transitions," *Evolutionary biology*, vol. 43, no. 4, pp. 553–581, 2016.

[104] D. Roze and R. E. Michod, "Mutation, multilevel selection, and the evolution of propagule size during the origin of multicellularity," *The American Naturalist*, vol. 158, no. 6, pp. 638–654, 2001.

[105] R. E. Michod and D. Roze, "Cooperation and conflict in the evolution of multicellularity," *Heredity*, vol. 86, no. 1, pp. 1–7, 2001.

[106] M. Abedin and N. King, "Diverse evolutionary paths to cell adhesion," *Trends in cell biology*, vol. 20, no. 12, pp. 734–742, 2010.

[107] C. E. Tarnita, C. H. Taubes, and M. A. Nowak, "Evolutionary construction by staying together and coming together," *Journal of theoretical biology*, vol. 320, pp. 10–22, 2013.

[108] L. Becks, S. P. Ellner, L. E. Jones, and N. G. Hairston Jr, "Reduction of adaptive genetic diversity radically alters eco-evolutionary community dynamics," *Ecology letters*, vol. 13, no. 8, pp. 989–997, 2010.

[109] S. Jacobeen, E. C. Graba, C. G. Brandys, T. C. Day, W. C. Ratcliff, and P. J. Yunker, "Geometry, packing, and evolutionary paths to increased multicellular size," *Physical Review E*, vol. 97, no. 5, p. 050 401, 2018.

[110] O. Kempthorne and O. B. Tandon, "The estimation of heritability by regression of offspring on parent," *Biometrics*, vol. 9, no. 1, pp. 90–100, 1953.

[111] E. Gullberg, S. Cao, O. G. Berg, C. Ilbäck, L. Sandegren, D. Hughes, and D. I. Andersson, "Selection of resistant bacteria at very low antibiotic concentrations," *PLoS pathogens*, vol. 7, no. 7, 2011.

[112] D. E. Dykhuizen, "Experimental studies of natural selection in bacteria," *Annual Review of Ecology and Systematics*, vol. 21, no. 1, pp. 373–398, 1990.

[113] J. E. Bouma and R. E. Lenski, "Evolution of a bacteria/plasmid association," *Nature*, vol. 335, no. 6188, pp. 351–352, 1988.

[114] V. López Rodas, E. Maneiro, and E. Costas, "Adaptation of cyanobacteria and microalgae to extreme environmental changes derived from anthropogenic pollution," *limnetica*, vol. 25, no. 1-2, pp. 403–410, 2006.

[115] B. Baselga-Cervera, E. Costas, E. Bustillo-Avendaño, and C. Garcıa-Balboa, "Adaptation prevents the extinction of chlamydomonas reinhardtii under toxic beryllium," *PeerJ*, vol. 4, e1823, 2016.

[116] A. Gerstein, L. Cleathero, M. Mandegar, and S. Otto, "Haploids adapt faster than diploids across a range of environments," *Journal of evolutionary biology*, vol. 24, no. 3, pp. 531–540, 2011.

[117] G. Vogt, "Stochastic developmental variation, an epigenetic source of phenotypic diversity with far-reaching biological consequences," *Journal of Biosciences*, vol. 40, no. 1, pp. 159–204, 2015.

[118] M. B. Elowitz, A. J. Levine, E. D. Siggia, and P. S. Swain, "Stochastic gene expression in a single cell," *Science*, vol. 297, no. 5584, pp. 1183–1186, 2002.

[119] S. Ballouz, M. T. Pena, F. M. Knight, L. B. Adams, and J. A. Gillis, "The transcriptional legacy of developmental stochasticity," *bioRxiv*, p. 2019.12.11.873265, Dec. 2019. eprint: 2019.12.11.873265.

[120] N. Q. Balaban, J. Merrin, R. Chait, L. Kowalik, and S. Leibler, "Bacterial persistence as a phenotypic switch," *Science*, vol. 305, no. 5690, pp. 1622–1625, 2004.

[121] J. A. Lee, S. Riazi, S. Nemati, J. V. Bazurto, A. E. Vasdekis, B. J. Ridenhour, C. H. Remien, and C. J. Marx, "Microbial phenotypic heterogeneity in response to a metabolic toxin: Continuous, dynamically shifting distribution of formaldehyde tolerance in methylobacterium extorquens populations," *PLos Genet.*, vol. 15, no. 11, e1008458, 2019.

[122] M. M. Salek, F. Carrara, V. Fernandez, J. S. Guasto, and R. Stocker, "Bacterial chemotaxis in a microfluidic t-maze reveals strong phenotypic heterogeneity in chemotactic sensitivity," *Nature communications*, vol. 10, no. 1877, pp. 1–11, 2019.

[123] J. S. Kain, C. Stokes, and B. L. de Bivort, "Phototactic personality in fruit flies and its suppression by serotonin and white," *Proceedings of the National Academy of Sciences*, vol. 109, no. 48, pp. 19 834–19 839, 2012.

[124] M. D. Herron, S. Ghimire, C. R. Vinikoor, and R. E. Michod, "Fitness trade-offs and developmental constraints in the evolution of soma: An experimental study in a volvocine alga," *Evolutionary ecology research*, vol. 16, no. 3, p. 203, 2014.

[125] W. Schuett, S. R. X. Dall, J. Baeumer, M. H. Kloesener, S. Nakagawa, F. Beinlich, and T. Eggers, "Personality variation in a clonal insect: The pea aphid, acyrthosiphon pisum," *Developmental psychobiology*, vol. 53, no. 6, pp. 631–640, Sep. 2011.

[126] G. Vogt, M. Huber, M. Thiemann, G. van den Boogaart, O. J. Schmitz, and C. D. Schubart, "Production of different phenotypes from the same genotype in the same environment by developmental variation," *Journal of Experimental Biology*, vol. 211, no. 4, pp. 510–523, 2008.

[127] G. Doulcier, A. Lambert, S. D. Monte, and P. B. Rainey., "Eco-evolutionary dynamics of nested darwinian populations and the emergence of community-level heredity," *eLife*, vol. 9, no. 4, e53433, 2020.

[128] J. L. Payne, A. G. Boyer, J. H. Brown, S. Finnegan, M. Kowalewski, R. A. Krause, and S. K. L. et al, "Two-phase increase in the maximum size of life over 3.5 billion years reflects biological innovation and environmental opportunity," *Proceedings of the National Academy of Sciences*, vol. 106, no. 1, pp. 24–27, 2009.

[129] N. A. Heim, J. L. Payne, S. Finnegan, M. L. Knope, M. Kowalewski, S. K. Lyons, D. W. McShea, P. M. Novack-Gottshall, F. A. Smith, and S. C. Wang, "Hierarchical complexity and the size limits of life," *Proceedings of the Royal Society B: Biological Sciences*, vol. 284, no. 1857, p. 20 171 039, 2017.

[130] L. G. Nagy, G. M. Kovács, and K. Krizsán, "Complex multicellularity in fungi: Evolutionary convergence, single origin, or both?" *Biological Reviews*, vol. 93, no. 4, pp. 1778–1794, 2018.

[131] C. A. Solari, J. O. Kessler, and R. E. Goldstein, "A general allometric and life-history model for cellular differentiation in the transition to multicellularity," *The American Naturalist*, vol. 181, no. 3, pp. 369–380, 2013.

[132] R. Fisher, J. Shik, and J. Boomsma, "The evolution of multicellular complexity: The role of relatedness and environmental constraints.," *Proceedings of the Royal Society B*, vol. 287, no. 1913, p. 20 192 963, 2020.

[133] A. Boudaoud, "An introduction to the mechanics of morphogenesis for plant biologists," *Trends in plant science*, vol. 15, no. 6, pp. 353–360, 2010.

[134] S. Höhn, A. R. Honerkamp-Smith, P. A. Haas, P. K. Trong, and R. E. Goldstein, "Dynamics of a volvox embryo turning.," *Physical review letters*, vol. 114, no. 17, p. 178 101, 2015.

[135] M. Delarue, J. Hartung, C. Schreck, P. Gniewek, L. Hu, S. Herminghaus, and O. Hallatschek, "Self-driven jamming in growing microbial populations," *Nature physics*, vol. 12, no. 8, pp. 762–766, 2016.

[136] J. W. Westbrook, K. Kitajima, J. G. Burleigh, W. J. Kress, D. L. Erickson, and S. J. Wright, "What makes a leaf tough? patterns of correlated evolution between leaf toughness traits and demographic rates among 197 shade-tolerant woody species in a neotropical forest," *The American Naturalist*, vol. 177, no. 6, pp. 800–811, 2011.

[137] S. P. Veres and J. M. Lee, "Designed to fail: A novel mode of collagen fibril disruption and its relevance to tissue toughness," *Biophysical journal*, vol. 102, no. 12, pp. 2876–2884, 2012.

[138] V. N. Prakash, M. S. Bull, and M. Prakash, "Motility-induced fracture reveals a ductile-to-brittle crossover in a simple animal's epithelia," *Nature Physic*, vol. 17, no. 4, pp. 1–8, 2021.

[139] E. C. Heinrich, M. Farzin, C. J. Klok, and J. F. Harrison, "The effect of developmental stage on the sensitivity of cell and body size to hypoxia in drosophila melanogaster," *Journal of Experimental Biology*, vol. 214, no. 9, pp. 1419–1427, 2011.

[140] M. Stratford and S. Assinder, "Yeast flocculation: Flo1 and newflo phenotypes and receptor structure," *Yeast*, vol. 7, no. 6, pp. 559–574, 1991.

[141] T. J. Deerinck, E. A. B. T. M. Shone, R. Ramachandra, S. T. Peltier, and M. H. Ellisman, "High-performance serial block-face sem of nonconductive biological samples enabled by focal gas injection-based charge compensation," *Journal of microscopy*, vol. 142, no. 4, pp. 142–149, 2018.

[142] C. E. Edwards, D. J. Mai, S. Tang, and B. D. Olsen, "Molecular anisotropy and rearrangement as mechanisms of toughness and extensibility in entangled physical gels," *Physical Review Materials*, vol. 4, no. 1, p. 015 602, 2020.

[143] E. Brown, A. Nasto, A. G. Athanassiadis, and H. M. Jaeger, "Strain stiffening in random packings of entangled granular chains," *Physical review letters*, vol. 108, no. 10, p. 108 302, 2012.

[144] D. M. Raymer and D. E. Smith, "Spontaneous knotting of an agitated string," *Proceedings of the National Academy of Sciences*, vol. 103, no. 42, pp. 16 432–16 437, 2007.

[145] J. Wilhelm and E. Frey, "Elasticity of stiff polymer networks," *Physical review letters*, vol. 91, no. 10, p. 108 103, 2003.

[146] R. S. Hoy and M. O. Robbins, "Strain hardening of polymer glasses: Effect of entanglement density, temperature, and rate," *Journal of Polymer Science Part B: Polymer Physics*, vol. 91, no. 10, pp. 3487–3500, 2006.

[147] K. A. Erk, K. J. Henderson, and K. R. Shull, "Strain stiffening in synthetic and biopolymer networks," *Biomacromolecules*, vol. 59, no. 12, pp. 1358–1363, 2010.

[148] Y. Wang, Z. Xu, M. Lovrak, V. A. le Sage, K. Zhang, X. Guo, R. Eelkema, E. Mendes, and J. H. van Esch, "Biomimetic strain-stiffening self-assembled hydrogels," *Angewandte Chemie International*, vol. 59, no. 12, pp. 4830–4834, 2020.

[149] A. Baryshnikova, "Spatial analysis of functional enrichment (safe) in large biological networks.," *In Computational Cell Biology*, pp. 249–268, 2018.

[150] M. Watanabe, D. Watanabe, S. Nogami, S. Morishita, and Y. Ohya, "Comprehensive and quantitative analysis of yeast deletion mutants defective in apical and isotropic bud growth.," *Current genetics*, vol. 55, no. 4, pp. 365–380, 2009.

[151] R. Sopko, B. Papp, S. G. Oliver, and B. J. Andrews, "Phenotypic activation to discover biological pathways and kinase substrates," *Cell cycle*, vol. 5, no. 13, pp. 1397–1402, 2006.

[152] D. Yanni, S. Jacobeen, P. Márquez-Zacarías, J. S. Weitz, W. C. Ratcliff, and P. J. Yunker, "Topological constraints in early multicellularity favor reproductive division of labor," *eLife*, vol. 9, e54348, 2020.

[153] B. T. Larson, "Regulation of form in multicellular choanoflagellates and the evolutionary cell biology of morphogenesis," *PhD diss*, UC Berkeley, 2019.

[154] T. Brunet, B. T. Larson, T. A. Linden, M. J. Vermeij, K. McDonald, and N. King, "Light-regulated collective contractility in a multicellular choanoflagellate," *Science*, vol. 366, no. 6463, pp. 326–334, 2019.

[155] P. C. Hinkle, M. A. Kumar, A. Resetar, and D. L. Harris, "Mechanistic stoichiometry of mitochondrial oxidative phosphorylation," *Biochemistry*, vol. 30, no. 14, pp. 3576–3582, 1991.

[156] J. Raymond and D. Segrè, "The effect of oxygen on biochemical networks and the evolution of comple life," *Science*, vol. 311, no. 5768, pp. 1764–1767, 2006.

[157] A. P. Gumsley, K. R. Chamberlain, W. Bleeker, U. Söderlund, M. O. de Kock, E. R. Larsson, and A. Bekker, "Timing and tempo of the great oxidation event.," *Proceedings of the National Academy of Sciences*, vol. 114, no. 8, pp. 1811–1816, 2017.

[158] P. Bourrat, "Evolutionary transitions in heritability and individuality," *Theory in Biosciences*, vol. 138, no. 2, pp. 305–323, 2019.

[159] P. Bourrat, "Transitions in evolution: A formal analysis," *Synthese*, pp. 1–33, 2019.

[160] N. P. Edgington, M. J. Blacketer, T. A. Bierwagen, and A. M. Myers, "Control of saccharomyces cerevisiae filamentous growth by cyclin-dependent kinase cdc28," *Molecular and cellular biology*, vol. 19, no. 2, pp. 1369–1380, 1999.

[161] M. Watanabe, D. Watanabe, S. Nogami, S. Morishita, and Y. Ohya, "Comprehensive and quantitative analysis of yeast deletion mutants defective in apical and isotropic bud growth," *Current genetics*, vol. 55, no. 4, pp. 365–380, 2009.

[162] R. D. Gietz and R. A. Woods, "Yeast transformation by the liac/ss carrier DNA/PEG method," in *Yeast Protocol*, Springer, 2006, pp. 107–120.

[163] C. Janke, M. M. Magiera, N. Rathfelder, C. Taxis, S. Reber, H. Maekawa, A. Moreno-Borchart, G. Doenges, E. Schwob, E. Schiebel, *et al.*, "A versatile toolbox for pcr-based tagging of yeast genes: New fluorescent proteins, more markers and promoter substitution cassettes," *Yeast*, vol. 21, no. 11, pp. 947–962, 2004.